Norwegian University of Life Sciences

**Master's Thesis 2021 60 ECTS**

Faculty of Biosciences

# Sensitivity to gamma radiation of Scots pine seedlings grown from seeds developed under elevated levels of ionizing radiation

Md Mahfuzur Rahman

Master of Science in Plant Sciences

Norwegian University of Life Sciences

Norges miljø- og biovitenskapelige universitet

Master's thesis

# Sensitivity to gamma radiation of Scots pine seedlings grown from seeds developed under elevated levels of ionizing radiation

**Md Mahfuzur Rahman**

Department of Plant Sciences

Faculty of Biosciences

Norwegian University of Life Sciences

Post Box 5003, NO-1432 Ås, Norway

Ås, 2021

## Table of contents

## Abstract

As being sessile, plants are generally exposed to background levels of ionizing radiation in their natural environment due to cosmic radiation as well as alpha-, beta- or gamma- emitting radionuclides in naturally occurring radioactive materials (NORM) including thorium, uranium and their progeny radionuclides in bedrocks, sediments and soils. Also, some areas have elevated, potentially harmful levels of radiation arising particularly from anthropogenic sources including fuel cycles and nuclear power plant accidents, tests and use of nuclear weapons as well as medical use. Such radiation at low and high doses can induce various physiological, biochemical and molecular responses in plants and can cause adverse effects such as reduction in growth and reproduction, and damage to DNA, proteins and lipids.

Due to its high energy, gamma radiation has high penetration power in biological tissues and its effects on living organisms have accordingly been much studied. Long-term study results in plants have demonstrated detrimental effects and mutations even at low levels of ionizing radiation. Coniferous plants are suggested to be among the most radiosensitive plant species, and pine trees showed high-level of radiosensitivity after the Chernobyl and Fukushima nuclear power plant accidents. However, studies of sensitivity to gamma radiation of plant seedlings under controlled exposure conditions are scarce, especially for low to moderate dose rates. Also, there is limited information about how elevated levels of ionizing radiation during seed development affect the radiosensitivity in the plants grown from these seeds.

The present study aimed to investigate the sensitivity to gamma radiation in seedlings of the ecologically and economically important gymnosperm Scots pine when grown from seeds from different areas in the Chernobyl region with background (CON), intermediate (INT) and high (TR22) levels of ionizing radiation. Such seedlings were exposed to gamma dose rates from 0-100 mGy $h^{-1}$ from a $^{60}Co$ (Cobalt-60) source for 144 h and studied across multiple levels of biological organization at the end of the gamma irradiation and up to 29 days post-irradiation. In addition to growth and development, DNA damage, total antioxidant capacity and expression analysis of genes involved in control of cell division and DNA repair were assessed.

In spite of significantly increased root and shoot lengths of TR22 seedlings at 10 mGy $h^{-1}$ and 0-40 mGy $h^{-1}$, respectively, compared to the unexposed CON seedlings, at the end of the gamma irradiation, there was no clear dose-response relationship between the gamma dose

rates and plant lengths for any of the plant types. Post-irradiation, the number of needles and shoot diameter were reduced at ≥ 40 mGy $h^{-1}$ for all three plant types, but shoot elongation was not significantly affected. However, there was no overall significant difference in growth in response to the different gamma irradiation dose rates between the plant types.

All the plant types showed a clear dose-rate dependent DNA damage as assessed by the COMET assay at the end of the 144 h gamma irradiation and at day 30 post-irradiation. At the end of the irradiation, the TR22 and INT plants showed significantly lower DNA damage than the CON plants at ≥ 40 mGy $h^{-1}$. Such differences were also observed day 30 post-irradiation, but most pronounced so for TR22. Despite the differences in DNA damage, the different plant types did not show any significant differences in total antioxidant capacity measured by the FRAP assay after 144 h gamma irradiation. The relative transcript level of the cell division controlling gene *CYCB1;1* was then significantly reduced in TR22 seedlings at 100 mGy $h^{-1}$ compared to the unexposed CON seedlings, but the *CDKB1;2* expression did not differ significantly between the different dose rates and plant types. The transcript level of the DNA repair-related *RAD51* gene was significantly downregulated in TR22 seedlings at 10 mGy $h^{-1}$ as compared to unexposed CON seedlings, whereas the *SOG1* transcript level did not differ significantly between the plant types. Thus, except for a possible slight trend of a dose-rate dependent reduction in *CYCB1;1* expression and more so in the TR22 than the CON plants, there was no clear, systematic dose-response relationship between the gamma dose rates or plant types and transcript levels of the analyzed genes.

In conclusion, in spite of that, more DNA damage in the CON plants than the INT and TR22 plants after gamma irradiation at 40 and 100 mGy $h^{-1}$ suggested lower radiosensitivity in the plants grown from seeds developed under elevated levels of ionizing radiation, this was not reflected in their growth, total antioxidant capacity or expression of selected cell division- and DNA damage repair-related genes.

**Keywords:** Ionizing radiation, gamma radiation, radiosensitivity, dose rate, DNA damage, Scots pine, *Pinus sylvestris*, gene expression

## Acknowledgement

This MSc thesis was funded by the Norwegian University of Life Sciences and the Research council of Norway through its Centre of Excellence (CoE) funding scheme (Grant 223268/F50). The work was done within a subproject on radiosensitivity in plants within the Centre for Environmental Radioactivity (CoE CERAD).

I would like to express my gratitude to my supervisor Professor Jorunn Elisabeth Olsen for her help, dynamic guidance, constant encouragement and support, and constructive suggestions during the period of this thesis work. I acknowledge her intellectual input and supervision. I am very grateful for her help in statistical analyses and valuable comments and feedback during the thesis writing. I am also obliged and thankful to my co-supervisor Dr. Payel Bhattacharjee for her cordial help and guidance with all the laboratory experiments.

The COMET assays for measuring DNA damage after gamma irradiation were performed by scientist Dr. YeonKyeong Lee. I am very thankful to her for letting me use these results in my MSc thesis for completeness, since these data are important background information for the antioxidant capacity and gene expression studies. I am also thankful to senior engineer Tone Ingeborg Melby of Plant Cell Laboratory for her support on aspects of the gene expression analyses. I also express my regards to all the teaching- and non-teaching staffs of Plant Cell Laboratory.

I would like to thank researcher Dr. Dag Anders Brede for all his help and assistance with setting up gamma irradiation experiments and for general discussions about the experiments. Professor Valery Kashparov and his team at the University of Kiev, Ukraine, are also to be thanked for providing the Scots pine seeds used in this thesis work, as well as information regarding the sampling sites and for valuable suggestions and discussions. Professor Brit Salbu (former head of CERAD) and Dr. Ole Christian Lind (current Research Director of CERAD) are also gratefully acknowledged for all their input and discussions during the planning and performance of the work included in this MSc thesis.

I am thankful to my loving parents, brothers, sister-in-law and my nieces Parin and Doreen, and my lovely wife for their blessing, continuous inspiration and mental support. It is my pleasure to dedicate this work to them.

Finally, I would like to put into record that all those whose names I may inadvertently left out, will always have a place in my heart for whatever the assistance rendered directly or indirectly which has made possible the completion of this work.

Md Mahfuzur Rahman

August, 2021

## Abbreviations

| Short form | Full form |
|---|---|
| ChEZ | Chernobyl Exclusion Zone |
| ChNPP | Chernobyl Nuclear Power Plant |
| SAM | Shoot apical meristem |
| RAM | Root apical meristem |
| ROS | Reactive oxygen species |
| ATM | Ataxia Telangiectasia Mutated |
| ATR | Ataxia Telangiectasia Mutated Rad3-related |
| Gy | Gray |
| DDR | DNA Damage Response |
| CPDs | Cyclobutane-type pyrimidine dimers |
| DNA | Deoxyribonucleic acid |
| cDNA | Complementary DNA |
| $H_2O_2$ | Hydrogen peroxide |
| ssDNA | Single strand DNA |
| dsDNA | Double strand DNA |
| SDB | Single strand DNA breaks |
| DSB | Double strand DNA breaks |
| MMR | Mismatch Repair |
| BER | Base Excision Repair |
| NER | Nucleotide Excision Repair |
| NHEJ | Non-homologous End Joining |
| HR | Homologous Recombination |
| APX/APOD | Ascorbate peroxidase |
| CAT | Catalase |
| POD | Peroxidase |
| SOD | Superoxide dismutase |
| SPX/SPOD | Syringaldazine peroxidase |
| GPX/GPOD | Guaiacol peroxidase |
| GR | Glutathione reductase |
| *CYC* | *CYCLIN* |
| *CDK* | *CYCLIN-DEPENDENT KINASE* |
| *SOG1* | *SUPPRESSOR OF GAMMA-RESPONSE 1* |
| *RAD51* | *RADIATION 51* |
| ANOVA | Analysis of variance |
| glm | General linear model |
| qPCR | Quantitative Real Time Polymerase Chain Reaction |

# 1. Introduction

## 1.1 Overview

Plants are frequently exposed to various environmental conditions and stresses, including biotic and abiotic stresses such as pathogen infection, drought, freezing, nutrient deficiency and radiation and therefore have developed complex mechanisms to quickly respond and finally adapt to these stresses. In the environment, radiation is found as either ionizing radiation such as alpha (α), beta (β) and gamma (γ) radiation or non-ionizing radiation such as ultraviolet (UV) radiation (UV-A, UV-B), visible light, infra-red, microwave and radio wave radiation.

Ionizing radiation is emitted from many natural environmental sources which include cosmic radiation and naturally occurring radioactive materials (NORM) including thorium, uranium and their progeny radionuclides in bedrocks, sediments and soils (Paschoa, 1998). Furthermore, there are several anthropogenic sources of ionizing radiation including nuclear power plant releases and accidents, nuclear testing, nuclear weapon test fallout, stockpiles of nuclear waste as well as radionuclides used for medical diagnostics and therapeutic operations (United Nations Scientific Committee on the Effects of Atomic Radiation [UNSCEAR], 2010, 2017).

Such radiation can induce various physiological, biochemical and molecular responses in organisms and give rise to somatic and genetic effects in subsequent generations. The somatic effects can lead to cell damage and even cell death (Choppin et al., 2013). When a plant experiences too much exposure to ionizing radiation, it is plausible that a high enough total absorbed dose (measured in the unit Gray (Gy) which is a measure of the total energy deposited in a unit mass of matter) delivered over a certain threshold rate can result in deleterious effects, and even death. Several studies have reported that ionizing radiation has positive and negative effects on plants at low and high doses, respectively (Jan et al., 2012). It has also been widely reported that acutely delivered high doses of ionizing radiation have noticeable negative effects on plants.

DNA damage and other consequences at the molecular level are heavily highlighted in studies utilizing acute doses, and many such studies have been centered on mutagenesis. Because there are significantly fewer studies of effects of low to moderate doses of ionizing radiation, particularly in the laboratory under controlled conditions, significantly less is

known about the biological effects of ionizing radiation at lower doses and/or the threshold for dosages at which there would be "no effect." Nevertheless, generally plants are considered more radio-resistance than humans and other animals and the presence of ambient background ionizing radiation is not usually thought to cause stress to plants (Caplin & Willey, 2018).

Among different types of ionizing radiation, the effects of external gamma radiation on living organisms have been most studied (Van Hoeck et al., 2015), and long-term study results indicated that plants experience detrimental effects and mutations even at low levels of ionizing radiation (Real et al., 2005). Woody conifer plants (gymnosperms) are suggested to be among the most radiosensitive plant species, and pine trees showed high-level of radiosensitivity after the Chernobyl and Fukushima nuclear power plant accidents that occurred in April 1986 and Mach 2011, respectively (Yoschenko et al., 2018). Despite extensive field and laboratory research on the effects of ionizing radiation on plants, our understanding of biological processes and oxidative stress responses in plants caused by low to moderate levels of gamma radiation at different levels of organization (molecular, cellular, and organismal level) is still limited particularly under standardized exposure conditions in the absence of possible confounding factors.

### 1.2 Ionizing radiation

Ionizing radiation is made up of subatomic particles or electromagnetic waves with enough energy to ionize atoms or molecules by detaching their electrons. Ionizing radiation includes α, β and γ radiation (electromagnetic spectrum, Figure 1).

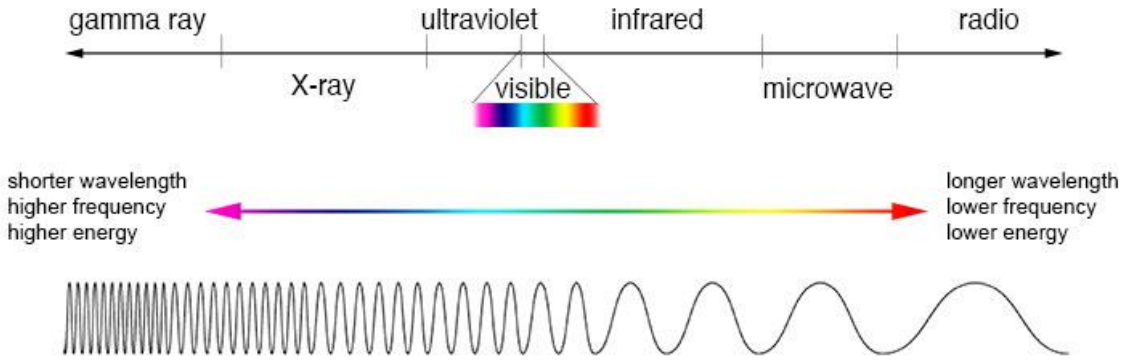


Figure 1. The electromagnetic spectrum showing relative frequency, wavelength and energy of different sources of ionizing and non-ionizing radiation (https://imagine.gsfc.nasa.gov/Images/science/EM_spectrum_compare_level1_lg.jpg; Accessed on 16 June, 2021).

The interaction of ionizing radiation with target atoms or molecules of the exposed cells results in excitation or ionization of molecules (Lachumy et al., 2013). The energy absorbed from ionizing radiation damages the molecular structure of cells by two different ways either by direct or indirect action (Figure 2).

In direct action, ionizing radiation induces ionization of cellular macromolecules such as DNA, proteins and lipids. The emitted energy induces electron loss of molecules and thus, causes bond breakage which leads to functional changes in those cellular molecules (Hosoya & Miyagawa, 2014). This process of ionizing radiation becomes very common with high doses of radiation and high-LET (linear energy transfer) radiation, i.e. α particles and neutrons.

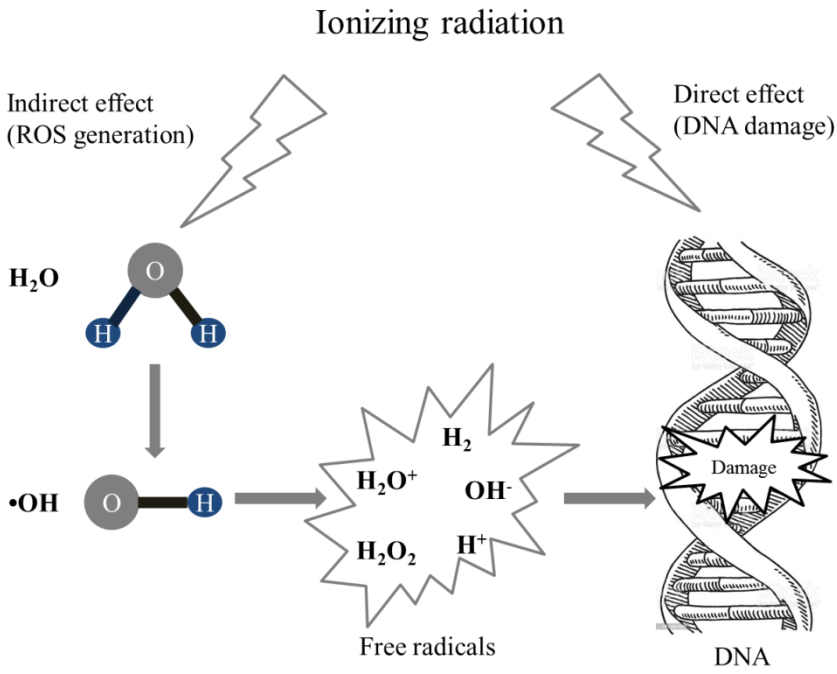


Figure 2. Action mechanism of ionizing radiation. In direct effects, secondary electrons interact with macromolecules such as DNA, whereas in indirect effects, the secondary electrons interact with water molecules which lead to formation of ROS. Modified from Dowlath et al. (2021). Abbreviations: ROS (Reactive oxygen species); $H_2O_2$ (Hydrogen peroxide); •OH (Hydroxyl radical); $OH^-$ (Hydroxide ion); $H^+$ (Hydrogen ions); $H_2O^+$ (Oxoniumyl).

On the other hand, in the indirect action of ionizing radiation, the absorbed energy interacts directly with the water molecules present in the cells instead of the macromolecules. The water molecules become ionized, thereby forming free radicals (Figure 2). Recombination of free radicals produces reactive oxidative species (ROS). As water comprises about three-

fourths of the cellular mass, the water molecules experience most of the ionization reactions induced by ionizing radiation (Sreedhar et al., 2013). In the process of ionization in living organisms, production of hydroxyl radicals (•OH), and hydrogen ions ($H^+$) upon splitting of water molecules and the formation of hydrogen peroxide ($H_2O_2$) internally in cells can damage the cellular structures and cellular biomolecules like DNA.

The radioactivity (or simply activity) of a radioactive source is measured in the unit Becquerel (Bq), which indicates the number of disintegrations of atoms per time unit (United Nations Scientific Committee on the Effects of Atomic Radiation [UNSCEAR], 2010). **A**bsorbed dose (energy) describes the amount of radiation absorbed by an object or a living organism (i.e. the amount of energy that radioactive sources deposit in materials through which they pass) which is given by the unit of Gray (Gy) where 1 Gy is equal to 1 J $kg^{-1}$. Sievert (Sv) is the SI unit for ionizing radiation dose that measures the quantity of energy absorbed in a human body per unit mass (J $kg^{-1}$). Sievert is regarded as a risk unit which is not used for organisms like plants. It practically takes into account the random effects and the risk of developing negative health effects like cancer in humans. Mostly based on health effects, currently low gamma doses and dose rates are defined as ≤ 100 mGy and ≤ 6 mGy $h^{-1}$, respectively (Averbeck et al., 2018; United Nations Scientific Committee on the Effects of Atomic Radiation [UNSCEAR], 2017). The current global mean natural background dose rate is about 2.5 mGy per year, which corresponds to about 0.29 μGy $h^{-1}$ (Caplin & Willey, 2018). However, there are many areas that experience naturally elevated ionizing radiation because of high radionuclide contents in the bedrock, for instance Ihla Grande island in Brazil, Ramsar in Iran and the Fen field in Norway where radiation dose rates have been measured at 14-15 μGy $h^{-1}$, 4.4 μGy $h^{-1}$ and 8 μGy $h^{-1}$ respectively (Caplin & Willey, 2018; Freitas & Alencar, 2004; Mrdakovic Popic et al., 2012).

### 1.3 Non-ionizing radiation

Unlike ionizing radiation, non-ionizing radiation has sufficient energy for excitation of atoms or molecules, but the energy is not sufficient to ionize the atoms or molecules. It does also not possess sufficient energy to break chemical bonds when it meets biological materials. Non-ionizing radiation can be divided into two main areas in the electromagnetic spectrum: optical radiation and electromagnetic fields. Optical radiation includes ultraviolet (UV) radiation, visible light and infrared radiation, whereas electromagnetic fields cover

microwave and radio wave radiation (Figure 1). Non-ionizing radiation originates from both natural and man-made sources. Sunlight or lighting discharges etc. are natural sources of non-ionizing radiation, whereas man-made sources of non-ionizing radiation are found in wireless communications, industrial, scientific and medical applications. Based on wavelengths, non-ionizing UV radiation in the solar electromagnetic spectrum can be further classified into three types as UV-A, UV-B and UV-C. UV-A, UV-B and UV-C have wavelengths ranging from 315-400 nm, 290-315 nm and 100-280 nm respectively (Gill et al., 2015; Jansen, 2017). UV-C has comparatively shorter wavelengths which makes it the most damaging type of UV radiation. The ozone layer absorbs the UV-C completely and therefore prevents it to reach the earth's surface. In contrast to UV-C, UV-B radiation contains comparatively longer wavelengths that can reach the earth's surface. This makes UV-B the most high-energy type of UV radiation of significance to living organisms on the earth's surface. UV-B is a highly active component of the solar radiation, making up only less than 1% of the total solar energy. It can cause potential damage to plant genomes by oxidative damage and crosslinks between DNA-DNA and DNA-protein, at least under high UV-B levels or high UV-B: PAR ratios or in plants with weak UV-B protection mechanisms (Ganguly & Duker, 1991; Gill et al., 2015; Rastogi et al., 2010). However, UV-B radiation is influenced by various abiotic factors i.e. thickness of the ozone layer, geographical area, season, altitude, latitude, cloud cover, and even time of the day (Jansen, 2017).

### 1.4 Effects of ionizing radiation on plant growth and development

The Chernobyl accident and Fukushima Dai-Ichi accident occurring in 1986 and 2011, respectively, are the two recent most devastating nuclear power plant accidents in human history. In both accidents, the released radioactive components were mostly composed of volatile radionuclides of noble gases, $^{137}$Cs, $^{131}$I, $^{90}$Sr, Zr, Tellurium etc. However, the amounts of refractory elements (including actinides) emitted in the course of the Chernobyl accident was approximately four magnitudes higher than during the Fukushima accident (Steinhauser et al., 2014). Acute irradiation has a major impact on forest ecosystem as well as plant growth and development.

The accident happened at the 4$^{th}$ block of Chernobyl Nuclear Power Plant (ChNPP) on April 26$^{th}$, 1986 and the near 30-km zone of the Chernobyl Exclusion Zone (ChEZ) was the most heavily contaminated with various radioactive materials (Kashparov et al., 2001, 2003) and

more than half of the original radioactive fallout was intercepted by the canopy of coniferous trees (Tikhomirov & Shcheglov, 1994). The coniferous tree species Scots pine is very prominent in this region. One month after the accident, the extremely high levels of acute radiation in the ChEZ had destroyed pine forests at close proximity to the source of release and resulted in sub-lethal and moderate damage zones at further distances. Four zones were identified with different radiation effects in the coniferous forests of the area around the ChNPP (Table 1) (Holiaka et al., 2020; Kozubov & Taskaev, 1994).

Table 1. Different zones and corresponding damage to coniferous forests (Scots pine and Norway spruce) in the area around the Chernobyl Nuclear Power Plant (ChNPP) (adopted from Kozubov & Taskaev, 1994).

| Zone | Basic effects | Dose rate[1] (mGy $h^{-1}$) |
|---|---|---|
| 1 | Coniferous death (4–6 $km^2$): complete death of pines, partial damage to deciduous trees | >4 |
| 2 | Sub-lethal effect (38 $km^2$): death of most growth points, death of some coniferous trees, morphological changes to deciduous trees | 2–4 |
| 3 | Medium damage (120 $km^2$): suppressed reproductive ability, dried needles, morphological changes | 0.4–2 |
| 4 | Minor damage: disturbances in growth, reproduction and morphology of coniferous trees | <0.2 |

Note: [1] Dose rate of gamma radiation at 1 m above the soil surfaces on June 1, 1986

A very high level of contamination of canopies of pine trees was caused within a 7 km radius of the ChNPP and eventually, those trees incurred lethal doses of radiation. The measured absorbed gamma dose amounted to 80–100 Gy in the needles of the dead pine trees (Kashparova et al., 2020). The first signs of radiation injury caused to Scots pine trees (*Pinus sylvestris* L) were yellowing and needle death. These trees were growing in close proximity to the reactor and the injury was visible within 2-3 weeks after the Chernobyl accident. The area of the radiation damage expanded up to 5 km in the west direction and up to 7 km in the north-northwest direction from the ChNPP unit no. 4 during the summer of the year 1986 (Kashparov et al., 2003; Kozubov et al., 1990). This small forest comprising an area of about 4 $km^2$ became known as “Red Forest” due to that the pine needles turned ginger-brown after

they died. This was the most readily observable effect of radiation damage on organisms in the area and is the best-known illustration of impacts of acute radiation on a forest ecosystem (Alexakhin et al., 2007; Beresford et al., 2020; IAEA, 2006).

The effects of radiation in higher plants are of concern to ecology, horticulture and agriculture. Many studies have reported the effects of ionizing radiation on plant growth and aberrations in the Chernobyl region. For example, Mousseau et al. (2013) reported substantial decreases in Scots pine growth rates living in contaminated areas. A dendrochronological analysis of 105 pine trees were done across the spectrum of radiation levels in the ChEZ. In their studies, they measured the growth rates of pine trees (which is easily measured in pine trees) using annual growth rings both before and after the Chernobyl accident in 1986. Their analysis using annual growth rings showed very prominent decreases in growth rates in the most radioactive areas for 3 years after the accident, which was followed by smaller decreases especially in years of drought. This was most likely due to the exposure of trees to extremely high doses at the time of the accident, and that the radiation level decreased dramatically over time (Mousseau & Møller, 2020). The effects of radiation have been demonstrated to be particularly harmful to Scots pine. In several studies, younger trees were found to be particularly vulnerable to the effects of radiation, with considerable alterations in growth and wood quality (Mousseau et al., 2013; Tulik & Rusin, 2005). Different field studies, including those conducted in Chernobyl and Fukushima, have found that conifer species in general are particularly sensitive to gamma radiation (Arkhipov et al., 1995; Watanabe et al., 2015; Woodwell, 1962; Woodwell & Rebuck, 1967; Yoschenko et al., 2018). Many of the pine trees in Chernobyl's most contaminated areas have undergone remarkable morphological alterations with unusual branching, indicating meristem damage shortly after the accident (Kozubov & Taskaev, 2002). Following the Fukushima disaster, Japanese red pine (*Pinus densiflora*) and Japanese fir (*Abies firma*) trees both revealed developmental abnormalities similar to those reported in Chernobyl (Watanabe et al., 2015; Yoschenko et al., 2016). This provides a strong support for the possibility that exposure to gamma radiation during growth was the causal factor associated with these developmental aberrations (Mousseau & Møller, 2020). At present, there is limited detailed information about the genetic and physiological mechanisms underlying these effects. During the initial period after the Chernobyl accident, Scots pine trees underwent several types of physiological and developmental changes including death of sprouts, dying needles, variability in needle length, dwarfed or even needles, necrosis of growth points, decreased reproductive capacity,

chromosomal aberrations and mutations in enzyme loci (Kozubov & Taskaev, 2002, 2007; Steinhauser et al., 2014; Zelena et al., 2005).

Studies of another conifer species Norway spruce (*Picea abie*s) also demonstrated alterations of a wide range of characters upon the Chernobyl accident. This, as well as other plant species in the Chernobyl zone showed different morphological abnormalities (Fesenko et al., 2005; Geras'kin et al., 2003, 2008; Geras'kin & Volkova, 2014; Kalchenko et al., 1993; Kozubov & Taskaev, 1994; Shevchenko et al., 1996; Shevchenko & Grinikh, 1995; Sorochinsky & Zelena, 2003). Pine seeds collected near the Chernobyl accident site were found to have abnormalities when compared to seeds collected from control sites (Kal'chenko & Fedotov, 2001). Increased mutations in persistently irradiated pines were found to be significantly related to levels of radiation exposure in more recent studies (Geras'kin & Volkova, 2014; Geras'kin et al., 2011; Makarenko et al., 2016). Such observations provide evidence that ionizing radiation has long-term impacts.

Effects of gamma radiation on growth have also been reported for other plants, including in studies under controlled conditions. For instance, Vandenhove et al. (2010) reported negative effect on growth but no apparent effect on oxidative stress pathways of different gamma dose rates ranging from 81-2336 μGy $h^{-1}$ for 24-54 days on the radio-resistant herbaceous plant *Arabidopsis thaliana*. Furthermore, Vanhoudt et al. (2014) found increased photosystem II (PSII) efficiency at gamma doses of 3.9 and 3.7 Gy, and maximum electron transportation rate ($ETR_{max}$) at 3.9, 6.7 and 14.8 Gy. *A. thaliana* also showed differences in gene expression when subjected to acute gamma radiation from external $^{60}Co$ exposure at 90,000 mGy $h^{-1}$ for 40 s with a total dose of 1 Gy and chronic gamma irradiation from internal $^{137}CsCl$ (about 24% of the total radiation) and external $^{60}Co$ (about 76%) at 2 mGy $h^{-1}$ for 21 days with a total dose of 0.93 Gy (Kovalchuk et al., 2007). Xie et al. (2019) reported a dose-rate dependent reduction in growth in aquatic macrophyte *Lemna minor* for different growth parameters such as frond number, frond size and frond weight at ≥ 24 mGy $h^{-1}$ after 7 days exposure to gamma radiation from an external $^{60}Co$ source under controlled conditions. A recent study of comparative sensitivity to gamma radiation among Norway spruce, Scots pine and *A. thaliana* showed an evident dose-rate dependent severe inhibition of shoot and root developmental parameters in two conifers to ≥ 40 mGy $h^{-1}$ after 144 h gamma exposure from an external $^{60}Co$ source under controlled laboratory conditions and also post-irradiation, whereas *A. thaliana* showed delayed lateral root formation after 144 h and 360 h gamma exposure to ≥ 400 mGy $h^{-1}$ and post-irradiation delayed development of flower buds and

inflorescence elongation (Blagojevic et al., 2019a). In their study, it is shown that the effect of the gamma irradiation on growth and development of these species was usually stronger post-irradiation than at the end of the 144 h gamma exposure. Another recent study by Blagojevic et al. (2019b) reported growth inhibition of Scots pine seedlings in response to the gamma dose rates of 42.9 and 125 mGy $h^{-1}$ in shoots and 125 mGy $h^{-1}$ in roots as a result of the effect of 144 h of gamma radiation on root or shoot elongation. However, growth parameters such as shoot elongation, number of needles and shoot diameter were negatively affected post-irradiation by 20 mGy $h^{-1}$ in those seedlings. Gamma radiation results in dose-dependent changes in plant growth and development by inducing the production of harmful free radicals in cells, which leads to the damage of cellular nucleic acids, proteins and membrane-lipids (Kovács & Keresztes, 2002).

### 1.5 Characteristics and biology of Scots pine as conifer species

Conifers are a group of cone-bearing seed plants that cover around 39% of the world forests. It is the most dispersed group of gymnosperms with 600-630 species in 69 genera (Armenise et al., 2012; De La Torre et al., 2014; Wang & Ran, 2014). Conifers are well characterized by a long juvenile period, long life span and high heterozygosity. They are pollinated by wind and are the dominant plants over large areas of land; most notably the temperate zone taiga forests of the northern hemisphere (Campbell, 2005; De La Torre et al., 2014; Mackay et al., 2012). In those ecosystems, conifer species play a significant role in global carbon cycle. They are widely used in reforestation and are vital for prevention of soil erosion (Mackay et al., 2012). The pine family (*Pinaceae*) with its 11 genera includes a wide range of important forest trees such as different pines (*Pinus*), spruces (*Picea*), firs (*Abies*) and Douglas fir (*Pseudotsuga*). Scots pine (*Pinus sylvestris*) is an evergreen conifer tree that grows up to 35 m (Rushforth, 1986) in height and 1 m trunk diameter at maturation. However, on very productive sites, it can grow exceptionally over 45 m tall and 1.7 m trunk diameter (Marinich & Powell, 2017).

The forestry and evolutionary studies of Scots pine have a long history of fundamental and practical research. Its adaptive variation patterns and function in forest economics and ecological systems have been researched for about 275 years and its detailed demography and mating system have been studied for a century and more than 50 years, respectively. However, the reference genome sequence of Scots pine is not yet available and its genomic

studies have also been lagging compared to, for instance, two other economically important conifers Norway spruce (*Picea abis*) and loblolly pine (*Pinus taeda*) (Pyhäjärvi et al., 2020).

Compared to the herbaceous model plant *A. thaliana* (which has the genome size of approximately 135 Mbp with 25,498 genes (2n = 10 chromosomes) (The Arabidopsis Genome, 2000), conifers have a large genome size. For instance, the recently sequenced genome of Norway spruce has an estimated genome size of 19.6 Gbp and the information about the total number of genes and its full-length sequences are still incomplete due to its large genome size, but around 66,000 genes has been estimated (De La Torre et al., 2014; Nystedt et al., 2013).

The first sequenced genome of any pine species was loblolly pine (*Pinus taeda*) (2n = 24 chromosomes) which has a 20.1 Gbp genome size (NCBI, 2019; Neale et al., 2014; Wegrzyn et al., 2014; Zimin et al., 2014). Although many studies are ongoing and a draft sequence has been proposed, the complete sequence of Scots pine is yet to be published. Bennett & Leitch (2012) reported a large genome size of Scots pine with $22 \times 10^9$ bp. However, on the basis of the closely related loblolly pine reference genome, it has been estimated that only approximately 0.2% of Scots pine genome consists of protein coding regions (Wegrzyn et al., 2014). Like loblolly pine, Scots pine also has 24 chromosomes (NCBI, 2019). *Pinus* genomes feature high repetitive content, remarkably long introns (Stival Sena et al., 2014), large gene families, and perhaps over 50,000 genes (Stevens et al., 2016; Wegrzyn et al., 2014).

### 1.6 DNA damage

DNA damage is a type of error that creates abnormal chemical structure in DNA. It causes alterations in the structure of the genetic material, preventing the replication mechanism from functioning properly. DNA damage occurs naturally in living organisms, but it can also be caused by a range of external genotoxic agents such as UV radiation, ionizing radiation, and chemical mutagens (Manova & Gruszka, 2015). In humans, mitochondrial DNA is more sensitive to oxidative stress than nuclear DNA. This is due to the lack of chromatin organization in mitochondria and lower mitochondrial DNA repair activities (Yakes & Van Houten, 1997).

Overproduction of ROS may lead to DNA damage. ROS generation can occur as a by-product of cellular metabolic activities or due to abiotic stress such as UV light. DNA

damage includes single strand DNA (ssDNA) breaks (SDB) or double strand DNA (dsDNA) breaks (DSB), loss or modification of a base to form an abasic site or a miscoding or noncoding lesion or breakage of the DNA sugar-phosphate backbone (Manova & Gruszka, 2015; Singh et al., 2010; Vonarx et al., 1998). Plant genome instability, reduced growth, development, and productivity, as well as the organism's immediate survival, may occur from the accumulation of mutations induced by such damages (Biedermann et al., 2011; Gill & Tuteja, 2010; Singh et al., 2010; Tuteja et al., 2001; Waterworth et al., 2011). Thus, to preserve the plant genome stability, it is essential to reduce the risk of permanent genetic modifications/alterations by efficient DNA repair involving detection of DNA damage, removal of damaged nucleotides and replacement of undamaged nucleotides via DNA synthesis (Gill & Tuteja, 2010; Roy et al., 2009; Waterworth et al., 2011). Plants need light to grow photo-autotrophically, but exposure to UV radiation induces DNA photoproducts. The most common DNA photoproducts induced by exposure to UV light are cyclobutane-type pyrimidine dimers (CPDs) and the pyrimidine (6, 4) pyrimidone dimers (Hutchinson et al., 1988), while gamma radiation induces 8-oxoguanine (8-Oxo-G), 6-O-methylquanine ($O^6$meG) and N3-methyladenine ($N^3$MeA) to form DNA lesions. Apart from inducing the DNA photoproducts, UV exposure and gamma radiation may induce DNA-protein cross-links, DNA strand breaks, and insertion or deletion of base pairs (Esnault et al., 2010; Kim et al., 2004; Kovács & Keresztes, 2002; Kovalchuk et al., 2007; Manova & Gruszka, 2015; Vandenhove et al., 2010; Wi et al., 2005).

### 1.7 DNA repair

Despite the high frequency of DNA damage in plant cells, the estimated mutation rate is very low. The genome-wide average mutation rate was calculated to be roughly $7 \times 10^{-9}$ per site per generation using whole genome sequencing of *A. thaliana* lines propagated from a single seed descendant for 25–30 generations (Ossowski et al., 2010; Weng et al., 2019). This indicates less than one single mutation in the entire genome per generation, and the mutation rate is at least 10 times lower than the error rate of the replication machinery for a single cell cycle and provides strong evidence of how efficiently DNA damage is detected and further repaired in the cells (Nisa et al., 2019). DNA damage can be repaired through multiple pathways, although the action of the repair system is influenced by the type of cell, its proliferative condition, the phase of the cell cycle, type of damage/lesion, and its genomic context (Britt, 1999; Manova & Gruszka, 2015).

The majority of lesions, including UV-induced CPDs, mismatches, and so on, are detected and repaired by specialized machinery such as photolyases or complexes involved in Mismatch Repair (MMR), Base Excision Repair (BER) or Nucleotide Excision Repair (NER) (Jackson & Bartek, 2009; Manova & Gruszka, 2015; Spampinato, 2017). If not repaired properly, such lesions might hamper DNA replication or create DSBs, which require particular DNA repair pathways such as Non-homologous End Joining (NHEJ) or Homologous Recombination (HR) (Amiard et al., 2013). In this case, a complex signaling pathway known as the DNA Damage Response (DDR) allow the activation of cell cycle checkpoints and of particular DNA repair mechanisms (Hu et al., 2016; Yoshiyama et al., 2013).

In animals, the activation of DDR depends on two protein kinases including Ataxia Telangiectasia Mutated (ATM) and Ataxia Telangiectasia Mutated Rad3-related (ATR) (Maréchal & Zou, 2013). Both of these protein kinases belong to the phosphatidylinositol 3-kinase-like family. ATM primarily responds to double strand break-inducing factors, whereas ATR is sensitive to replication stress and is activated by single stranded DNA and defects in replication fork progression (Maréchal & Zou, 2013). Both of the ATM and ATR proteins activate downstream components of DDR signaling pathway. In *A. thaliana*, the homologues of ATM and ATR have been isolated and *atm* and *atr* mutants characterized (Culligan et al., 2004; Garcia et al., 2003). Both the *atm* and *atr* mutants are hypersensitive to DNA DSBs induced by γ-irradiation and only *atr* is involved in replicative stress response (Culligan et al., 2006).

An overview of current knowledge of the plant DDR signaling is summarized in Figure 3. ATM and ATR recognize different types of lesions and are activated through different mechanisms. Plant ATM recognizes DSBs and is activated by the MRN (MRE11, RAD50 and NBS1) complex (Amiard et al., 2010; Puizina et al., 2004; Waterworth et al., 2007). ATR is recruited to single stranded DNA by Replication Protein A (RPA) through ATRIP (ATR Interacting Protein) and activated by a number of factors including 9-1-1 and RAD17/RFC complexes (Saldivar et al., 2017). DNA polymerase ε (pol ε) can also activate the ATR through an unknown mechanism (García-Rodríguez et al., 2015). The ATM/ATR signaling converges to the SUPPRESSOR OF GAMMA-RESPONSE 1 (SOG1) transcription factor. SOG1 is the central regulator of the plant DDR that belongs to the NAC (NAM, ATAF1/2, and CUC2) family (Yoshiyama et al., 2009). It controls the expression of numerous genes involved in cell cycle regulation, cell death control and DNA repair (Nisa et al., 2019). DNA

repair is also controlled via E2Fa/RBR complexes by regulating DNA repair genes. The E2Fa/RBR complexes also recruit *RADIATION 51* (*RAD51*) and *BREAST CANCER SUSCEPTIBILITY 1* (*BRCA1*) at the DNA damage sites. However, the function of E2Fa/RBR complexes in plant DDR depends on ATM/ATR and CYCB1/CDKB activity (Nisa et al., 2019).

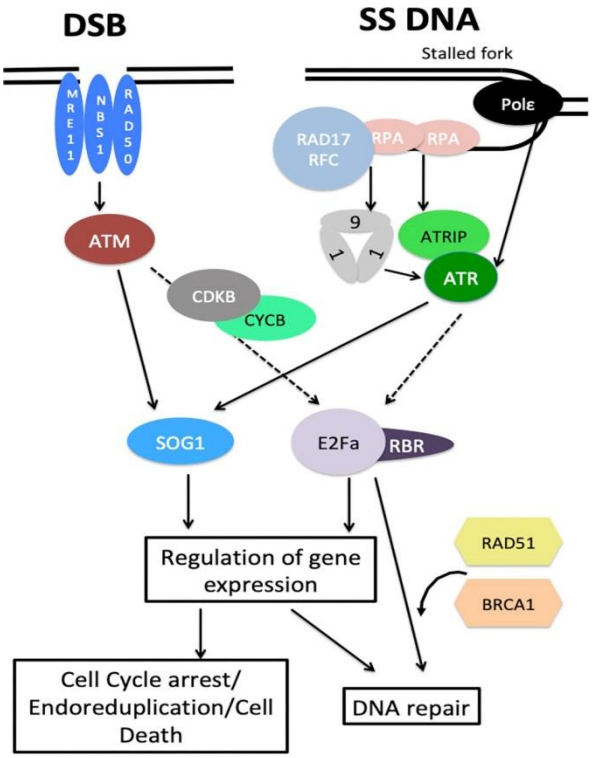


Figure 3. Overview of the plant DNA Damage Response (DDR) (Nisha et al., 2019). ATM recognizes DNA double strand breaks (DSBs) and is activated by the MRN (MRE11, RAD50, and NBS1) complex, whereas RPA proteins recruits ATR to single stranded DNA through ATRIP. ATR is activated by the 9-1-1, RAD17/RFC complexes and DNA polymerase ε (pol ε). Pol ε activates ATR via an unknown mechanism. Both ATM and ATR converge to SOG1 that controls the expression of numerous genes involved in cell cycle regulation, apoptosis and DNA repair. E2Fa/RBR complexes also control DNA repair by modulating DNA repair genes which recruit *RAD51* and *BRCA1* at DNA damage sites. In DDR, the role of E2Fa/RBR complexes depends on CYCB1/CDKB and ATM/ATR activity, but the exact molecular mechanisms are unknown. Dashed arrows represent putative/possibly indirect regulations.

Upon exposure to acute or chronic irradiation, plants exhibit different gene expression responses depending on the duration and level of exposure (Kovalchuk et al., 1999, 2007). The *RAD51* gene induced by gamma radiation is involved in the homologous recombination (HR) DNA repair mechanism (Yoshiyama et al., 2013). The ATM/ATR signaling pathways recruits the accumulation of a phosphorylated histone variant γH2AX at the DNA damage

sites in response to irradiation-induced DSBs (Amiard et al., 2010; Friesner et al., 2005). In *A. thaliana*, several genes including *KU70*, *KU80I*, *DNA LIGASE IV* (*LIGIV*), *BRCA1* and *HOMOLOG OF X-RAY REPAIR CROSS COMPLEMENTING 4* (*XRCC4*) showed upregulation in gene expression after gamma exposure. All these genes encode proteins that are required for the initiation and completion of the NHEJ DNA repair mechanism (Bleuyard et al., 2005; Doutriaux et al., 1998; Lafarge & Montané, 2003; Tamura et al., 2002; West et al., 2000).

Several genes encoding proteins involved in homologous recombination (HR), for example *BRCA1*, *BRCA2*, *RAD51*-like, *RAD51B*, *RAD5C*, *XRCC2*, *XRCC3*, *MEIOTIC RECOMBINATION 11* (*MRE11*) and the genes of the regulatory proteins *BRCA1* and *BRCA2* showed induced gene expression in particular plant species following gamma exposure. Similar gamma-induced DNA repair has also been reported in the woody angiosperm species *Populus nigra* where the expression of *RAD51*, *LIG4*, *KU70*, *XRCC4* and *PROLIFERATING CELLULAR NUCLEAR ANTIGEN* (*PCNA*) genes were increased upon gamma exposure (Bleuyard et al., 2005; McIlwraith et al., 2000). Moreover, SOG1 modulate multiple genes in the DNA repair pathway through DDR signaling, which sequentially activate canonical pathways involved in DNA repair, apoptosis and endoreduplication (Yoshiyama et al., 2013).

### 1.8 Cell cycle regulation in response to DNA damage

The DNA damage sites produce biochemical signals that activate checkpoints which are responsible for delay in cell cycle progression. Checkpoints are necessary for plants to accommodate time for adequate DNA repair. The replication of damaged DNA is stopped at the checkpoint in the G1/S and S stages, while the checkpoint in the G2/M stage stops chromosome segregation (Belli et al., 2002). If DNA damage cannot be repaired, checkpoints attempt to destroy severely damaged cells by causing irreversible cell cycle arrest or cell death (apoptosis). The ATR protein is necessary for the G2-phase checkpoint as it activates cell-cycle checkpoints and induces cell cycle arrest to give time for proper DNA repair in response to DNA damage (Culligan et al., 2004). The SOG1 protein has been suggested to be a central transcription factor in genomic stress and responsible for inducing cell-cycle checkpoint genes and γ-induced short-term transcriptional changes of multiple genes (Yoshiyama et al., 2009, 2013). The cell-cycle checkpoints target the cyclin (CYC)/cyclin-dependent kinase (CDK)-complex that generally promotes cell cycle progression (Deckbar et

al., 2011). SOG1 directly regulate the genes encoding plant-specific B1-type cyclins (CYCB1s) and B1-type CDKs (CDKB1s). These are suggested to be major regulators of HR in plants (Weimer et al., 2016). For example, *CYCB1;1* was upregulated in response to DNA damage-inducing chemicals (Adachi et al., 2011; Chen et al., 2003; Culligan et al., 2004, 2006; Ricaud et al., 2007). Furthermore, in cell cycle arrest, SOG1 is involved together with a protein encoded by the *WEE1 KINASE HOMOLOG* (*WEE1*) gene which showed upregulation in *A. thaliana* following gamma exposure (De Schutter et al., 2007). However, specific cell cycle genes in *A. thaliana* such as *CYCB1;1* and *CDKB2;1* were induced and suppressed respectively, 1.5 h after exposure to 100 Gy (2 days of irradiation) of gamma radiation (Culligan et al., 2006; Yoshiyama et al., 2009).

### 1.9 Antioxidants in plants

Upon exposure to ionizing radiation plants experience indirect damage, which is caused by formation of ROS such as such as hydroxyl radical (•OH), hydrogen peroxide ($H_2O_2$), superoxide anion ($O_2•^-$) and singlet oxygen ($^1O_2$), which are generated by water radiolysis and thus lead to oxidative stress (Esnault et al., 2010; Desouky et al., 2015; Gill & Tuteja, 2010; Kovács & Keresztes, 2002; Luckey, 2006; Miller & Miller, 1987; Quintiliani, 1986). The highly reactive hydroxyl radical (•OH) can quickly oxidize cell macromolecules causing DNA damage, protein oxidation, and lipid peroxidation (Esnault et al., 2010; Gill & Tuteja, 2010). Cells undergo oxidative stress when a severe imbalance exists within ROS formation and antioxidant defense (Ahmad et al., 2010).

Plants modulate their own antioxidant defense systems to scavenge ROS under oxidative stress conditions. Plants utilize two types of antioxidant machineries i.e. enzymatic and non-enzymatic antioxidants to scavenge ROS. The enzymatic machinery includes antioxidant enzymes such as ascorbate peroxidase (APX), catalase (CAT), peroxidase (POD), and superoxide dismutase (SOD), whereas the non-enzymatic machinery comprises antioxidant metabolites such as ascorbate and glutathione or phytochemicals such as anthocyanins, carotenoids, and phenolic compounds (Gill & Tuteja, 2010; Hong et al., 2018; Roldán-Arjona & Ariza, 2009).

SOD plays a defense role by converting superoxide anion into $H_2O_2$ when plant is subjected to gamma radiation (Gill & Tuteja, 2010). In *A. thaliana*, enhanced SOD and APX capacities but reduced activities of CAT, syringaldazine peroxidase (SPX) and guaiacol peroxidase

(GPX) were observed on the subcellular level in roots under gamma irradiation, while leaves expressed simply increased level of GPX (Vanhoudt et al., 2014). CAT and POD also perform important roles in cellular detoxification of $H_2O_2$ and therefore protect cellular components like lipids and proteins from oxidation (Wi et al., 2007). Previous studies reported POD induction in pumpkin cells upon gamma exposure, while POD, APX, CAT and SOD capacities were induced due to gamma irradiation (Kim et al., 2011; Van Hoeck et al., 2015). A significant change in CAT activity was found in the freshwater duckweed *L. minor* upon 7 days exposure to gamma radiation at a dose rate of 27 mGy $h^{-1}$ (Van Hoeck et al., 2015). Volkova (2017) reported no significant changes in the activities of SOD, CAT and POD in Scots pine under the natural background dose rates in the range of 0.03 - 38.6 mGy $year^{-1}$ and suggested that this range of dose rates is insufficient to induce any essential biological effect.

### 1.10 Quantitative Real Time Polymerase Chain Reaction (qRT-PCR)

A real-time polymerase chain reaction (real-time PCR) is a molecular biology technique that uses the polymerase chain reaction (PCR). It tracks the amplification of a specific DNA molecule during the PCR (in real-time), rather than at the end, as in traditional PCR. Real-time PCR can be employed quantitatively (quantitative real-time PCR) or semi-quantitatively (number of DNA molecules above/below a given threshold) (semi-quantitative real-time PCR). According to the Minimum Information for Publication of Quantitative Real-Time PCR Experiments (MIQE) recommendations, quantitative real-time PCR should be abbreviated as qPCR, while reverse transcription–qPCR should be abbreviated RT-qPCR (Bustin et al., 2009). The qPCR method detects a fluorescent DNA stain, such as SYBR Green, and measures the amplification of the target DNA during each PCR cycle. The fluorescence level grows to a detectable point during the log-linear phase of magnification, which is known as the threshold cycle (CT). Thus, the qPCR results include amplification; standard curves log concentration vs CT, which are plotted using serial dilutions of a known magnitude of standard DNA, and this standard curve can identify the quantity of DNA or complementary DNA (cDNA) in an unknown specimen as a CT value (Singh et al., 2014). The fact that qPCR combines amplification and detection into a single step, eliminates the need for any post-amplification processing of the targeted DNA (Mackay, 2004). Several types of polymerases, including high precision, hot start, and enzymes with high and rapid activity, are used to assist various types of qPCR processes. qPCR machines are designed to

carry out these reactions, which include a thermal cycler for DNA amplification, an optical environment to stimulate fluorophores and capture generated fluorescence from the detection chemistry, and special software to collect and analyze the quantitative data emitted. The most important benefit of qPCR is that it has a low level of contamination from PCR products like cDNA and RNA. However, this technique has certain drawbacks, such as the high cost of reagents. This approach is a very sensitive procedure, and knowing the experimental design is critical for precise and valuable results (Wong & Medrano, 2005). In comparison to the conventional PCR process, qPCR is preferred over endpoint PCR for several reasons, including the ability to amplify short DNA fragments, the ability of fluorescent detection, which allows the detection of minor amounts of amplified products, and increased tolerance to inhibit materials interfering with DNA purification. Furthermore, with qPCR equipment, operating as a single process helps minimize post-PCR contamination leading to false-positive results. Lastly, the absence of a gel electrophoresis step in qPCR makes the process simple to automate and ideal for use in a variety of applications (Ravnikar et al., 2016).

## 2. Aims and specific objectives of this study

It may be hypothesized that plants grown under elevated, non-lethal ionizing radiation may have better adaptability for radiation compared to plants grown in natural background radiation. Moreover, it is speculated that seeds from such plants might be epigenetically primed to make the seedlings grown from them more radioresistant. In our study, Scots pine seeds were obtained from three different areas in the Chernobyl region with background (CON), intermediate (INT) and high (TR22) levels of ionizing radiation (described in Materials and methods) and seedlings grown from those seeds were exposed to gamma radiation dose rates ranging from 0 to 100 mGy $h^{-1}$ in controlled laboratory conditions for 144 h. The overall aim of this work was to study whether Scots pine seedlings grown from seeds developed under different levels of ionizing radiation in the Chernobyl area show any differences in radiosensitivity.

The specific objectives in this respect were to study effects of the 144 h of gamma radiation 7-12 days after sowing on the following traits in gamma-irradiated CON, INT and TR22 seedlings:

- The root length and shoot length at the end of the irradiation.
- Post-irradiation growth parameters in time courses of about one month, i.e. cumulative shoot elongation, number of needles and shoot diameter.
- DNA damage at the end of the irradiation and post-irradiation.
- Total antioxidant capacity at the end of the irradiation.
- The relative transcript levels of specific cell division controlling genes (*CYCKB1;1* (*CYC = CYCLIN*), *CDKB1;2* (*CDK = CYCLIN-DEPENDENT KINASE*)) and DNA repair genes (*RADIATION 51* (*RAD51*), *SUPPRESSOR OF GAMMA RESPONSE 1* (*SOG1*)) in shoots at the end of the irradiation.

# 3. Materials and methods

## 3.1 Sampling sites description and plant materials

Scots pine (*Pinus sylvestris* L) was used as plant material throughout this study. Cones of Scots pine were collected from three different locations in the Chernobyl Exclusion Zone (ChEZ), Ukraine, based on their level of ionizing radiation due to different levels of radionuclide contamination (Figure 4) and eventually seeds were extracted from cones by drying in a lab oven at 45°C for 2 days (Figure 5). The sampling locations were all in open-air areas (forest edges, meadows), had the same sod-podzolic sandy soil type and similar forest conditions (illumination, moistures, etc). The geographical coordinates of each sampling site were determined by a GPSmap 78s receiver (Garmin, USA).

The sampling site Near Trench 22 of the Red forest is located approximately 2 km west-southwest of the Chernobyl Nuclear Power Plant (ChNPP) in the Red forest radioactive waste area (Table 2) (Kashparov et al., 2012). Seeds extracted from cones were collected from two trees, on the site Near Trench 22 of Red forest (Figure 4; Table 2). After the ChNPP accident, radioactive materials, including radioactively contaminated pine trees (and possibly some other vegetation remnants), topsoil layer and forest litter, were bulldozed into trenches or under the embankment, made of the local sandy soil. Having done this, the cleared territory was covered by a shielding of 30–50 cm thick relatively "clean" soil cover layer (from the sandy soil excavated while digging the trenches). The sampled trees are approximately 30 m away from the Trench 22. The average values of $^{137}$Cs and $^{90}$Sr activity concentrations, measured in the radioactive materials in Trench 22 (around which the sampled trees were selected), were 280 ± 110 kBq kg$^{-1}$ and 135 ± 53 kBq kg$^{-1}$, respectively (Kashparova et al., 2020). Moreover, the $^{137}$Cs and $^{90}$Sr activity concentrations, measured in the seeds from the site Near Trench 22 were 40 ± 4 kBq kg$^{-1}$ and 71.5 ± 5.3 kBq kg$^{-1}$ (n = 305), respectively (Table 2). Seeds from the site Near Trench 22 of the Red forest were used as high radiation type seeds where the dose rate in the air 1 m above the ground was about 12 mGy h$^{-1}$.

The sampling site Near Lake Glubokoye is located approximately 4 km north-northeast of the ChNPP. Seeds extracted from cones of Scots pine were collected from two trees in the site Near lake Glubokoye (Figure 4; Table 2). The activity concentrations of $^{137}$Cs and $^{90}$Sr, measured in the seeds from the site Near Lake Glubokoye were 10.5 ± 1 kBq kg$^{-1}$ and 23.9 ± 1.9 kBq kg$^{-1}$ (n = 248), respectively (Table 2). Seeds from the site Near Lake Glubokoye

were used as intermediate radiation level seeds where the absorbed dose rate in the air at a height of 1 m above the ground was about 3 mGy $h^{-1}$.

The reference sampling site is situated approximately 55 km south-southwest of the ChNPP near the town Ivankiv. Seeds were collected from the Ivankiv forestry, where the radioactive contamination is evenly distributed, and is significantly lower than within the ChEZ. The activity concentrations of radionuclides (i.e. $^{137}Cs$ and $^{90}Sr$) in the seeds from this site were lower than the minimum detectable level. All trees at this sampling site were artificially planted in rows after the Chernobyl accident. The absorbed dose rate in the air at a height of 1 m above the ground at this site was about 0.1 μGy $h^{-1}$ and corresponds to the level of natural background radiation (Kashparova et al., 2020) (Figure 4; Table 2). Seeds from this site were used as control type of seeds.

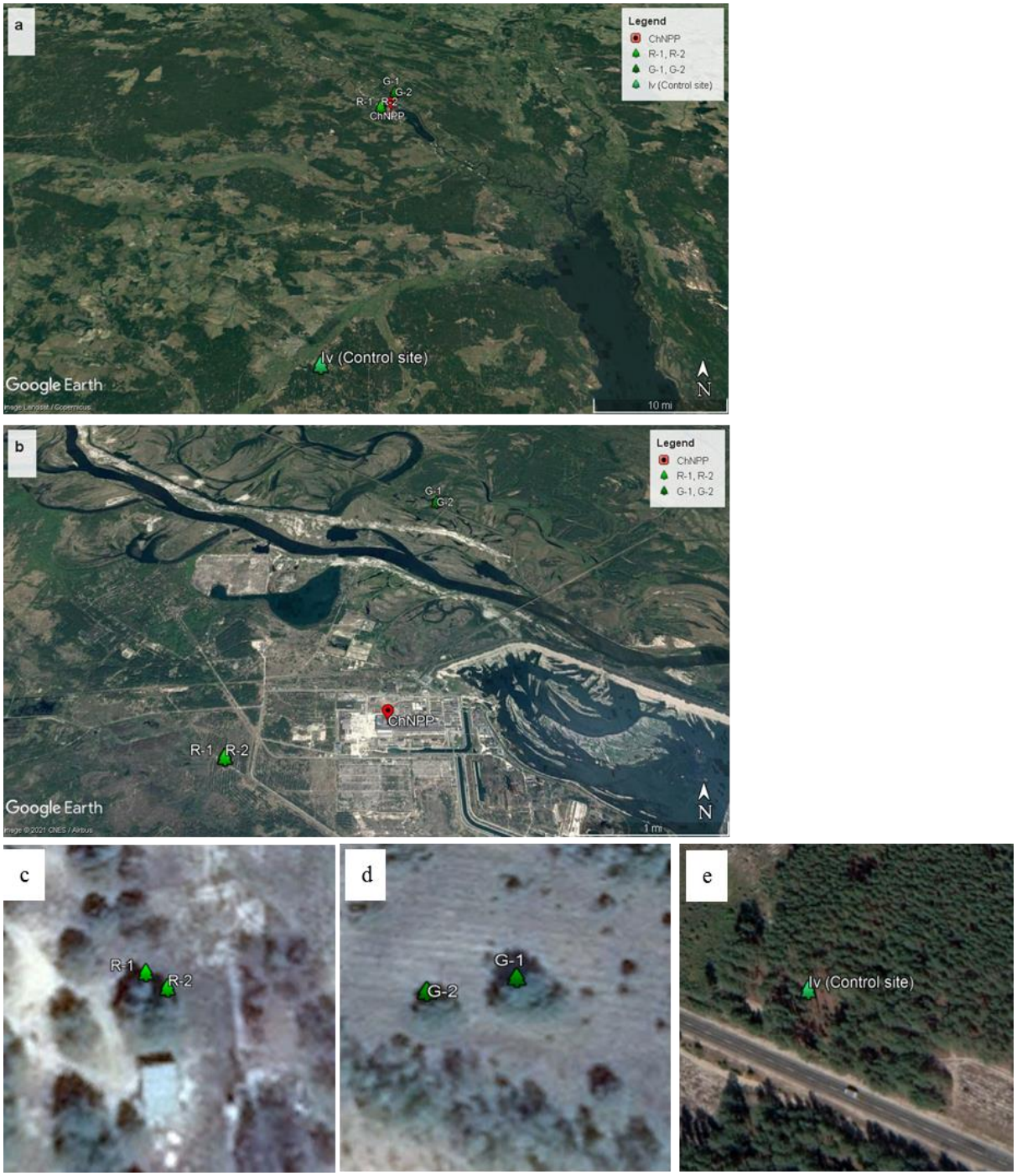


Figure 4. Overview of the seed sampling sites in the Chernobyl Exclusion Zone (ChEZ) based on their level of ionizing radiation; Near Trench 22 of Red forest (R site; denoted TR22 in this thesis), Near Lake Glubokoye (G site; denoted INT in this thesis) and Ivankiv forestry (Iv-Control site; denoted CON in this thesis). Seeds were collected from two trees on the sites Near Trench 22 of Red forest (R-1 and R-2), Near Lake Glubokoye (G-1 and G-2). a) The three individual seed collection sites and the Chernobyl Nuclear Power Plant (ChNPP). b) A zoom-in of the positions of the two trees in the site Near Trench 22 of Red forest (R-1 and R-2) and the Near Lake Glubokoye (G-1 and G-2). c), d) and e) Close-up views of the three seed collection sites.

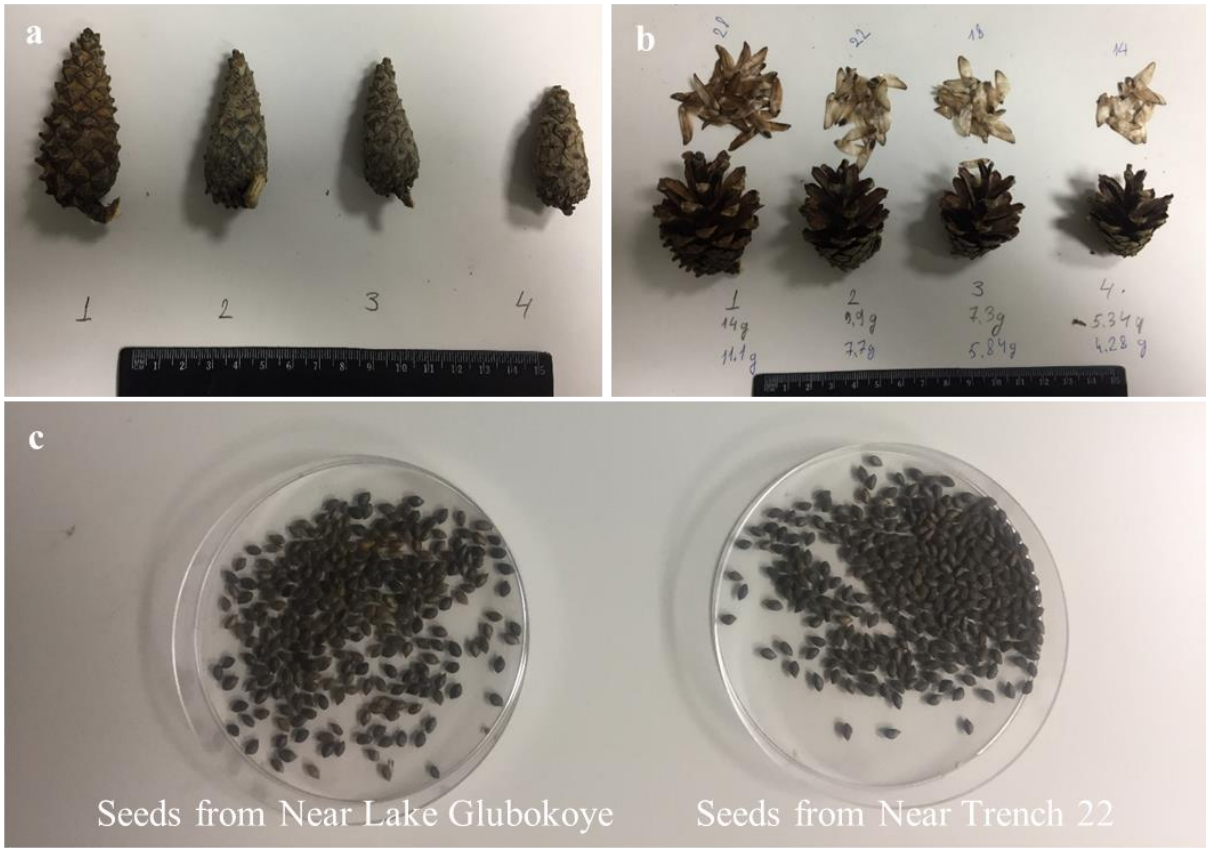


Figure 5. Cones and seeds of Scots pine collected in the Chernobyl nuclear power plant (CNPP) area. a) and b) The cones before and after drying. c) The extracted seeds from the location Near Lake Glubokoye and Near Trench 22 of the Red forest. The absorbed dose rate of these sites was about 3 and 12 mGy $h^{-1}$ respectively, in the air at a height of 1 m above the ground.

Although all the experimental sites in this study have the same sod-podzolic sandy soil type, the soil conditions for particular trees vary slightly. The trenches of the Red forest have the most fertile environment. However, in general, all other environmental conditions at different sampling sites are very similar except the absorbed radiation dose rates (Yoschenko et al., 2011). For convenience, the control, intermediate and high radiation type seeds (based on their radiation level) collected from the site Ivankiv forestry, Near Lake Glubokoye and Near Trench 22 of Red forest were termed as CON, INT and TR22, respectively, throughout this study. The seeds from these different trees at each of the sites were pooled before being transported to the Norwegian University of Life Sciences, Ås, Norway.

Table 2. Overview of the sampling sites and activity concentrations of the Scots pine seeds collected in the Chernobyl Nuclear Power Plant (ChNPP) area (mean ± SD shown for dose rate and activity concentration).

| Site | | Sample name termed in this study based on seed collection site | Distance and direction from the ChNPP | Coordinates of pine tree | | Average external dose rate in air 1 m (mGy $h^{-1}$) | Activity concentration (kBq $kg^{-1}$) | |
|---|---|---|---|---|---|---|---|---|
| | | | | N | E | | $^{137}Cs$ | $^{90}Sr$ |
| R | Near Trench 22 of **R**ed forest, pine tree No. 1 | TR22 | 1.955 km, 253.54° | 51.384188 | 30.072432 | 12 ± 1 | 40 ± 4 | 71.5 ± 5.3 |
| | Near Trench 22 of **R**ed forest, pine tree No. 2 | | 1.9513 km, 253.40° | 51.384155 | 30.072504 | | | |
| G | Near lake **G**lubokoye, pine tree No. 1 | INT | 4.2226 km, 12.44° | 51.426239 | 30.112559 | 3 ± 1 | 10.5 ± 1 | 23.9 ± 1.9 |
| | Near lake **G**lubokoye, pine tree No. 2 | | 4.2168 km, 12.25° | 51.426216 | 30.112340 | | | |
| Iv | Ivankiv forestry | CON | 55.4701 km, 190.62° | 50.898991 | 29.952973 | 0.0001 | <LoQ | <LoQ |

LoQ = Limit of Quantification

### 3.2 Seed sterilization and pre-growing conditions

Approximately 300-350 seeds of CON, INT and TR22 seeds were taken into 50 ml plastic centrifuge tube. For surface sterilization of the seeds, 1% Sodium hypochlorite (NaOCl) was added to each tube and kept for 5 minutes. Gentle mixing and shaking were done by turning the tubes upside down 2-3 times. NaOCl was then removed by a pipette and the seeds were rinsed with autoclaved distilled water. The CON, INT and TR22 seeds were rinsed 9, 12 and 16 times respectively, with distilled water to ensure the removal of brownish/yellowish color at the end of the washing. The seeds were then placed on autoclaved filter paper to dry for 45 minutes to ensure that the seeds were dried completely prior to the next step. The dried seeds were then evenly sown on ½ MS medium ((Murashige & Skoog, 1962); Duchefa Biochemie B.V., Haarlem, The Netherlands, Product code M0221.0050)) with 0.8% agar (Plant agar, A1296-1KG, Sigma-Aldrich, St Louis, MO, USA) in 50 mm diameter Petri dishes (ThermoFisher Scientific, USA). About 30-35 seeds were sown per Petri dish and the germination rate was approximately 50–60%. The pH of the ½ MS medium was maintained to 5.6. The seed sterilization was done in a clean laminar air flow bench. Thereafter, the seeds were kept for germination in a growth chamber for 6 days at 20°C under a photosynthetic photon flux density (PPFD) of 30 μmol $m^{-2}$ $s^{-1}$ at 400–700 nm (TL-D 58 W/840 lamps, Philips, Eindhoven, The Netherlands) in a 16 h photoperiod. The irradiance was measured at the top of the Petri dishes with a Li-Cor Quantum/Radiometer/Photometer (model LI-250, LI-COR, Lincoln, Nebraska, USA).

### 3.3 Gamma irradiation of seedlings using a $^{60}$Co source and growing conditions during the exposure

Petri dishes with six days old seedlings from CON, INT and TR22 type seeds were carried in a box to the FIGARO low dose gamma irradiation facility ($^{60}$Co source; 1173.2 and 1332.5 keV γ-rays) at the Norwegian University of Life Sciences, Ås, Norway (Lind et al., 2019). The Petri dishes with the seedlings were then exposed to gamma radiation with different gamma dose rates ranging from 1 to 100 mGy $h^{-1}$ for 144 h 7-12 days after sowing (Figure 6; Table 3) and the seedlings were grown in the Petri dishes during the entire gamma exposure period. The Petri dishes with seedlings were placed in two rows in front of the collimator. The Petri dishes were rotated 180° in the middle of each experiment to reduce dose variability between irradiated samples and thus to ensure more even irradiance and gamma radiation. The gamma exposure experiment was repeated five times in total. The first three

experiments were performed during January 2020 and February 2020 whereas the last two gamma exposure experiments were carried out during November 2020. The room temperature was set at 20˚C ± 1°C with a 12 h photoperiod during the gamma exposure. The photon flux density during the gamma exposure was measured to 45 μmol $m^{-2}$ $s^{-1}$ and 40 μmol $m^{-2}$ $s^{-1}$ (400 - 700 nm) for the first three experiments and last two experiments, respectively, and was provided by high pressure metal halide lamps (HPI-T Plus 250 W lamps, Philips, Eindhoven, The Netherlands) mounted above the Petri dishes. The irradiance was measured with the Li-Cor Quantum/Radiometer/Photometer described above. The red:far red (R:FR) ratio for the first three experiments and last two experiments were 2.7 and 2.2 respectively and measured by a 660/730 nm Skye sensor (Skye Instruments, Powys, Wales, UK). Furthermore, Petri dishes with CON, INT and TR22 type seedlings were placed behind lead walls outside the radiation sector in the same room and were used as unexposed control samples (0 mGy $h^{-1}$) (Figure 6). The unexposed samples were kept under the same light and temperature conditions as the gamma irradiated seedlings.

For dosimetry of the seedlings exposed to gamma radiation, an established protocol was followed (Hansen et al., 2019). Petri dishes with the CON, INT and T22 type seedlings were positioned at different distances from the gamma radiation source to obtain the nominal dose rates to water 1, 10, 20, 40 and 100 mGy $h^{-1}$ and total dose rates presented in Table 3. The dose rates to water in the center of the Petri dishes were estimated according to Hansen et al. (2019) and used as a proxy for dose rates to the seedlings. To confirm calculated dose rates at different positions, actual air kerma rates for each position were obtained from 4 nanodot dosimeter measurements per position (MicroStar, Landauer Inc. Greenwood, IL, USA). Total doses (0.14-14.4 Gy; Table 3) were calculated from the estimated absorbed dose rates to water, multiplied by total exposure time (144 h).

Table 3. The gamma radiation dose rates and total doses applied in experiments with exposure of Scots pine seedlings for 144 h at day 7-12 after sowing, using a $^{60}Co$ source. The seedlings were grown from seeds obtained from different areas in the Chernobyl region with background (CON), intermediate (INT) and high (TR22) levels of ionizing radiation.

| Dose rate (mGy $h^{-1}$) | Total dose (Gy) after 144 h exposure |
|---|---|
| 100 | 14.4 |
| 40 | 5.8 |
| 20 | 2.9 |
| 10 | 1.4 |
| 1 | 0.14 |
| 0 | 0 |


Figure 6. Gamma radiation exposure experiment set-up at the FIGARO low dose gamma irradiation facility. Petri dishes with six days old seedlings that were grown from seeds obtained from different areas in the Chernobyl region with background (CON), intermediate (INT) and high (TR22) levels of ionizing radiation (see Table 2) and the seedlings were exposed to gamma radiation with gamma dose rates ranging from 1 to 100 mGy $h^{-1}$ for 144 h 7-12 days after sowing. a) The gamma radiation facility where the Petri dishes were positioned at different distances from the gamma radiation source to obtain the nominal dose rates. b) The gamma radiation experiment room showing the shielded lead wall where the unexposed samples were kept outside the radiation sector. c) The Petri dishes with seedlings that were placed behind the lead wall. All seedlings were in the same room under the same light and temperature conditions.

### 3.4 Post-irradiation growing conditions

After 144 h of gamma exposure, CON, INT and TR22 seedlings were transferred from the Petri dishes to pots (5 cm diameter and 5 cm height) filled with S-soil (45% low moist peat, 25% high moist peat, 25% perlite and 5% sand; Hasselfors Garden AS, Örebro, Sweden). Each seedling was potted in a single pot and cultivated in growth chambers (manufactured by Norwegian University of Life Sciences, Ås, Norway) for one month. The temperature of the growth chambers was fixed at 20°C under a 24 h photoperiod with a 12 h main light period followed by 12 h day extension with low-intensity light from incandescent lamps only (8-10 μmol $m^{-2}$ $s^{-1}$) and the relative air humidity (RH) was adjusted to 78%, corresponding to 0.5 kPa water vapor pressure deficiency. The temperature and relative air humidity were

controlled by a Priva computer system (Priva, de Lier, The Netherlands). The main light phase was provided by high-pressure metal halide lamps (HPI-T Plus 250 W, Phillips, Eindhoven, The Netherlands) with the R:FR ratio adjusted to 1.7 with incandescent lamps (Osram, Munich, Germany). The irradiance during the main light phase was gradually increased from 50 to 180 μmol $m^{-2}$ $s^{-1}$ during 7 days. The irradiance and R:FR ratio were measured as described above. The plants were watered as needed.

### 3.5 Growth parameter recordings after the gamma exposure and post-irradiation

After termination of the gamma irradiation, CON, INT and TR22 seedlings were scanned by placing the seedlings between two transparent plastic sheets with millimeter paper on top. Image J software (US National Institutes of Health, Bethesda, MD, USA; http:/imagej.nih.gov/ij/) was used to measure the shoot and root lengths of the scanned seedlings. The lengths of 4-9 plants were measured per gamma dose rate for each CON, INT and TR22 plant type in each of the five repeated experiments, adding up to a total of 20-45 seedlings in total per gamma dose rate and plant type. An overview of the measured growth parameters and other analyzed parameters (described below) directly after the radiation and post-irradiation is shown in Table 4.

During the post-irradiation period, plant needle number was counted, and plant height and shoot diameter were measured in time courses of 29 days for the CON, INT and TR22 type seedlings to study the post-irradiation growth (Figure 7). Plant height was measured from the pot edge to the shoot apical meristem (SAM). Afterwards cumulative growth was calculated by subtracting the height at each subsequent time point from the first measurement. Shoot diameter was measured from needle tip to needle tip across the plant at the shoot apex with two perpendicular measurements per plant. Then the average for the two measurements was calculated. Two-14 CON, INT and TR22 type of plants for each gamma dose rate in each of three repeated experiments were used to measure the plant growth, needle number and shoot diameter.

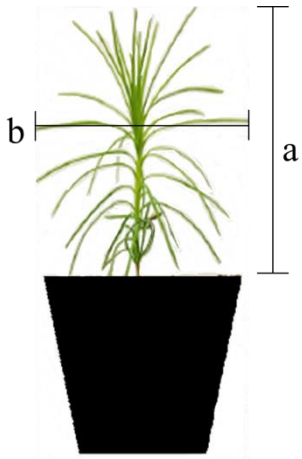


Figure 7. Post-irradiation growth parameter recordings in Scots pine seedlings. a. Plant height, b. Shoot diameter

Table 4. Overview of the gamma exposure experiments of CON, INT, TR22 type of Scots pine plants from the Chernobyl nuclear power plant (ChNPP) area and recorded parameters/analyses performed

| Duration of gamma exposure (h) | Number of repeated experiments | | Age of plants during gamma radiation exposure | Dose rates (mGy $h^{-1}$) |
|---|---|---|---|---|
| 144 | 5 | | 7–12 days after sowing | 0, 1, 10, 20, 40, 100 |
| Time point | Parameter | Number of experi-ments | Number of plants (plant $type^{-1}$ dose $rate^{-1}$ $experiment^{-1}$) | Frequency |
| Details for different analyses | | | | |
| At the end of the irradiation | Shoot and root length | 5 | 4–6 | At the end of the irradiation |
| | Transcripts | 1 | 4 | At the end of the irradiation |
| | DNA damage | 2 | 3 | At the end of the irradiation |
| | Antioxidant assay | 1 | 4 | At the end of the irradiation |
| Post-irradiation, 29 days (time course for growth) | Shoot elongation | 3 | 2-4 | Four times: at day 9, 15, 22 and 29 |
| | Number of needles | 3 | 2-4 | Four times: at day 9, 15, 22 and 29 |
| | Shoot diameter | 3 | 2-4 | Four times: at day 9, 15, 22 and 29 |
| | DNA damage | 2 | 3 | At day 30 post-irradiation |

### 3.6 Analyses of DNA damage by COMET assay

DNA damage of single and double strand breaks was quantified in seedlings after gamma exposure for 144 h 7-12 days after sowing by the COMET assay according to Gichner et al. (2003) with some modifications. To check for persistence of the DNA damage, this assay was also performed at day 30 post-irradiation. The principle of the COMET assay (also known as single cell gel electrophoresis assay (SCGE)) is that damaged DNA moves out of the cell nucleus of lysed cells/cell nuclei during electrophoresis in an agarose gel, and visualization of this is possible by a fluorescence microscopy. DNA breaks are quantified based on the intensity and length of the elongated cell nucleus (a COMET-like structure) due to damaged DNA, relative to the head. Three biological replicates of each of the CON, INT and TR22 plants were examined individually for DNA damage per dose rate, with each sample consisting of 3-4 mm of the shoot tip.

To avoid light-induced DNA damage, the COMET assay was carried out under inactinic red light. In a 9 cm Petri dish plate, approximately 200 mg plant material was placed, followed by the addition of 400 µl cold extraction buffer (PBS, pH 7.0, 200 mM EDTA). The plant materials were chopped vigorously for 30 s using a razor blade to isolate the cell nuclei. The nuclei solution free of plant debris was then collected. 50 µl of 1% low melting point agarose (NuSieve GTG Agarose, Lonza, Basel, Switzerland) prepared in distilled water at 40°C were gently mixed with 75 µl nuclear suspension and 10 µl aliquots was placed on pre-coated (with 1% low melting point agarose) microscope slides**.** The slides (gels) were kept on ice for 1 min, followed by 10 min incubation in a horizontal gel electrophoresis tank containing newly prepared cold electrophoresis buffer (1 mM $Na_2EDTA$ and 300 mM NaOH; pH 13) in order to unwind DNA prior to electrophoresis. Electrophoresis was carried out at 20 V (300 mA) for 5 min at 4°C, and the slides were then rinsed with distilled water and neutralized in PBS buffer for 10 min. After that, the slides were rinsed further in distilled water, fixed in 95% ethanol and dried overnight. The dried slides were stained for 20 min with SYBR Gold (Life Technologies Ltd, Paisley, UK; dilution 1:5000) and washed three times in distilled water for 5 min each time. 'COMETS' (elongated cell nuclei due to damaged DNA) were scored using Comet IV (Perceptive Instruments Ltd, Bury St. Edmunds, UK) and an Olympus BX51 fluorescence microscope with a CCD camera (Olympus, Tokyo, Japan). Two sets of experiments were performed to analyze DNA damage after 144 h gamma irradiation and 30 days post-irradiation. In each experiment, three technical replicates (gels) were performed for each of the three biological replicates per gamma treatment. For each technical replicate, 19-

20 nuclei were scored, adding up to 57-60 nuclei per biological replicate and totally 179 nuclei per dose rate per plant type. The median value for each biological replicate was calculated, followed by the average of these values for the three biological replicates, according to the recommendation of Koppen et al. (2017).

### 3.7 Analyses of total antioxidant capacity

At termination of the gamma exposure, seedling samples were harvested at the site laboratory of FIGARO low dose gamma irradiation facility in 2.0 ml Biosphere plus Safeseal Screw capped Micro Tubes (Sarstedt, Nümbrecht, Germany) in liquid nitrogen. Therefore, the samples were stored at -80ºC in an ultrafreezer (-86°C ULT Chest Freezer, Forma Series, ThermoFisher Scientific, USA) for later analysis. Totally four samples were harvested per dose rate for each of the CON, INT and TR22 type gamma treated seedlings. To analyze the total antioxidant capacity of the gamma treated samples, the OxiSelect Ferric Reducing Antioxidant Power (FRAP) Assay Kit (Cat no STA-859, Cell Biolabs, San Diego, USA) was used according to the manufacturer's instructions (https://www.cellbiolabs.com/sites/default/files/STA-859-frap-assay-kit.pdf). The whole plant samples were transferred from the 2.0 ml Biosphere Micro Tubes to 2.0 ml Eppendorf tube at the beginning of the assay.

Samples were weighed and grinded into fine powder using a TissueLyser Mixer Mill Type MM301 (Retsch, Haan, Düsseldorf, Germany) at 25 Hz for 30 seconds twice with small 5 mm stainless steel carbide beads in the tubes and at the same time cooled down by liquid nitrogen. Thereafter, pre-chilled 1× Assay buffer was added to the tissue lysates to maintain 10 mg $ml^{-1}$ concentration, followed by centrifugation of the homogenate at 12,000 rpm for 15 min at 4°C and collection of the supernatant to new 2.0 ml microcentrifuge tubes. Sufficient volume of reaction reagent was prepared freshly prior to the assay by diluting the Colorimetric Probe and Iron Chloride Solution in 1:10 ratio in 1× Assay buffer and kept on ice. Thereafter, 10 mg Iron standard crystals was measured in a 2.0 ml microcentrifuge tube and 1.0 ml RNase free water was added to make a 10 mg $ml^{-1}$ solution which is equivalent to a concentration of 36 mM. A 1 mM iron (II) standard solution (equivalent to 1000 µM) was prepared from freshly made 36 mM iron (II) stock solution by diluting 125 µl of 36 mM iron (II) stock solution into 4.375 ml of RNase free water. This 1 mM iron (II) standard solution was later used to prepare a series of standards according the manufacturer's recommendations.

For the assay, 100 µl of each of standard, samples or control was added to a 96-well microplate and 100 µl of reaction reagent was added to each well. The plate was then wrapped with aluminium foil to protect it from light and placed on a vertical shaker for 10 min. This was done for proper mixing as well as for incubation at room temperature. Three technical replicates were used for each sample and standard. The microplate was positioned in a microplate reader (Biochrom Asys UVM 340 with KIM, UK) immediately after the incubation to detect the absorbance (optical density) using 540 nm as the primary wavelength. The average absorbance values for each sample and standard were determined and the net absorbance values were calculated by subtracting the zero standard value from samples and standards. The sample results were therefore compared to the standard curve to determine the quantity of antioxidant potential, as µM $Fe^{2+}$ iron equivalents (FRAP value), present in the sample and normalized by weight.

### 3.8 Gene expression analyses

#### 3.8.1 Sample collection

For sample collection, the CON, INT and TR22 seedlings were divided into roots and shoots with a scalpel and harvested at the termination of the gamma irradiation in 2.0 ml Biosphere plus Safeseal Screw capped Micro Tubes in liquid nitrogen. Thereafter, the samples were stored at -80ºC in the ultrafreezer for later analysis. Totally four repeated shoot samples were harvested per dose rate for each of the CON, INT and TR22 type gamma treated seedlings.

#### 3.8.2 RNA extraction and purification

RNA was extracted and purified following the protocol of Masterpure™ Plant RNA Purification Kit (Epicentre, Wisconsin, USA) with some modifications to the manufacturer's protocol, i.e. addition of 0.5% polyvinylpyrrolidone (PVP) (MW 360000, Sigma-Aldrich, Steinheim, Germany) to the extraction buffer and replacement of 1,4-dithiothreitol (DTT) by 3 µl *β*-mercaptoethanol per sample, as briefly described below.

#### 3.8.2.1 Lysis of the tissue samples

The shoot tissue samples were transferred from the 2.0 ml Biosphere Micro Tubes to 2.0 ml Eppendorf tube. Samples were grinded into fine powder using a TissueLyser Mixer Mill Type MM301 at 25 Hz for 30 seconds twice with small 5 mm stainless steel carbide beads in the tubes and at the same time cooled down by liquid nitrogen.

Thereafter, a solution containing 600 µl of Tissue and Cell Lysis Solution and 1 µl of Proteinase K in addition to 3 µl of *β*-mercaptoethanol (Sigma-Aldrich, St. Louis, MO, USA) and 5 µg of PVP added to each sample. The samples were then vortexed vigorously by a vortexer for 1 min following incubation of the samples at 60°C for 15 min in a heat block, with gentle vortexing every 5 min for 25-30 seconds to improve the yield of nucleic acids. The samples were centrifuged afterwards at 10,000 g (Centrifuge 5415R, Eppendorf, Hamburg, Germany) at room temperature (23°C) for 5 min to pellet the debris. The clarified supernatant was transferred to a new 2.0 ml microcentrifuge tube by minimizing the carryover of particulates, followed by placing the samples on ice for 5 min.

#### 3.8.2.2 Precipitation of nucleic acids

250 µl of MPC Protein Precipitation Reagent (from the MasterPure kit) was added to each sample and mixed thoroughly by upside down inversion for 10 seconds. The samples were centrifuged at 10,000 g at 4°C for 10 min to pellet the debris. The supernatant was transferred to a new 2.0 ml microcentrifuge tube and the pellet was discarded following addition of 500 µl of isopropanol (Arcus, Oslo, Norway) to the recovered supernatant. The microcentrifuge tubes were thoroughly inverted 30-40 times by hand to precipitate the nucleic acids. The nucleic acids were pelleted by centrifugation at 10,000 g at 4°C for 10 min. All of the residual isopropanol was carefully removed by pipette without dislodging the total nucleic acid pellet. The tubes were kept open for 2-3 minutes to evaporate isopropanol.

#### 3.8.2.3 Removal of contaminating DNA from RNA preparations

The nucleic acid pellet was completely resuspended by finger tapping in 200 µl of DNase I solution containing 195 µl of 1× DNase buffer from the MasterPure kit and 5 µl of RNase free DNase I for each sample followed by incubation at 37°C for 30 min. Thereafter, 200 µl of 2× T and C Lysis Solution was added and mixed by gently tapping with finger for 5 sec.

Then 200 µl of MPC Protein Precipitation Reagent was added, mixed by gently tapping for 10 sec and placed on ice for 15 min. The samples were then centrifuged at 12,000 g (Centrifuge 5417 R, Eppendorf, Germany) at 4°C for 10 min to pellet the debris. The supernatant containing RNA was transferred to a new clean microcentrifuge tube and pellet was discarded. This step of centrifugation and supernatant transfer were done twice. Therefore, 500 µl of isopropanol was added to the supernatant and the tubes were inverted 30-40 times to precipitate the RNA. The precipitated RNA was pelleted by centrifugation at 11,000 g for 10 min at 4°C in a microcentrifuge tube and the isopropanol was removed without dislodging the RNA pellet. The RNA pellet was washed twice with 70% ethanol and centrifuged briefly at 10,000 g at 4°C for 5 min and all the residual ethanol was removed with a pipette. The RNA pellet was dried for 2-3 min under a laminar air flow and resuspended in 20 µl RNase free water. 1 µl of RiboGuard RNase Inhibitor was added to the RNA isolates to protect its quality and prevent RNA degradation and were stored at -80°C in the ultrafreezer for later use.

### 3.8.3 cDNA synthesis and reverse transcription

The concentration of the extracted total RNA was measured using a NanoDrop One/One$^{c}$ Spectrophotometer (ThermoFisher Scientific, USA), and the quality of the RNA was analyzed with a bioanalyzer (2100 Bioanalyzer, Agilent, California, USA). For cDNA preparation, 1 µg of RNA from each sample was used to synthesize cDNA in a 20 µl reaction volume with random primers and reverse transcriptase using SuperScript VILO cDNA Synthesis Kit (Invitrogen, ThermoFisher Scientific, Massachusetts, USA), according to the manufacturer's instruction manual. The enzyme uses RNA as a template, and the initial product is a single stranded cDNA sequence, which is complimentary to the RNA. Each 20 µl reaction volume contained 4 µl of 5× VILO Reaction Mix, 2 µl of 10× Superscript Enzyme Mix and 1,000 ng of sample RNA. RNase-free water was added to make the final volume 20 µl. Generally, the amount of sample RNA (to maintain 1,000 ng in reaction volume) and RNase-free water comprise 14 µl of the reaction volume.

Reactions without reverse transcriptase (-rt) were also prepared for each sample which contained an amount of RNA (µl) equivalent to 500 ng of RNA, 2 µl of 5× VILO Reaction Mix and RNase-free water to make the total reaction volume 10 µl. All the samples with (rt) and without (-rt) reverse transcriptase were incubated in a PCR machine (DNA Engine Tetrad

Pelitier Thermal Cycler, BioRad Laboratories, Hercules, California, USA) and the reaction program was 25°C for 10 min, 42°C for 60 min, 85°C for 5 min and 4°C for forever. After the cycling program ended, the synthesized cDNA was chilled on ice and the rt and –rt samples were diluted by adding 80 µl and 40 µl of RNase free water to each rt and –rt sample, respectively.

#### 3.8.3.1 Check for contaminating DNA

The quality of the newly made cDNA was checked for any contaminating or genomic DNA in the samples in a real time PCR (qPCR) machine (7500 Fast Real Time PCR system, Applied Biosystems Life Technologies, Thermo Fisher Scientific, Massachusetts, USA) following the same method as described below in the section 3.8.4, but with only one technical replicate for each sample. The –rt samples were used as control i.e. any gene expression from the control samples is an indication of DNA contamination. All the rt and –rt samples were tested with the primers of a reference gene actin.

### 3.8.4 Quantitative Real Time Polymerase Chain Reaction (qRT-PCR)

The real time qPCR assay for the amplification of the target genes were performed with the 7500 Fast Real Time PCR system in 96-well reaction plates (MicroAmp Fast Optical 96-Well Reaction Plate, Applied Biosystems, Thermo fisher Scientific, Massachusetts, USA). A master mix was made in a PCR cabinet (Biosan VVC/T-M-AR, Life Technologies, Thermo Fisher Scientific, Massachusetts, USA) in advance.

The reaction volume was 20 µl for each well with four technical replicates of each reference gene and target gene. Each of the 20 µl reaction volumes contained 2 µl of cDNA templates, 7 µl of RNase-free water, 10 µl of SYBR green dye (SYBR Selected master mix, Life technologies, Thermo Fisher Scientific, USA) along with 0.5 µl of forward and reverse primers with a primer concentration in the total reaction volume of 250 nM. There were also non-template controls (NTC) for each primer pairs, which contained RNase-free water instead of template. *ACTIN* (*ACT*) and *GLYCERALDEHYDE 3-PHOSPHATE DEHYDROGENASE* (*GAPDH*) were used as reference genes for the quantification of the relative transcript levels of target genes. A two-steps qPCR cycling program was used for amplification: a first step of 50ºC for 2 min followed by 95ºC for 2 min and a second step of

40 cycles of 95ºC for 15 sec and 60ºC for 1 min. The florescence of the samples was measured along the different steps and cycles.

### 3.8.4.1 Primer design and primer sequences

There were total six genes used in this study for the quantification of relative transcript level. Among them, two were reference genes, i.e. *ACT* and *GAPDH*. The 4 target genes were *CYCLIN B1;1* (*CYCB1;1*), *CYCLIN DEPENDENT KINASE B1;2* (*CDKB1;2*), *RADIATION 51* (*RAD51*) and *SUPPRESSOR OF GAMMA RESPONSE 1* (*SOG1*).

Briefly, Primer3 software (Rozen & Skaletsky, 2000) was used to design the gene-specific primers with default parameters and amendments according to the following criteria: melting temperature around 60°C and product size between 100 and 150 bp. All the qPCR primers used in this study were synthesized by Invitrogen (ThermoFisher Scientific, USA) and tested for their product size (base pair length) on 1% agarose gel (Agar, Sigma-Aldrich, Steinheim, Germany). The gene-specific primers are listed in Table 5.

### 3.8.4.2 Calculation of relative transcript level

Relative quantification (RQ) was used when calculating the results of the qPCR. The relative transcript level of different gamma treated samples of the CON, INT and TR22 plants were compared with the unexposed CON sample (i.e. 0 mGy $h^{-1}$). The comparative Cycle threshold (Ct) method (ΔΔCt method) was used to calculate the relative transcript level which normalizes the transcript levels of the target genes to the reference genes and quantifies the transcript levels relative to a control (calibrator) group. The average of transcript levels of the two reference genes was used to normalize transcript levels of the target genes for each sample. The Ct values of control samples were also averaged.

For each sample and gene, the following formulas were used:

1. $\Delta Ct_{\text{sample}} = Ct_{\text{target gene-treated sample}} - Ct_{\text{reference gene-treated sample}}$
2. $\Delta Ct_{\text{control}} = Ct_{\text{target gene control sample}} - Ct_{\text{reference gene control sample}}$
3. $\Delta\Delta Ct_{\text{treated sample}} = \Delta Ct_{\text{treated sample}} - \Delta Ct_{\text{control (calibrator) sample}}$
4. Fold difference (RQ) = $2^{-\Delta\Delta Ct}$

To get the relative transcript levels of all gamma treated samples including unexposed controls, the fold changes of 4 biological replicate samples were analyzed and averaged using 3-4 technical replicates. The fold change shows the transcript level of each sample relative to the control (calibrator).

### 3.9 Statistical analyses

Different growth and developmental parameters (i.e. shoot and root lengths at the termination of the gamma exposure, post-irradiation shoot elongation, number of needles, shoot diameter), DNA damage after gamma irradiation, post-irradiation DNA damage, total antioxidant capacity and relative transcript levels of gamma irradiated CON, INT and TR22 samples were assessed by two-way analysis of variance (ANOVA) in the general linear model (glm) mode using the Minitab statistical software (Minitab 19, Minitab Inc, Pennsylvania, USA) with a significance level of 95% ($p \leq 0.05$). Prior to the ANOVA, the data were checked for equal variance and normal distribution using Levene`s and Ryan-Joiner tests. A Tukey's post hoc test was used ($p \leq 0.05$) to test for differences between means. The final time point data was considered only in the analyses of the post-irradiation growth parameters i.e. shoot elongation, number of needles, shoot diameter. The relative transcript levels data were log-transformed before analyses, whereas the DNA damage after gamma irradiation and post-irradiation DNA damage data were square root-transformed. Each data set derived from each experiment was analyzed separately. Therefore, data from all repeated experiments were included together for final statistical analysis.

Table 5. Gene-specific primers used for quantitative RT-PCR (qPCR) assays in Scots pine

| Gene | Accession number | Forward primer (5’ – 3’) | Reverse primer (3’ – 5’) | Purpose |
|---|---|---|---|---|
| *CYCB1;1* | PITA_000017697-RA | CTGCAGTCTACACCGCTCAA | GGAATGCCACCATCAGTCTT | qPCR |
| *CDKB1;2* | PITA_000082194-RA | GGGAACGTATGGCAAAGTGT | GTGGGAGGAACTCCCTCTTC | qPCR |
| *RAD51* | EU513162.1 | TATGGGGAATTTCGAACAGG | GTTCCCTCGGCATCAATAAA | qPCR |
| *SOG1* | PITA_000080155-RA | ATGGAATCTGCTCTGCTCGT | GCGTTTACGGTTGCCTGTAT | qPCR |
| *GAPDH* | L07501 | GTGCATTCCATCACAGCAAC | GTTGAAACCAGCTACTCTGC | qPCR |
| *ACT* | FN546174 | TGACATGGAGAAGATTTGGC | CATACATAGCAGGCACATTG | qPCR |

# 4. Results

## 4.1 Effect of gamma radiation on plant growth

To evaluate the effect of ionizing radiation during seed development on later plant growth and development, Scots pine seedlings grown from seeds from different areas in the Chernobyl region with background (CON), intermediate (INT) and high (TR22) levels of ionizing radiation were exposed to gamma radiation ranging from 0 to 100 mGy $h^{-1}$ for 144 h 7-12 days after sowing.

Overall, at the end of the 144 h gamma irradiation, the root length differed significantly between the plant types ($p < 0.001$) and gamma dose rates ($p < 0.001$). There was also a significant interaction between plant type and dose rate ($p < 0.001$) (Table 6). Within each of the CON and INT seedling types, the root length did not differ significantly between the different gamma dose ranging from 0 to 100 mGy $h^{-1}$. However, the root length of TR22 seedlings was significantly increased at 10 mGy $h^{-1}$ compared to the unexposed seedlings of this and the other two plant types (Figure 8a).

Specifically, the root length did not differ significantly between the different plant types for 0, 1, 40 and 100 mGy $h^{-1}$. At 10 mGy $h^{-1}$, the root length of TR22 seedlings was significantly increased compared to the CON and INT seedlings. Also, the root length of CON seedlings was significantly reduced at 20 mGy $h^{-1}$ compared to the INT and TR22 seedlings. However, overall, there was no clear dose-response relationship between root length and the gamma irradiation in any of the plant types (Figure 8a).

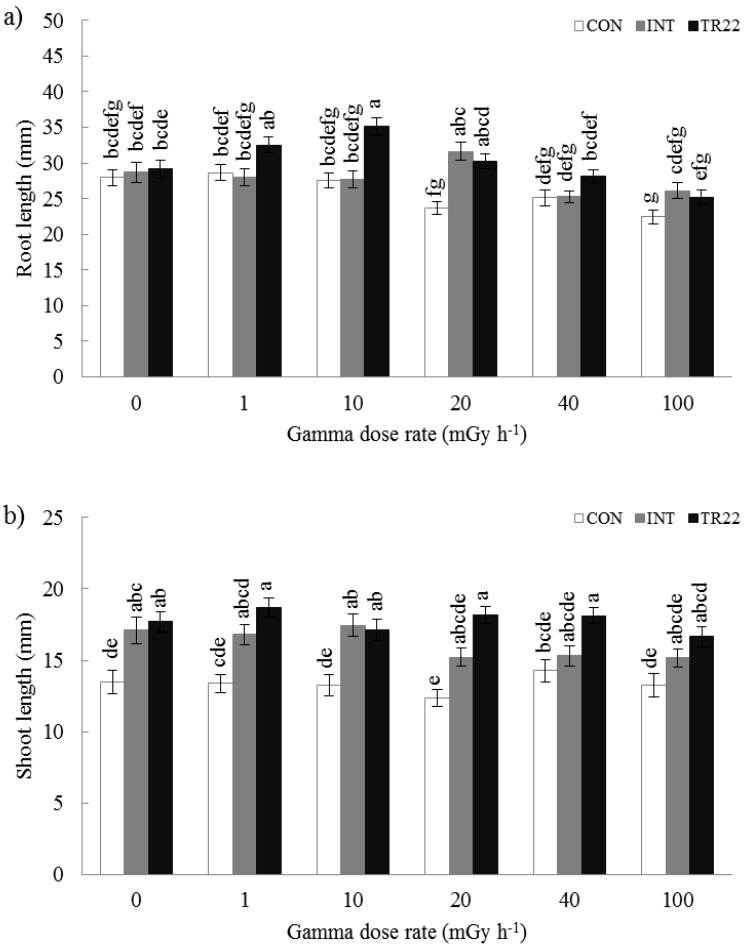


Figure 8. Effect of 144 h exposure to gamma radiation 7–12 days after sowing on a) root length and b) shoot length of Scots pine seedlings grown from seeds from different areas in the Chernobyl region with background (CON), intermediate (INT) and high (TR22) levels of ionizing radiation (see Table 2). The results are mean ± SE of 4-6 plants per dose rate and per plant type (seed source) in each of five experiments (totally n = 20-30). Different letters within each plant type indicate significant differences ($p \leq 0.05$) based on two-way ANOVA in the general linear model mode followed by Tukey's post hoc test.

At the end of the gamma radiation exposure, the shoot length differed significantly between the plant types ($p < 0.001$). However, there was no overall significant effect of the gamma dose rate on shoot length ($p = 0.210$), as well as no significant interaction between plant type and dose rate ($p = 0.275$) (Table 6).

The TR22 seedlings showed significant increase in shoot length at 0 to 40 mGy $h^{-1}$, compared to the unexposed CON seedlings. The CON seedlings showed decrease in shoot length at 0 and 10 mGy $h^{-1}$ as compared to the two other plant types. However, overall, there was no clear dose-response relationship between shoot length and the gamma irradiation in or between any of the plant types (Figure 8b).

Table 6. ANOVA (general linear model) table for the overall effect of 144 h exposure to gamma radiation (0, 1, 10, 20, 40 and 100 mGy $h^{-1}$) 7-12 days after sowing on root and shoot length of seedlings of Scots pine grown from seeds from different areas in the Chernobyl region with background (CON), intermediate (INT) and high (TR22) levels of ionizing radiation (see Table 2). There were 4-6 plants per dose rate and plant type in each of five experiments (totally n = 20-30).

| Source | DF | Adj SS | Adj MS | F-Value | P-Value |
|---|---|---|---|---|---|
| **Root length** | | | | | |
| Plant type | 2 | 4070 | 2034.89 | 21.45 | 0.000 |
| Dose rate | 5 | 4895 | 978.97 | 10.32 | 0.000 |
| Plant type*Dose rate | 10 | 3405 | 340.48 | 3.59 | 0.000 |
| Error | 1339 | 127047 | 94.88 | | |
| Total | 1356 | 139778 | | | |
| **Shoot length** | | | | | |
| Plant type | 2 | 4565.7 | 2282.85 | 58.98 | 0.000 |
| Dose rate | 5 | 277.0 | 55.41 | 1.43 | 0.210 |
| Plant type*Dose rate | 10 | 471.3 | 47.13 | 1.22 | 0.275 |
| Error | 1339 | 51822.6 | 38.70 | | |
| Total | 1356 | 57287.7 | | | |

"*" indicates interaction between the factor Plant type and Dose rate

### 4.2 DNA damage after 144 h gamma exposure

To measure the DNA damage in response to gamma radiation in the Scots pine seedlings grown from seeds from the different radiation levels in the Chernobyl region, the COMET assay was performed after 144 h gamma exposure.

A significant dose-rate dependent increase was observed in DNA damage assessed as percentage (%) COMET tail intensity after 144 h gamma exposure. Overall, the % tail DNA differed significantly between the plant types ($p < 0.001$) and gamma dose rates ($p < 0.001$). There was also a significant interaction between plant type and dose rate ($p < 0.001$) (Table 7).

As compared to the unexposed CON seedlings which had 0.05% tail DNA, CON seedlings showed significantly increased DNA damage after gamma exposure with 0.6-11% tail DNA at 1-20 mGy $h^{-1}$ and significantly increasing DNA damage up to 18% and 23% tail DNA at 40 and 100 mGy $h^{-1}$, respectively. As compared to the unexposed CON and INT seedlings, gamma exposed INT seedlings also exhibited significantly higher DNA damage with 0.6-10%

tail DNA at 1-40 mGy $h^{-1}$ with increasing DNA damage up to 15% tail DNA at the highest dose rate analyzed in this study, i.e. 100 mGy $h^{-1}$. Similarly, the TR22 seedlings showed significantly increased DNA damage like CON and INT seedlings with 1-9% tail DNA at 1-40 mGy $h^{-1}$ with increasing DNA damage up to 14% tail DNA at 100 mGy $h^{-1}$, compared to the unexposed seedlings of this and the other two plant types (Figure 9).

Furthermore, the DNA damage differed significantly between the plant types for 1-100 mGy $h^{-1}$. DNA damage did not differ significantly between the plant types for the unexposed seedlings, i.e. 0 mGy $h^{-1}$. At 1 mGy $h^{-1}$, the TR22 seedlings exhibited higher DNA damage compared to the CON and INT seedlings. At 10 and 20 mGy $h^{-1}$, the CON and TR22 seedlings exhibited increased DNA damage compared to the INT seedlings, although, no significant difference in DNA damage between CON and TR22 seedlings was detected at these two dose rates. The CON seedlings displayed significantly higher DNA damage than the plant types at 40 and 100 mGy $h^{-1}$ (Figure 9).

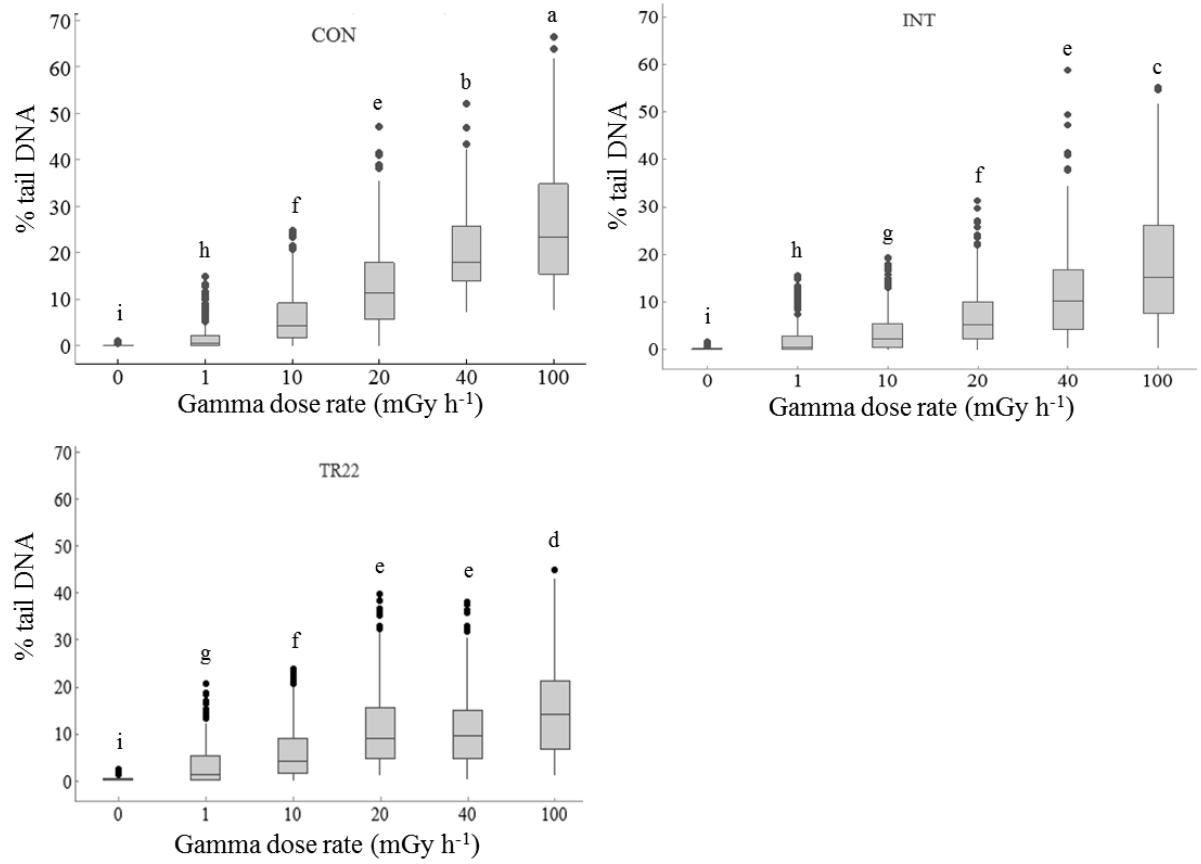


Figure 9. Effect of 144 h exposure to gamma radiation 7–12 days after sowing on DNA damage analyzed by COMET assay in Scots pine seedlings grown from seeds from different areas in the Chernobyl region with background (CON), intermediate (INT) and high (TR22) levels of ionizing radiation (see table 2). The results are mean ± SE of the median values for

3 biological replicates per dose rate with 3 technical replicates (gels) for each sample which 19–20 nuclei scored in each gel, and per plant type (seed source) in each of two experiments. Lower and upper box boundaries = 25 and 75% percentiles, error bars = 10 and 90% percentiles with data points outside these shown as dots. Different letters indicate significant differences ($p \leq 0.05$) based on two-way ANOVA in the general linear model mode with plant type and dose rate as factors, followed by Tukey's post hoc test.

Table 7. ANOVA (general linear model) table for the overall effect of 144 h exposure to gamma radiation (0, 1, 10, 20, 40 and 100 mGy $h^{-1}$) 7-12 days after sowing on DNA damage in seedlings of Scots pine grown from seeds from different areas in the Chernobyl region with background (CON), intermediate (INT) and high (TR22) levels of ionizing radiation (see Table 2). The main effects of plant type and dose rate and their interactions were analyzed. There were two factors (Plant type: CON, INT and TR22; Dose rate: 0, 1, 10, 20, 40 and 100 mGy $h^{-1}$). The results are mean ± SE of the median values for 3 biological replicates (n = 3) with 3 technical replicates (gels) per dose rate and per plant type in each of two experiments. The data were square root-transformed before analysis.

| **Source** | **DF** | **Adj SS** | **Adj MS** | **F-Value** | **P-Value** |
|---|---|---|---|---|---|
| Plant type | 2 | 424.4 | 212.20 | 176.64 | 0.000 |
| Dose rate | 5 | 11404.3 | 2280.86 | 1898.64 | 0.000 |
| Plant type*Dose rate | 10 | 646.2 | 64.62 | 53.79 | 0.000 |
| Error | 6441 | 7737.7 | 1.20 | | |
| Total | 6458 | 20211.1 | | | |

"*" indicates interaction between the factor Plant type and Dose rate

### 4.3 Effect of gamma radiation on total antioxidant capacity

Overall, the plant types differed significantly (p = 0.028; ANOVA glm) in their total antioxidant capacity as analyzed by the FRAP assay, but there were no significant differences between the dose rates (p = 0.483) and no significant interaction between plant type and dose rate (p = 0.349) (Table 8).

However, there was no clear difference (Tukey`s test) between the plant types in their dose-response relationship with respect to the effect of gamma radiation on their total antioxidant capacity, only a possible trend of higher antioxidant capacity in the TR22 than in the CON seedlings for 0 and 100 $mGy^{-1}$ and possibly for the INT plants at 100 $mGy^{-1}$ (Figure 10).

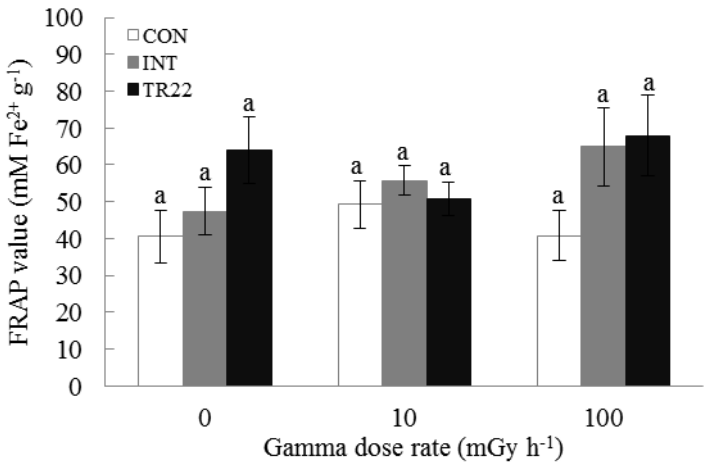


Figure 10. Effect of 144 h gamma radiation 7-12 days after sowing on total antioxidant capacity (Ferric reducing antioxidant power (FRAP) assay) in entire seedlings of Scots pine grown from seeds from different areas in the Chernobyl region with background (CON), intermediate (INT) and high (TR22) levels of ionizing radiation (see Table 2). The results are mean ± SE of 4 biological replicates (n = 4) with 3 technical replicates per sample. The treatments started when the seedlings were 6 days old. Different letters within diagram indicate significant differences ($p \leq 0.05$) based on two-way ANOVA in the general linear model mode followed by Tukey's post hoc test.

Table 8. ANOVA (general linear model) table for the overall effect of total antioxidant capacity (Ferric reducing antioxidant power (FRAP) assay) in entire seedlings of Scots pine grown from seeds from different areas in the Chernobyl region with background (CON), intermediate (INT) and high (TR22) levels of ionizing radiation (see Table 2) for 144 h gamma irradiation 7–12 days after sowing. The main effects of plant type and dose rate and their interactions were analyzed. There were 3 levels for each factor (Plant type: CON, INT and TR22; Dose rate: 0, 10 and 100 mGy $h^{-1}$). The results are mean ± SE of 4 biological replicates (n = 4) with 3 technical replicates per sample.

| **Source** | **DF** | **Adj SS** | **Adj MS** | **F-Value** | **P-Value** |
|---|---|---|---|---|---|
| Plant type | 2 | 1932.8 | 966.4 | 4.09 | 0.028 |
| Dose rate | 2 | 353.1 | 176.5 | 0.75 | 0.483 |
| Plant type*Dose rate | 4 | 1097.9 | 274.5 | 1.16 | 0.349 |
| Error | 27 | 6378.1 | 236.2 | | |
| Total | 35 | 9761.9 | | | |

"*" indicates interaction between the factor Plant type and Dose rate

### 4.4 Post-irradiation effect of gamma radiation on plant growth

Post-irradiation effects of gamma radiation on different plant growth parameters, i.e. cumulative shoot elongation, number of needles and shoot diameter were investigated for 29 days in the Scots pine seedlings grown from the seeds from the different areas in the Chernobyl region.

At day 29, the cumulative growth did not differ significantly between the plant types ($p = 0.616$) or dose rates ($p = 0.595$). There was also no significant interaction between plant type and dose rate for this growth parameter ($p = 0.515$) (Table 9; Figure 11).

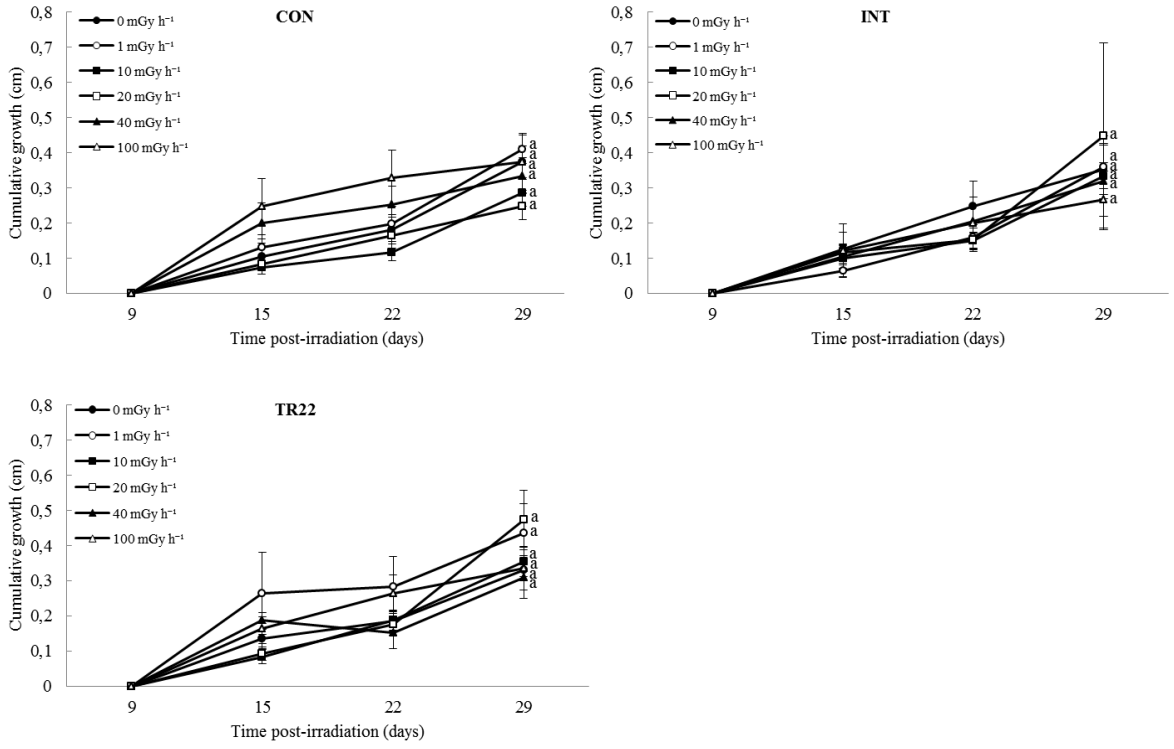


Figure 11. Post-irradiation effect of 144 h exposure to gamma radiation 7–12 days after sowing on cumulative growth of Scots pine seedlings grown from seeds from different areas in the Chernobyl region with background (CON), intermediate (INT) and high (TR22) levels of ionizing radiation (see Table 2). The results are mean ± SE of 2-4 plants per dose rate and plant type (seed source) in each of three repeated experiments (totally n = 6-12). Different letters indicate significant differences ($p \leq 0.05$) at day 29 based on two-way ANOVA in the general linear model mode with plant type and dose rate as factors, followed by Tukey's post hoc test. The results for the final time point only (41 days after sowing) were analyzed.

Table 9. ANOVA (general linear model) table for the overall post-irradiation effect of 144 h exposure to gamma radiation (0, 1, 10, 20, 40 and 100 mGy $h^{-1}$) 7-12 days after sowing on cumulative growth of seedlings of Scots pine grown from seeds from different areas in the Chernobyl region with background (CON), intermediate (INT) and high (TR22) levels of ionizing radiation (see Table 2). The results for the final time point only (day 41 after sowing) were analyzed. There were 2-4 plants per dose rate and plant type in each of three experiments (totally n = 6-12).

| **Source** | **DF** | **Adj SS** | **Adj MS** | **F-Value** | **P-Value** |
|---|---|---|---|---|---|
| Plant type | 2 | 0.0954 | 0.04772 | 0.48 | 0.616 |
| Dose rate | 5 | 0.3638 | 0.07275 | 0.74 | 0.595 |
| Plant type*Dose rate | 10 | 0.9058 | 0.09058 | 0.92 | 0.515 |
| Error | 379 | 37.3143 | 0.09845 | | |
| Total | 396 | 38.7174 | | | |

"*" indicates interaction between the factor Plant type and Dose rate

On the other hand, overall, at day 29, the number of needles differed significantly between the plant types ($p < 0.001$) and dose rates ($p < 0.001$). There was also a significant interaction between plant type and dose rate ($p < 0.001$) (Table 10).

For the CON seedlings, there was a significant increase in the number of needles at 1 mGy $h^{-1}$ as compared 20 to 100 mGy $h^{-1}$. However, the number of needles did not differ significantly between the unexposed CON seedlings and those irradiated with 1 to 20 mGy $h^{-1}$. By contrast, the number of needles was reduced significantly in the CON seedlings at 40 and 100 mGy $h^{-1}$ compared to the unexposed ones. For the INT seedlings, there was a significant increase at day 29 in the number of needles at 1 mGy $h^{-1}$, compared to 10 to 100 mGy $h^{-1}$, but, the number of needles did not differ significantly between 0 and 1 mGy $h^{-1}$. However, for this plant type, the number of needles was significantly reduced at 10, 40 and 100 mGy $h^{-1}$ as compared to the unexposed seedlings. At day 29, the TR22 seedlings exposed to 20 to 100 mGy $h^{-1}$ showed significantly, gradually reduced number of neeedles as compared to 0 mGy $h^{-1}$, but there was no significant difference between 0, 1 and 10 mGy $h^{-1}$ (Figure 12).

At 0 and 10 mGy $h^{-1}$, the TR22 seedlings had significantly more needles than the CON seedlings. By contrast, at 1, 20, 40 and 100 mGy $h^{-1}$, no significant difference was detected between the CON, INT and TR22 seedlings. Thus, overall, the different plant types all showed similar response to the gamma radiation with reduced number of needles at 40 and 100 mGy $h^{-1}$ (Figure 12).

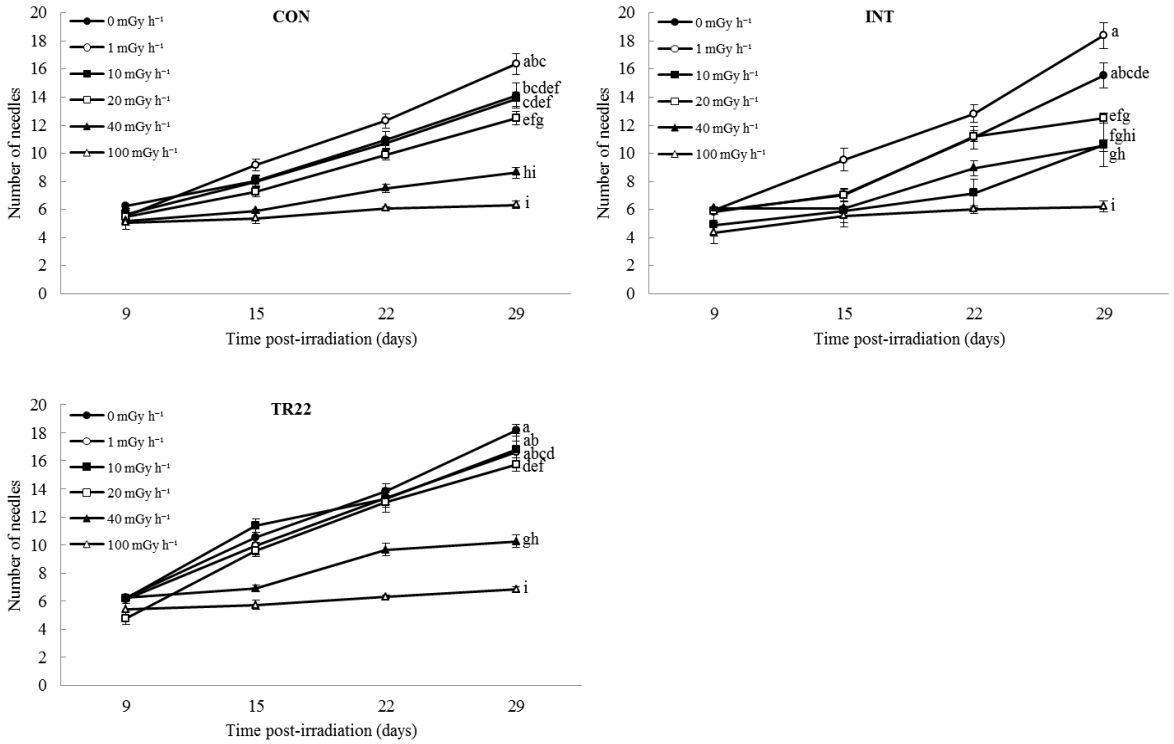


Figure 12. Post-irradiation effect of 144 h exposure to gamma radiation 7–12 days after sowing on number of needles of Scots pine seedlings grown from seeds from different areas in the Chernobyl region with background (CON), intermediate (INT) and high (TR22) levels of ionizing radiation (see Table 2). The results are mean ± SE of 2-4 plants per dose rate and plant type (seed source) in each of three repeated experiments (totally n = 6-12). Different letters indicate significant differences ($p \leq 0.05$) at day 29 based on two-way ANOVA in the general linear model mode with plant type and dose rate as factors, followed by Tukey's post hoc test. The results for the final time point only (41 days after sowing) were analyzed.

Table 10. ANOVA (general linear model) table for the overall post-irradiation effect of 144 h exposure to gamma radiation (0, 1, 10, 20, 40 and 100 mGy $h^{-1}$) 7-12 days after sowing on number of needles of Scots pine seedlings grown from seeds from different areas in the Chernobyl region with background (CON), intermediate (INT) and high (TR22) levels of ionizing radiation (see Table 2). The results for the final time point only (day 41 after sowing) were analyzed. There were 2-4 plants per dose rate and plant type in each of three experiments (totally n = 6-12).

| Source | DF | Adj SS | Adj MS | F-Value | P-Value |
|---|---|---|---|---|---|
| Plant type | 2 | 299.3 | 149.67 | 15.73 | 0.000 |
| Dose rate | 5 | 5329.6 | 1065.92 | 112.03 | 0.000 |
| Plant type*Dose rate | 10 | 387.9 | 38.79 | 4.08 | 0.000 |
| Error | 450 | 4281.5 | 9.51 | | |
| Total | 467 | 10867.1 | | | |

"*" indicates interaction between the factor Plant type and Dose rate

Overall, at day 29, the shoot diameter differed significantly between plant types ($p < 0.001$) and dose rates ($p < 0.001$). There was also a significant interaction between plant type and dose rate ($p < 0.001$) (Table 11).

At this time point, the shoot diameter of the CON seedlings did not differ significantly between 0 to 20 mGy $h^{-1}$. However, as compared to the corresponding unexposed seedlings, the shoot diameter of this plant type was significantly decreased at 40 and 100 mGy $h^{-1}$, but did not differ significantly between these two dose rates. The shoot diameter in the INT seedlings at day 29 did not differ significantly at 0, 1, 20 and 40 mGy $h^{-1}$. However, a significant decrease in shoot diameter was detected at dose rate 10 and 100 mGy $h^{-1}$ as compared to the unexposed INT seedlings. The shoot diameter of TR22 seedlings differed significantly at 40 and 100 mGy $h^{-1}$, compared to the unexposed TR22 plants, but no significant difference was detected between these two dose rates. On the contrary, the shoot diameter of TR22 seedlings did not differ significantly at 0 to 20 mGy $h^{-1}$ (Figure 13).

The statistical analysis showed a signficant difference in plant diameter between the CON and the other two seedling types at 20 mGy $h^{-1}$, but overall, all three plant types showed a similar dose-response relationship between shoot diameter and the gamma irradiation with decreased shoot diameter at the highest dose rate (Figure 13).

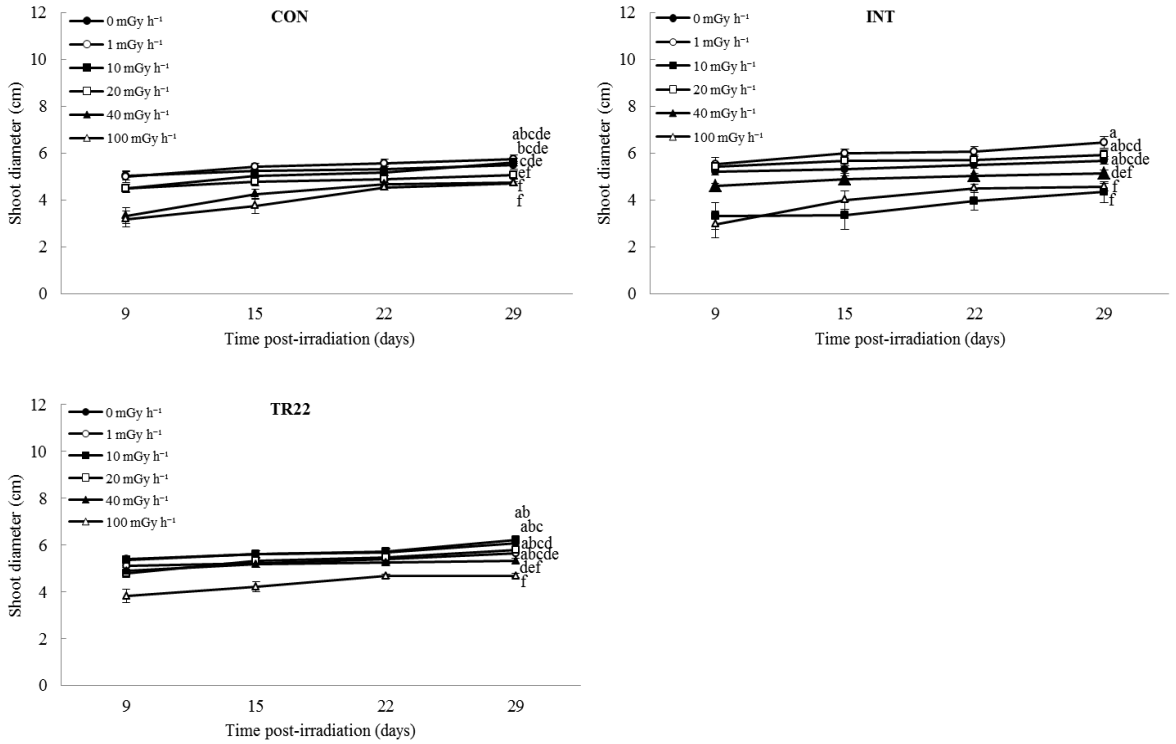


Figure 13. Post-irradiation effect of 144 h exposure to gamma radiation 7–12 days after sowing on shoot diameter of Scots pine seedlings grown from seeds from different areas in the Chernobyl region with background (CON), intermediate (INT) and high (TR22) levels of ionizing radiation (see Table 2). The results are mean ± SE of 2-4 plants per dose rate and plant type (seed source) in each of three repeated experiments (totally n = 6-12). Different letters indicate significant differences ($p \leq 0.05$) at day 29 based on two-way ANOVA in the general linear model mode with plant type and dose rate as factors, followed by Tukey's post hoc test. The results for the final time point only (41 days after sowing) were analyzed.

Table 11. ANOVA (general linear model) table for the overall post-irradiation effect of 144 h exposure to gamma radiation (0, 1, 10, 20, 40 and 100 mGy $h^{-1}$) 7-12 days after sowing on shoot diameter of seedlings of Scots pine grown from seeds from different areas in the Chernobyl region with background (CON), intermediate (INT) and high (TR22) levels of ionizing radiation (see Table 2). The results for the final time point only (day 41 after sowing) were analyzed. There were 2-4 plants per dose rate and plant type in each of three experiments (totally n = 6-12).

| Source | DF | Adj SS | Adj MS | F-Value | P-Value |
|---|---|---|---|---|---|
| Plant type | 2 | 12.15 | 6.0769 | 9.64 | 0.000 |
| Dose rate | 5 | 75.05 | 15.0107 | 23.81 | 0.000 |
| Plant type*Dose rate | 10 | 37.20 | 3.7203 | 5.90 | 0.000 |
| Error | 450 | 283.65 | 0.6303 | | |
| Total | 467 | 423.34 | | | |

"*" indicates interaction between the factor Plant type and Dose rate

### 4.5 Persistent post-irradiation DNA damage

To assess the persistence of the gamma-induced DNA damage in shoot tips of the Scots pine seedlings grown from seeds from different areas in the Chernobyl region, the COMET assay was performed at day 30 post-irradiation.

The % tail DNA values differed significantly between the plant types ($p < 0.001$) and gamma dose rates ($p < 0.001$). There was also a significant interaction between plant type and dose rate ($p < 0.001$) (Table 12).

In all three plant types, a significant dose-rate dependent increase in % tail DNA values was observed with increased gamma dose rate. As compared to the unexposed CON seedlings which had 0.04% tail DNA, CON seedlings exhibited significantly increasing DNA damage from 0.8-8% tail DNA at 1-100 mGy $h^{-1}$. There was 0.9%, 2%, 3%, 6% and 8% tail DNA after 1, 10, 20, 40 and 100 mGy $h^{-1}$. As compared to the unexposed CON and INT seedlings, gamma exposed INT seedlings showed significantly increased DNA damage with 0.4-5% tail DNA at 1-100 mGy $h^{-1}$. TR22 seedlings displayed significantly increased DNA damage with 2-3% tail DNA at 1-100 mGy $h^{-1}$, compared to the unexposed seedlings of this and the other two plant types (Figure 14).

Moreover, the % tail DNA did not differ significantly between different plant types at 1, 10 and 20 mGy $h^{-1}$. At 0 mGy $h^{-1}$, the INT seedlings showed higher DNA damage than CON seedlings. At 40 mGy $h^{-1}$, the CON seedlings exhibited increased DNA damage compared to other plant types, whereas, at 100 mGy $h^{-1}$, the CON seedlings showed increased DNA damage compared to TR22 seedlings (Figure 14).

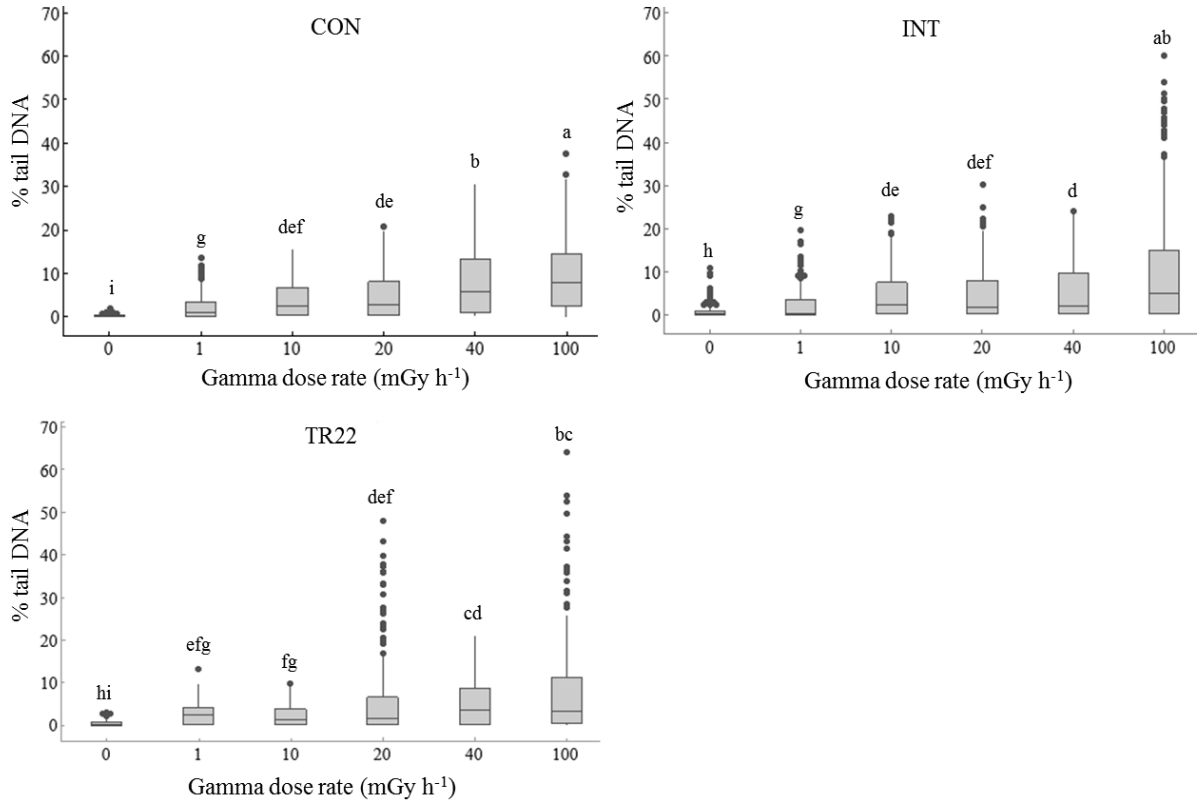


Figure 14. Post-irradiation effect on DNA damage measured by the COMET assay at day 30 post-irradiation (41 days after sowing) after 144 h exposure to gamma radiation 7–12 days after sowing in shoot tips with young needles of Scots pine seedlings grown from seeds from different areas in the Chernobyl region with background (CON), intermediate (INT) and high (TR22) levels of ionizing radiation (see table 2). The results are mean ± SE of the median values for 3 biological replicates per dose rate with 3 technical replicates (gels) for each sample which 19–20 nuclei scored in each gel, and per plant type (seed source) in each of two experiments. Lower and upper box boundaries = 25 and 75% percentiles, error bars = 10 and 90% percentiles with data points outside these shown as dots. Different letters indicate significant differences ($p \leq 0.05$) based on two-way ANOVA in the general linear model mode with plant type and dose rate as factors, followed by Tukey's post hoc test.

Table 12. ANOVA (general linear model) table for the overall post-irradiation effect at day 30 post-irradiation (41 days after sowing) after 144 h exposure to gamma radiation (0, 1, 10, 20, 40 and 100 mGy $h^{-1}$) 7-12 days after sowing on DNA damage in seedlings of Scots pine grown from seeds from different areas in the Chernobyl region with background (CON), intermediate (INT) and high (TR22) levels of ionizing radiation (see Table 2). The main effects of plant type and dose rate and their interactions were analyzed. There were two factors (Plant type: CON, INT and TR22; Dose rate: 0, 1, 10, 20, 40 and 100 mGy $h^{-1}$). The results are mean ± SE of the median values for 3 biological replicates (n = 3) with 3 technical replicates (gels) per dose rate and per plant type in each of two experiments. The data were square root-transformed before analysis.

| **Source** | **DF** | **Adj SS** | **Adj MS** | **F-Value** | **P-Value** |
|---|---|---|---|---|---|
| Plant type | 2 | 26,0 | 12,984 | 7,85 | 0,000 |
| Dose rate | 5 | 2007,2 | 401,435 | 242,56 | 0,000 |
| Plant type*Dose rate | 10 | 158,8 | 15,882 | 9,60 | 0,000 |
| Error | 5742 | 9502,9 | 1,655 | | |
| Total | 5759 | 11907,6 | | | |

"*" indicates interaction between the factor Plant type and Dose rate

### 4.6 Effect of gamma radiation on transcript levels of genes

To evaluate the effect of gamma irradiation on genes involved in control of cell division, transcript levels of the *CYCB1;1* and *CDKB1;2* genes were analyzed in the different plant types at 0, 10 and 100 mGy $h^{-1}$ (Figure 15).

Overall, the transcript level of *CYCB1;1* differed significantly between the plant types ($p = 0.049$) and dose rates ($p = 0.001$). There was no significant interaction between the plant type and dose rate ($p = 0.519$) (Table 13). *CYCB1;1* showed significantly lower transcript level by about 5.8-fold in the TR22 seedlings at 100 mGy $h^{-1}$, compared to the unexposed CON seedlings (Figure 15).

The transcript level of *CDKB1;2* showed no significant difference between the plant types ($p = 0.382$) or dose rates ($p = 0.141$), but there was a significant interaction between the plant type and dose rate ($p = 0.012$) (Table 13). Tukey`s test analyses showed a significant difference in transcript level in TR22 seedlings at 10 and 100 mGy $h^{-1}$ (Figure 15).

To evaluate the effect of gamma irradiation on genes involved in DNA repair, transcript levels of the *RAD51* and *SOG1* genes were analyzed in the different plant types at 0, 10 and 100 mGy $h^{-1}$ (Figure 15).

*RAD51* transcript levels showed significant difference between the plant types (p = 0.043) and dose rates (p = 0.036), but there was no significant interaction between plant type and dose rate (p = 0.146) (Table 13). *RAD51* exhibited significantly lower transcript levels in TR22 seedlings at 10 mGy $h^{-1}$ compared to the unexposed CON seedlings, with 3.2-fold lower transcript levels (Figure 15).

*SOG1* transcript levels showed no significant differences between the plant types (p = 0.610) or dose rates (p = 0.776). There was also no significant interaction between plant type and dose rate (p = 0.343) (Table 13; Figure 15).

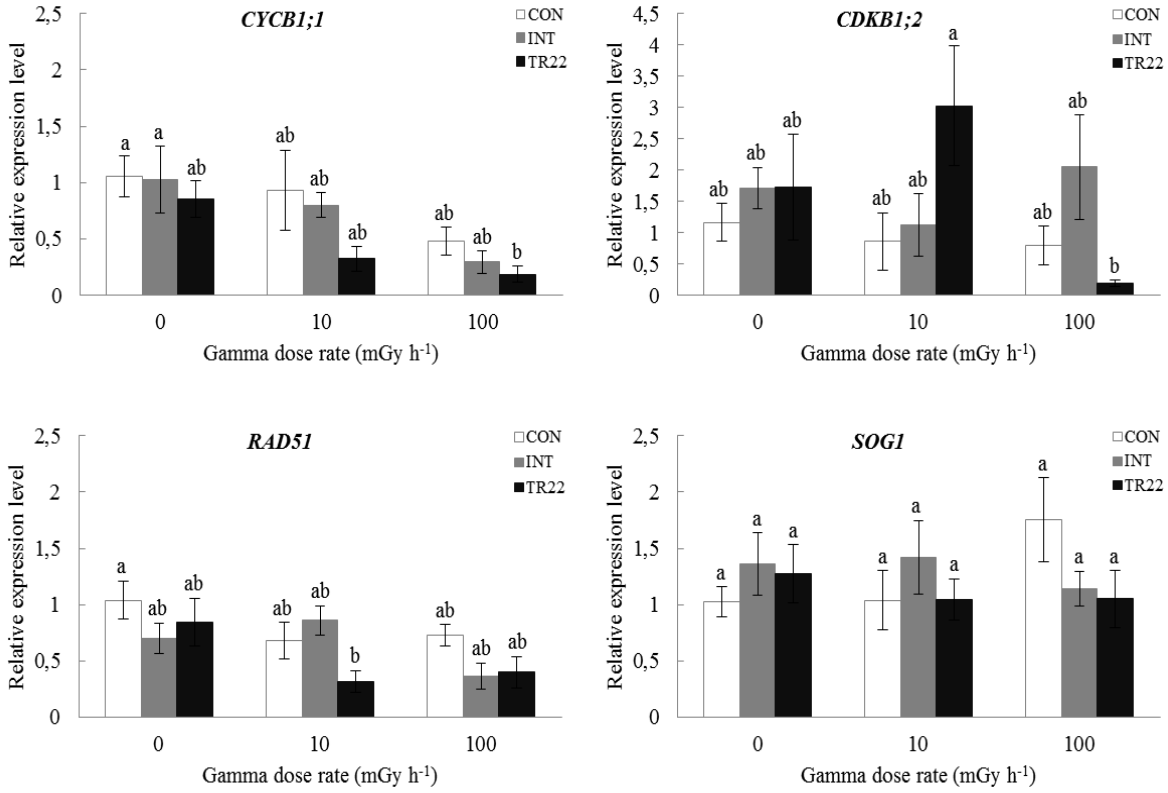


Figure 15. Effect of exposure to gamma radiation for 144 h 7–12 days after sowing on relative transcript levels of specific cell division controlling genes (*CYCKB1;1* (*CYC = CYCLIN*), *CDKB1;2* (*CDK = CYCLIN-DEPENDENT KINASE*)) and DNA repair genes (*RADIATION 51* (*RAD51*), *SUPPRESSOR OF GAMMA RESPONSE 1* (*SOG1*)) in shoots of Scots pine seedlings grown from seeds from different areas in the Chernobyl region with background (CON), intermediate (INT) and high (TR22) levels of ionizing radiation (see table 2). The transcript levels were normalized against *ACTIN* (*ACT*) and *GLYCERALDEHYDE-3-PHOSPHATE DEHYDROGENASE* (*GAPDH*) and shown relative to the unexposed control (i.e. CON 0). The results are mean ± SE of 4 biological replicates (n = 4) with 3–4 technical replicates per dose rate and plant type (seed source). Different letters within a diagram indicate significant differences ($p \leq 0.05$) based on two-way ANOVA in the general linear model mode followed by Tukey's post hoc test.

Table 13. ANOVA (general linear model) table for the overall effect of 144 h exposure to gamma radiation 7-12 days after sowing on relative transcript levels of *CYCB1;1*, *CDKB1;2*, *RAD51* and *SOG1* genes of Scots pine seedlings grown from seeds from different areas in the Chernobyl region with background (CON), intermediate (INT) and high (TR22) levels of ionizing radiation (see Table 2). The main effects of plant type and dose rate and their interactions were analyzed. There were 3 levels for each factor (Plant type: CON, INT and TR22; Dose rate: 0, 10 and 100 mGy $h^{-1}$). The results are mean ± SE of 4 biological replicates (n = 4) with 3–4 technical replicates. The data were log-transformed before analysis.

| **Source** | **DF** | **Adj SS** | **Adj MS** | **F-Value** | **P-Value** |
|---|---|---|---|---|---|
| ***CYCB1;1*** | | | | | |
| Plant type | 2 | 0.6862 | 0.34311 | 3.38 | 0.049 |
| Dose rate | 2 | 1.9735 | 0.98676 | 9.73 | 0.001 |
| Plant type*Dose rate | 4 | 0.3355 | 0.08388 | 0.83 | 0.519 |
| Error | 27 | 2.7371 | 0.10137 | | |
| Total | 35 | 5.7324 | | | |
| ***CDKB1;2*** | | | | | |
| Plant type | 2 | 0.3230 | 0.1615 | 1.00 | 0.382 |
| Dose rate | 2 | 0.6832 | 0.3416 | 2.12 | 0.141 |
| Plant type*Dose rate | 4 | 2.5896 | 0.6474 | 4.02 | 0.012 |
| Error | 25 | 4.0308 | 0.1612 | | |
| Total | 33 | 7.6768 | | | |
| ***RAD51*** | | | | | |
| Plant type | 2 | 0.4835 | 0.24173 | 3.54 | 0.043 |
| Dose rate | 2 | 0.5130 | 0.25650 | 3.76 | 0.036 |
| Plant type*Dose rate | 4 | 0.5085 | 0.12712 | 1.86 | 0.146 |
| Error | 27 | 1.8417 | 0.06821 | | |
| Total | 35 | 3.3466 | | | |
| ***SOG1*** | | | | | |
| Plant type | 2 | 0.03461 | 0.017306 | 0.50 | 0.610 |
| Dose rate | 2 | 0.01762 | 0.008808 | 0.26 | 0.776 |
| Plant type*Dose rate | 4 | 0.16205 | 0.040513 | 1.18 | 0.343 |
| Error | 27 | 0.92833 | 0.034383 | | |
| Total | 35 | 1.14261 | | | |

"*" indicates interaction between the factor Plant type and Dose rate

# 5. Discussion

In their natural environment, plants as sessile organism are generally exposed to low, non-damaging background levels of ionizing radiation such as gamma radiation. However, some areas in the environment have elevated, potentially harmful levels of radiation especially from anthropogenic sources including radioactive accidents, nuclear testing, nuclear weapon test fallout, nuclear power plants accidents, stockpiles of nuclear waste etc.

There have been a wide range of studies about the adverse effects of acute and chronic radiation after nuclear accidents like in Chernobyl and in laboratory studies (Tulik, 2001; Yoschenko et al., 2018; Zelena et al., 2005). Nevertheless, studies about sensitivity to gamma irradiation of plant seedlings under standardized exposure conditions is scarce, particularly for low-moderate dose rates, when seeds developed under elevated level of ionizing radiation. It is hypothesized that plants grown from seeds that developed under elevated level of ionizing radiation will show adaptation to such radiation in the sense that their radiosensitivity is enhanced. In the work of this thesis, we studied the sensitivity to gamma irradiation from a $^{60}$Co source in Scots pine seedlings grown from seeds from different areas in the Chernobyl region with background (CON), intermediate (INT) and high (TR22) levels of ionizing radiation. Thus, we aimed to investigate whether those seedlings had primed mechanisms contributing to tolerance to low-moderate gamma radiation levels.

## 5.1 Effect of gamma radiation on plant growth

Although there have been reports of negative effects of gamma radiation on conifer seed germination and seedling growth, as well as growth and cell abnormalities in older plants in response to ionizing radiation (Mergen & Strøm Johansen, 1964; Rudolph, 1971; Tulik, 2001; Yoschenko et al., 2018; Zelena et al., 2005), there is limited evidence on the effects of gamma radiation on young conifer seedlings.

In spite of some statistically significant small differences between plant types and specific dose rates in our study, like e.g. the increased root and shoot length in TR22 seedlings at 10 mGy $h^{-1}$ and 0-40 mGy $h^{-1}$, respectively compared to the unexposed CON seedlings, we have not found any clear overall dose-response relationship between root or shoot length and the gamma irradiation in or between the plant types after 144 h gamma irradiation (Figure 8). This is in contrast to a recent study showing an evident dose-response relationship with

significantly reduced seedling lengths (roots and shoots together) in Norway spruce and Scots pine after 144 h exposure to gamma radiation at dose rates ≥ 40 mGy $h^{-1}$ (Blagojevic et al., 2019a). Another study by Blagojevic et al. (2019b) reported growth inhibition in response to 6 days of gamma dose rates of 42.9 and 125 mGy $h^{-1}$ in shoots and 125 mGy $h^{-1}$ in roots but no additional adverse effect of simultaneous gamma and UV-B radiation on root or shoot lengths. Generally, the radiosensitivity in plants has been shown to depend on several factors such as species, plant developmental stage, cultivar, tissue architecture, physiology, plant genome organization and exposure scenario (Caplin & Willey, 2018; De Micco et al., 2011). Conifers including Scots pine are considered among the most sensitive species (Caplin & Willey, 2018; De Micco et al., 2011). The reason for specific small but significant differences between plant types at some dose rates only (e.g. at 10 mGy $h^{-1}$ but not the highest dose rates) in our study, which is different from the studies of Blagojevic et al. (2019a, b) remains elusive. A possible assumption could be that it may not be a real effect of gamma irradiation. As the seed materials were from three different areas in Chernobyl with background, intermediate and high levels of ionizing radiation, the seedlings grown from those seeds might have adapted to elevated radiation and do not exhibit any phenotypic changes when further exposed to gamma irradiation. However, as discussed below, at day 29 post-irradiation, reduced growth was observed. This implies that, these seedlings may need some time to exhibit growth changes. Also, in our study, slightly different environmental factors utilized during the gamma exposure experiment and the subsequent post-irradiation growth phase including light, temperature, air humidity etc. may possibly be potential sources of variability.

### 5.2 Post-irradiation effect of gamma radiation on plant growth

The growth inhibition in response to the 144 h gamma radiation during the post-irradiation phase included reduced number of needle and shoot diameter (i.e. length of needles) for all the CON, INT and TR22 seedlings of Scots pine at ≥ 40 mGy $h^{-1}$, but no significant alterations/changes in cumulative growth (i.e. shoot elongation) (Figure 11, 12, 13). Thus, although the CON, INT and TR22 seedlings did not show any significant difference in root and shoot length at the end of the 144 h gamma irradiation, the seedlings exhibited post-irradiation (recorded up to day 29) growth inhibition for at least some growth parameters. Overall, all the plant types showed a consistent reduction in number of needles at ≥ 40 mGy $h^{-1}$, compared to their corresponding unexposed seedlings (Figure 12). The CON seedlings

showed reduced number of needles at ≥ 40 mGy $h^{-1}$, compared to the unexposed CON seedlings, whereas the INT seedlings exhibited reduced number of needles at 10, 40 and 100 mGy $h^{-1}$ compared to the unexposed INT seedlings. On the other hand, the number of needles for the TR22 seedlings was reduced significantly at ≥ 20 mGy $h^{-1}$ compared to the unexposed TR22 seedlings. Overall, all the plant types showed a consistent reduction in shoot diameter at ≥ 40 mGy $h^{-1}$, compared to their corresponding unexposed seedlings (Figure 13). The CON and TR22 seedlings showed reduced shoot diameter at ≥ 40 mGy $h^{-1}$, compared to the unexposed CON and TR22 seedlings, whereas the INT seedlings exhibited reduced number of needles at 10 and 100 mGy $h^{-1}$, compared to the unexposed INT seedlings. However, in the current study, we did not observe any significant difference in reduction of number of needles and shoot diameter when comparing among those plant types at different dose rates, which may suggest that all the plant types responded in a similar manner towards the 144 h gamma exposure at different gamma dose rates post-irradiation irrespective of their seed source. The difference in delay in growth inhibition after 144 h gamma exposure and post-irradiation implies that the negative effect of gamma dose rates may take some time to be evidenced. Like at the end of the gamma radiation, there was also some variation in the post-irradiation growth responses for different growth parameters, such as the INT seedlings showing significantly reduced number of needles but not reduced shoot diameter at dose rate of 40 mGy $h^{-1}$.

The variation in growth between different dose rates of gamma irradiation, i.e. variation that was not due to a systematic dose-response relationship or systematic differences between the plant types in this respect, could possibly be explained at least to a slight extent by genetic variation since population materials were used. Since the seeds of the CON, INT and TR22 seedlings were collected from three different region of Chernobyl with different background radiation under seed development, they could have responded slightly differently to further gamma treatment. Also, variation in growth responses between some dose rates and plant types could possibly be due to differences in DNA damage and DNA repair between individuals.

Cell division and cell elongation in the shoot apical meristem (SAM) are required for shoot elongation, needle formation, growth and development and it thus follows that the gamma irradiation altered these basic growth processes (Blagojevic, 2019). When Scots pine seedlings subjected to up to 40 mGy $h^{-1}$ were grown further 7-8 months post-irradiation, the

growth inhibition in response to 144 h of gamma irradiation was no longer visible, indicating that cell division and cell elongation had been normalized (Blagojevic et al., 2019b).

Many studies are available on the alterations of growth and development of pine trees under acute and chronic radiation conditions. The lowest dose that caused morphologic effects in the Chernobyl accident zone (shoot growth reduction of pine trees, emergence of morphosis in the year after the accident) was found to be 0.43 Gy $year^{-1}$ (Sidorov, 1994). Under chronic radiation conditions, young Scots pine trees in Chernobyl and Japanese red pine and Japanese fir in the Fukushima zone lost their apical dominance (Yoschenko et al., 2018). One year after the Chernobyl accident, abnormal long needles of about 120 mm compared to the normal length of about 70 mm were observed in older Scots pine trees (Goltsova et al., 1991). Previous research on older Scots pine plants in the Bryansk area of Russia, which was polluted by the Chernobyl disaster, found an increased frequency of necrotic needles in response to ionizing radiation with increasing levels of radiation exposure ranging from 0.1 to 130 mGy $year^{-1}$ (calculated values for 2008) (Makarenko et al., 2016). Moreover, some studies have found growth stimulation in crops subjected to low doses of ionizing radiation, such as, increased callus fresh weight and dry weight in carrot (*Daucus carota*) and increased fruit yield weight in tomato (*Lycopersicon esculentum*) (Al-Safadi & Simon, 1990; Sidrak & Suess, 1973). Another study reported the symmetry of Scots pine needles from the Chernobyl Exclusion Zone (ChEZ) was not affected with the external and internal dose rate in the range of 0.1 - 40 μGy $h^{-1}$ and 0.1 - 273 μGy $h^{-1}$ respectively (Kashparova et al., 2020).

Blagojevic et al. (2019a) reported several reduced growth parameters such as shoot elongation, needle length (shoot diameter) and number of needles, post-irradiation in a dose-rate dependent manner from 40-540 mGy $h^{-1}$ in Norway spruce and Scots pine conifers after 144 h gamma irradiation. Another recent study by Blagojevic et al. (2019b) reported normal appearance of the SAM and needle anatomy at dose rates 0-125 mGy $h^{-1}$ 44 days post-irradiation. However, gamma-induced growth inhibition was then generally visible at lower dose rates post-irradiation than at the end of the irradiation, with growth parameters such as shoot elongation, number of needles and shoot diameter being negatively affected post-irradiation from 20 mGy $h^{-1}$ in Scots pine plants (Blagojevic et al., 2019b). In our study, the post-irradiation growth inhibition was manifested as reduced number of needles and shoot diameter at ≥ 40 mGy $h^{-1}$ for the CON, INT and TR22 seedlings. However, in our study, the shoot elongation did not show any significant difference for these seedling types. A possible explanation for the variation between the post-irradiation gamma effect on growth parameters

in the previous studies by Blagojevic et al. (2019a, b) and our study, which were all performed under controlled conditions, could be associated with several factors such as slightly different environmental conditions under the exposure to ionizing radiation and the post-irradiation cultivation as well as possibly slightly different developmental stages.

### 5.3 Effect of gamma radiation on DNA damage

DNA damage produces abnormal chemical structure in DNA. Ionizing radiation is a well-known factor that can produce DNA damage and acute high doses of 10-1000 Gy have been proposed as potentially lethal to plants (United Nations Scientific Committee on the Effects of Atomic Radiation [UNSCEAR], 1996). Ionizing radiation interacts with water molecules, resulting in the production of ionized water molecules ($H_2O^+$) and ROS. Interaction of ROS with DNA causes oxidative damage such as base alterations and single and double strand DNA breaks (Belli et al., 2002; Roldán-Arjona & Ariza, 2009). In order to reverse oxidative products and other chemical alterations, DNA repair mechanisms play an important role (Hu et al., 2016). Also, various DNA repair mechanisms are active during different phases of the cell cycle, allowing cells to repair DNA damage (Chatterjee & Walker, 2017). However, in most plant species, DNA repair mechanisms are less well studied than in *Arabidopsis* and a variety of other organisms. Despite the fact that radiosensitivity varies by plant species, it is widely known that plant cells are more resistant to the formation of dsDNA breaks and repair them quicker than animal cells (Hu et al., 2016; Yokota et al., 2005).

In our study, to check the radiosensitivity of the DNA, the COMET assay was performed to assess the DNA damage in the gamma-irradiated Scots pine seedlings grown from the seeds from different areas in the Chernobyl area with background (CON), intermediate (INT) and high (TR22) ionizing radiation (Figure 9, 14). Although the CON, INT and TR22 plant types did not show any significant effect of the gamma radiation on the root and shoot lengths at the end of the 144 h gamma irradiation, a dose-rate dependent DNA damage was present in all three plant types at 1 to 100 mGy $h^{-1}$. However, among the plant types, the CON seedlings showed higher radiosensitivity with respect to DNA damage at 40 and 100 mGy $h^{-1}$ compared to the INT and TR22 seedlings (Figure 9). Although a correlation could be expected between growth and DNA damage, our results revealed that DNA damage may be tolerated to some extent without affecting growth.

A recent study of comparative radiosensitivity of Scots pine, Norway spruce and the highly radioresistant herbaceous plant *A. thaliana* also showed dose-rate dependent DNA damage immediately after 144 h gamma irradiation (Blagojevic et al., 2019a). All species exhibited significantly increased DNA damage from 1 or 10 mGy $h^{-1}$ up to the highest tested dose rate 400 or 540 mGy $h^{-1}$ after 144 h of gamma irradiation as well after 360 h for *A. thaliana* (360 h not tested for the conifers) (Blagojevic et al., 2019a). Another study with 48 h of gamma irradiation of Norway spruce showed significantly increased DNA damage from 1 mGy $h^{-1}$ when growth inhibition was not observed (Blagojevic, 2019). DNA damage in a dose-rate dependent manner has also been reported in a variety of other plant species after gamma irradiation from a $^{60}$Co source. For example, tobacco (*Nicotiana tabacuum*) exposed to 0.39 and 0.47 Gy $min^{-1}$, Lombardy poplar (*Populus nigra*) exposed to dose rates ranging from 0.5 to 15 Gy $h^{-1}$ for 20 h, and rice (*Oryza sativa*) exposed to 25 and 50 Gy given as 0.28 Gy $min^{-1}$ or 50, 100, and 200 Gy provided as 5.15 Gy $min^{-1}$ (Macovei & Tuteja, 2013).

In the current study, dose-rate dependent DNA damage was also detected in the CON, INT and TR22 plant types day 30 post-irradiation (Figure 14). All the plant types then showed significantly increased DNA damage from 1 to 100 mGy $h^{-1}$, compared to their corresponding unexposed plants. As expected, our results showed correlation between post-irradiation DNA damage and growth inhibition at the highest dose rates (≥ 40 mGy $h^{-1}$) in all plant types. However, the CON seedlings showed more DNA damage at 40 and 100 mGy $h^{-1}$ compared to the TR22 seedlings (Figure 14) but the difference in DNA damage level between the plant types was not associated with any difference in growth. Also, at day 30, significantly increased DNA damage after exposure to the lowest gamma dose rates (1, 10 and 20 mGy $h^{-1}$) did not reflect any significant changes in number of needles and shoot diameter.

Blagojevic et al. (2019a) reported significantly increased level of DNA damage in Norway spruce and Scots pine shoot tips at ≥ 1 mGy $h^{-1}$ and ≥ 10 mGy $h^{-1}$, respectively 44 days post-irradiation. These dose rates were lower than those that affected the conifers' post-irradiation growth negatively (≥ 40 mGy $h^{-1}$). However, Scots pine roots then showed DNA damage at 40 and 100 mGy $h^{-1}$, while no increase in DNA damage in Norway spruce roots was observed in any of the tested dose rates. *A. thaliana* leaves exhibited increased level of DNA damage from 1 to 400 mGy $h^{-1}$ 44 days post-irradiation after 360 h gamma exposure (Blagojevic et al. 2019a). Another study by these authors showed the presence of DNA damage in Norway spruce at day 77 post-irradiation after 48 h of gamma exposure at dose rates from ≥ 1 mGy $h^{-1}$ (Blagojevic, 2019). This implies long term effects from short term gamma exposures.

Since the DNA damage in Scots pine and other species after short-term gamma irradiation was observed for an extended time period in our and previous studies (Figure 14; Blagojevic, 2019; Blagojevic et al., 2019a, b), we may assume that the gamma irradiation caused significant genomic instability. Another possibility is that DNA repair failed to counteract the long-term consequences of DNA damage, or that stem cells continued to produce damaged daughter cells that survived and grew. In animal cells, there is evidence of radiation-induced genomic instability, but this knowledge is limited in plants (Hurem et al., 2017; Morgan, 2003; Morgan et al., 1996; Mothersill & Seymour, 1998). However, following the initial insult, gamma irradiated tobacco cells produced constant micronuclei in progeny of multiple generations, providing direct evidence of radiation-induced genomic instability in higher plant cells (Yokota et al., 2010). Previous research showed that DNA repair genes, oxidative stress response genes, and signal transduction genes were activated in *A. thaliana* exposed to acute irradiation (1 Gy in 1 day), while expression of DNA repair genes and antioxidant genes was not changed upon exposure to more chronic irradiation (1 Gy in 21 days) (Ali et al., 2015; Kovalchuk et al., 2007).

### 5.4 Effect of gamma radiation on total antioxidant capacity

As discussed above, DNA damage can be induced by direct ionization or production of excess ROS, which can damage DNA and other macromolecules, when exposed to ionizing radiation such as gamma radiation. ROS has the capacity to induce oxidative damage to single bases of DNA, as well as single and double strand breaks in DNA (Biedermann et al., 2011). Cellular ROS production is counterbalanced by the activity of cellular antioxidant enzymes, macro or micro molecules and other redox molecules under normal physiological circumstances. Antioxidants are compounds with one or more free electrons that can be supplied to stabilize ROS. Antioxidants comprise both hydrophilic and lipophilic compounds able to metabolize ROS and these can be localized in different tissues or cells transiently. Due to their potentially damaging effects, excessive ROS must be quickly neutralized and removed from cells by a variety of antioxidant defense mechanisms.

Gamma radiation can induce the formation of ROS, such as $H_2O_2$, which can damage lipids, proteins and DNA (Biedermann et al., 2011; Gill & Tuteja, 2010). Plants are induced to produce antioxidant enzymes such as catalase (CAT), glutathione reductase (GR), ascorbate peroxidase (APOD), syringaldazine peroxidase (SPOD), and guaiacol peroxidase (GPOD) in

order to reduce elevated levels of singlet oxygen ($^1O_2$), superoxide radical ($O_2^-$), and hydrogen peroxide ($H_2O_2$) (Apel & Hirt, 2004; Van Hoeck et al., 2015).

A recent study showed a substantial dose-rate dependent increase in $H_2O_2$ level after gamma radiation in Scots pine seedlings at 42.9 and 125 mGy $h^{-1}$, which was consistent with observed dose-rate dependent growth inhibition and subsequent DNA damage (Blagojevic et al., 2019b). The level of phenolic compounds such as flavonoids kaempferol glycosides were induced by UV-B, whereas no effect of gamma radiation on such compounds was observed (Blagojevic et al., 2019b). An RNA-seq study of Norway spruce seedlings after 48 h gamma irradiation showed that genes involved in flavonoid biosynthesis process were upregulated at 100 mGy $h^{-1}$ (Blagojevic, 2019). Van Hoeck et al. (2017) also reported that transcription levels of a substantial number of genes in *L. minor* related to flavonoid and lignin biosynthesis were upregulated up to a dose rate of 232 mGy $h^{-1}$.

Some studies reported no major alterations in antioxidative enzyme capacities in *A. thaliana* exposed to gamma irradiation (Vandenhove et al., 2010; Vanhoudt et al., 2010, 2011). On the other hand, Vanhoudt et al. (2014) reported enhanced activities of SOD and APX in roots at a dose of 58.8 Gy, while no alterations in SOD, CAT and SPX capacities were observed in the leaves but GPX exhibited decreased level at the highest doses of 6.7 – 58.8 Gy, and increased level at the lowest dose of 3.9 Gy. A significant change in CAT activity was found in *L. minor* at a dose rate of 27 mGy $h^{-1}$ upon 7 days exposure to gamma radiation (Van Hoeck et al., 2015). Volkova (2017) reported no significant changes in the activities of SOD, CAT and POD in Scots pine under the natural background dose rates in the range of 0.03 - 38.6 mGy $year^{-1}$, implying that this range of dose rates is insufficient to induce any essential biological effect.

In our study, we measured the total antioxidant capacity of the CON, INT and TR22 seedlings exposed to three different gamma dose rates (i.e. 0, 10 and 100 mGy $h^{-1}$) after 144 h gamma irradiation (Figure 10). Although, there are many studies that reported gamma radiation and also UV-B induce the formation of different groups of antioxidants (Ahmad et al., 2010; Gill & Tuteja, 2010; Hahlbrock & Scheel, 1989; Jansen & Bornman, 2012; Mittler et al., 2004), we did not observe any significant effect of gamma treatments on total antioxidant capacity when entire seedlings were analyzed. The lack of a dose-response relationship with respect to effect of gamma radiation on the total antioxidant capacity in the different plant types in our study remains elusive. However, a similar result was found in a

recent study of Scots pine that showed no significant effect of gamma irradiation and UV-B treatments on total antioxidant capacity when entire seedlings or shoots only were analyzed (Blagojevic et al., 2019b).

Antioxidants are not evenly distributed in a plant. Different parts of a plant such as needles, shoots, roots etc. and cells may have different concentrations of antioxidant. In our study, we analyzed the whole seedling as a crude sample. For further research, we could analyze the total antioxidant capacity of different parts of seedlings separately. Furthermore, in our study, the sample number was comparatively limited and we choose three dose rates only (i.e. 0, 10 and 100 mGy $h^{-1}$) due to the cost of the analyses and available time for analysis. Selecting more gamma dose rates and smaller plant parts/tissues could possibly provide more elaborated scenario of these seedlings on total antioxidant capacity.

### 5.5 Effect of gamma radiation on transcript levels of genes

Although acute and chronic stress may elicit various responses in plants, previous research have suggested that plants respond to acute radiation and other stressors in similar ways, including immediate damage repair, activation of pro-survival mechanisms, and inhibition of cell division and differentiation (Kovalchuk et al., 2007).

The *CYCB1* gene, which encodes a B type mitotic cyclin, was significantly induced in *A. thaliana* following an 8 h gamma treatment of 100 Gy (Culligan et al., 2006). Another previous study showed upregulated transcript level of *CYCB1;2* upon 144 h gamma exposure in *A. thaliana* between 40 and 400 mGy $h^{-1}$ as compared to the unexposed control, 1 and 10 mGy $h^{-1}$, and in Scots pine between 10 and 40 mGy $h^{-1}$; whereas Norway spruce expressed no difference in transcript level among different gamma dose rates despite of similar DNA damage levels. On the other hand, *CYCD3;1* and *CDKB1;2* displayed no evidence of upregulation at their transcript level in any of these species (Blagojevic et al., 2019a). Ali et al. (2015) reported upregulation of *CYCD3;1* in *A. thaliana* after UV-B stress. However, in our study, the *CYCB1;1* transcript level was downregulated in TR22 seedlings at 100 mGy $h^{-1}$ after 144 h gamma irradiation as compared to the unexposed CON seedlings, while *CDKB1;2* transcript level did not show any significant difference between the CON, INT and TR22 seedlings (Figure 15). A recent RNA-seq study in Norway spruce seedlings subjected to 48 h gamma irradiation reported downregulation of *CYCB1;1* and *CYCB1;2* at 100 mGy $h^{-1}$ and upregulation of *CYCB2;3* and *CDKB2;2* only at 40 mGy $h^{-1}$ (Blagojevic, 2019).

We also quantified the transcript levels of the DNA repair-related genes *RAD51* and *SOG1* in the CON, INT and TR22 seedlings of Scots pine after 144 h gamma irradiation using qPCR (Figure 15). The *RAD51* transcript level appeared downregulated in TR22 seedlings at 10 mGy $h^{-1}$ after 144 h gamma irradiation as compared to the unexposed CON seedlings. In comparison, *SOG1* did not show any significant difference in transcript level in between any of the dose rates and plant types after the gamma radiation treatments (Figure 15). *RAD51* and *SOG1* were shown to be induced in *A. thaliana* exposed to 100 Gy of gamma radiation for 8 h (Culligan et al., 2006; Yoshiyama et al., 2009). A recent study demonstrated the induction of *RAD51* and *SOG1* in Scots pine and *A. thaliana* after 144 h gamma treatment, although the overall radiosensitivity with respect to growth and development, DNA damage and mortality was similar in Scots pine and Norway spruce; and *A. thaliana* was far less affected and showed no damage or mortality (Blagojevic et al., 2019a). In their study, *RAD51* gene expression was increased in Scots pine at 10 mGy $h^{-1}$ and in *A. thaliana* from 180 to 400 mGy $h^{-1}$, whereas Norway spruce did not show any difference. Also, *SOG1* expression did not exhibit any induction in any of those plant species after gamma irradiation (Blagojevic et al., 2019a).

However, overexpression of several DNA repair genes including *SOG1* (upregulated at 100 mGy $h^{-1}$), *DNA LIGASE 4* (*LIGIV*), *ATP-DEPENDENT DNA HELICASE 2 SUBUNIT KU80* (*KU80*), *X-RAY REPAIR CROSS-COMPLEMENTATION PROTEIN 2* (*XRCC2*), *X-RAY REPAIR CROSS-COMPLEMENTATION PROTEIN 3* (*XRCC3*) and *GAMMA RESPONSE 1* (*GR1*) were found in an RNA-seq study of Norway spruce after 48 h of gamma irradiation, as well as the *WEE1* gene, which is also involved in cell cycle arrest (Blagojevic, 2019). De Schutter et al. (2007) also reported a similar upregulation of *SOG1* and *WEE1* in *A. thaliana*.

Overall, although the transcript levels of certain genes were reduced in response to gamma irradiation among the CON, INT and TR22 Scots pine plants, there were no consistent differences that may assist to explain the DNA damage differences in response to gamma irradiation between these plant types. In addition, the differences in expression of specific genes between our study and previous studies may possibly also be due to several factors such as different exposure conditions, different radiation levels and growth conditions, as well as difference between plant types and species and their developmental stage.

### 5.6 Other factors that might have affected the results

In our study, different environmental factors employed in the gamma exposure experiments and subsequent growth including light, temperature, air humidity etc. may possibly be potential sources of variability. Moreover, since the seedlings were grown in 5 cm diameter Petri dishes when exposed to the gamma radiation, there was some variation in exposure among individual seedlings. Although the Petri dishes were rotated in the middle of the gamma exposure period in all experiments to get a more even irradiation, this may have led to some variation. To measure the total antioxidant capacity and to measure the transcript level of specific genes in qPCR, we selected samples that were irradiated with 0, 10 and 100 mGy $h^{-1}$. This was due to the cost of the analyses and the available time for analyses. This may act as possible factors causing variability and uncertainty between results. Hence, to get a better picture of the effects on gamma radiation on the gene expression during gamma irradiation, more gamma treatments should be included.

RNA quality could also be a factor that affects the gene expression of specific genes studied in this thesis. Although, proper care has been taken for handling the samples from RNA isolation to qPCR, we cannot ignore the errors during experimentation and the fact that Scots pine has inherently high levels of substances such as phenolic that may interfere with the RNA isolation. The specificity of qPCR primers of specific genes studied could be another possible factor for expressing variable transcript level of those genes. The genome sequence of Scots pine has not yet been published and the primer design had to be largely based on the published genome of another pine species (loblolly pine (*Pinus taeda*)).

## 6. Conclusions

The CON, INT and TR22 seedlings of Scots pine did not show any significant difference in root and shoot length after 144 h gamma irradiation, and there was also no clear dose-response relationship for any of the plant types. However, all the plant types showed clear dose-rate dependent DNA damage at the end of the gamma irradiation. Interestingly, the DNA damage then differed between the plant types, with less DNA damage in the TR22 seedlings than the CON plants at dose rates ≥ 40 mGy $h^{-1}$. Although post-irradiation shoot elongation did not differ significantly between these plant types, the number of needles and shoot diameter generally showed significant reduction at ≥ 40 mGy $h^{-1}$, and this correlated with persistent DNA damage at day 30 post-irradiation. In spite of the differences in DNA damage between different dose rates and plant types, the total antioxidant capacity, as analyzed by the FRAP assay, did not differ significantly between the plant types after the 144 h gamma exposure. The transcript levels of cell division controlling genes and DNA repair genes did also not show any consistent significant differences between the plant types and gamma dose rates after the 144 h gamma treatment. The *CDKB1;2* and *SOG1* showed no induction in gene expression compared to the unexposed CON seedlings, whereas *CYCB1;1* and *RAD51* expression were reduced in the TR22 seedlings at 100 and 10 mGy $h^{-1}$, respectively, compared to the unexposed CON seedlings. Further experimentation for specific antioxidants of these plant types and qPCR analysis of different target genes could possibly provide us more consistent results that would show their association with growth alterations and DNA damage. Although all the CON, INT and TR22 plant types showed a dose-rate dependent DNA damage after 144 h gamma radiation and post-irradiation, the CON plant type displayed higher radiosensitivity at cellular level particularly at higher dose rates of 40 and 100 mGy $h^{-1}$.

## 7. Further perspectives

The results of this study will contribute further to our knowledge about the radiosensitivity to gamma radiation of Scots pine seedlings grown from seeds developed under elevated levels of ionizing radiation in the Chernobyl area. Although DNA damage after gamma irradiation was higher in the CON seedlings grown from seeds developed under background level of ionizing radiation than in the INT and TR22 seedlings originating from seeds from higher radiation levels, no systematic differences were found for the other characteristics analyzed (growth, antioxidant capacity and expression of selected cell division- and DNA repair related genes). Thus, more biological parameters should be analyzed to try to explain the background of the different DNA damage in the different plant types.

In our study, the growth studies after 144 h gamma irradiation did not demonstrate any clear overall dose-response relationship between the plant types and dose rates, while some post-irradiation growth alterations were observed at higher dose rates. However, we did not perform any histological studies to detect the status of the tissues or cells of the different plants types at different dose rates. Study of histology of shoot and root apical meristems (SAM and RAM, respectively) as a further approach will possibly link between the plant growth and DNA damage.

Surprisingly, our result on total antioxidant capacity has no association with the DNA damage and the reason for this remains elusive. However, for further research, increasing the number of samples and gamma treatment levels, and analysis of root and shoot samples and possibly even different tissues separately are recommended for total antioxidant capacity analysis. Also, detailed analysis of ROS (such as $H_2O_2$), analysis of particular antioxidants and phenolic compounds will increase our understanding about how the different plant types react at the cellular level.

After 144 h of gamma irradiation, expression of the selected cell division- and DNA repair-related genes tested in this study showed no consistent differences between the plant types and gamma dose rates. Further qPCR analysis of multiple target genes or RNA-seq analyses might potentially provide results that may indicate something about the basis of the differences in DNA damage between the plant types and why these are not associated with differences in growth. More DNA repair-related genes from the different DNA repair pathways and specific antioxidant- and defense-related genes would be particularly

interesting to address. Also, epigenetics-related genes would be highly interesting to analyze since environmental conditions during embryogenesis (seed development) is known to induce an epigenetic memory effect impacting on gene expression in conifer species (Carneros et al., 2019). Moreover, producing mutants of our study materials and further functional analysis of different target genes including genes involved in defense mechanisms and antioxidant genes in parallel could provide us a better understanding of specific genes function at molecular level.

## 8. References


1. Adachi, S., Minamisawa, K., Okushima, Y., Inagaki, S., Yoshiyama, K., Kondou, Y., Kaminuma, E., Kawashima, M., Toyoda, T., Matsui, M., Kurihara, D., Matsunaga, S., & Umeda, M. (2011). Programmed induction of endoreduplication by DNA double-strand breaks in *Arabidopsis*. *Proceedings of the National Academy of Sciences of the United States of America*, *108*(24), 10004–10009. https://doi.org/10.1073/pnas.1103584108
2. Ahmad, P., Jaleel, C. A., Salem, M. A., Nabi, G., & Sharma, S. (2010). Roles of enzymatic and nonenzymatic antioxidants in plants during abiotic stress. *Critical reviews in biotechnology*, *30*(3), 161–175. https://doi.org/10.3109/07388550903524243
3. Alexakhin, R. M., Sanzharova, N. I., Fesenko, S. V., Spiridonov, S. I., & Panov, A. V. (2007). Chernobyl radionuclide distribution, migration, and environmental and agricultural impacts. *Health physics*, *93*(5), 418–426. https://doi.org/10.1097/01.HP.0000285093.63814.b7
4. Ali, H., Ghori, Z., Sheikh, S., & Gul, A. (2015). Effects of gamma radiation on crop production. In *Crop production and global environmental issues* (pp. 27-78). Springer, Cham.
5. Al-Safadi, B., & Simon, P. W. (1990). The effects of gamma irradiation on the growth and cytology of carrot (*Daucus carota* L.) tissue culture. *Environmental and experimental botany*, *30*(3), 361-371. https://doi.org/10.1016/0098-8472(90)90049-A
6. Amiard, S., Charbonnel, C., Allain, E., Depeiges, A., White, C. I., & Gallego, M. E. (2010). Distinct roles of the ATR kinase and the Mre11-Rad50-Nbs1 complex in the maintenance of chromosomal stability in *Arabidopsis*. *The Plant cell*, *22*(9), 3020–3033. https://doi.org/10.1105/tpc.110.078527
7. Amiard, S., Gallego, M. E., & White, C. I. (2013). Signaling of double strand breaks and deprotected telomeres in *Arabidopsis*. *Frontiers in plant science*, *4*, 405. https://doi.org/10.3389/fpls.2013.00405
8. Apel, K., & Hirt, H. (2004). Reactive oxygen species: metabolism, oxidative stress, and signal transduction. *Annual review of plant biology*, *55*(1), 373-399. https://doi.org/10.1146/annurev.arplant.55.031903.141701
9. Arkhipov, N. P., Kuchma, N. D., Askbrant, S., Pasternak, P. S., & Musica, V. V. (1994). Acute and long-term effects of irradiation on pine (*Pinus silvestris*) strands post-Chernobyl. *The Science of the total environment*, *157*(1-3), 383–386.
10. Armenise, L., Simeone, M. C., Piredda, R., & Schirone, B. (2012). Validation of DNA barcoding as an efficient tool for taxon identification and detection of species diversity in Italian conifers. *European journal of forest research*, *131*(5), 1337-1353. https://doi.org/10.1007/s10342-012-0602-0
11. Belli, M., Sapora, O., & Tabocchini, M. A. (2002). Molecular targets in cellular response to ionizing radiation and implications in space radiation protection. *Journal of radiation research*, *43 Suppl*, S13–S19. https://doi.org/10.1269/jrr.43.s13
12. Bennett, M. D., & Leitch, I. J. (2012). The Plant DNA C-values database (release 6.0, Dec. 2012, http://data.kew.org/cvalues)

13. Beresford, N. A., Scott, E. M., & Copplestone, D. (2020). Field effects studies in the Chernobyl Exclusion Zone: Lessons to be learnt. *Journal of environmental radioactivity*, *211*, 105893. https://doi.org/10.1016/j.jenvrad.2019.01.005
14. Biedermann, S., Mooney, S., & Hellmann, H. (2011). Recognition and repair pathways of damaged DNA in higher plants. *Selected topics in DNA repair*, InTech, 201-236.
15. Blagojevic, D. (2019). Sensitivity of plants exposed to gamma radiation. A physiological and molecular study (Accession No. 2019:100) [Doctoral dissertation, Norwegian University of Life Sciences]. https://nmbu.brage.unit.no/nmbu-xmlui/handle/11250/2711552.
16. Blagojevic, D., Lee, Y., Brede, D. A., Lind, O. C., Yakovlev, I., Solhaug, K. A., Fossdal, C. G., Salbu, B., & Olsen, J. E. (2019a). Comparative sensitivity to gamma radiation at the organismal, cell and DNA level in young plants of Norway spruce, Scots pine and *Arabidopsis thaliana*. *Planta*, *250*(5), 1567–1590. https://doi.org/10.1007/s00425-019-03250-y
17. Blagojevic, D., , Lee, Y., Xie, L., Brede, D. A., Nybakken, L., Lind, O. C., Tollefsen, K. E., Salbu, B., Solhaug, K. A., & Olsen, J. E., (2019b). No evidence of a protective or cumulative negative effect of UV-B on growth inhibition induced by gamma radiation in Scots pine (*Pinus sylvestris*) seedlings. *Photochemical & photobiological sciences*, *18*(8), 1945–1962. https://doi.org/10.1039/c8pp00491a
18. Bleuyard, J. Y., Gallego, M. E., Savigny, F., & White, C. I. (2005). Differing requirements for the *Arabidopsis* Rad51 paralogs in meiosis and DNA repair. *The Plant journal: for cell and molecular biology*, *41*(4), 533–545. https://doi.org/10.1111/j.1365-313X.2004.02318.x
19. Britt, A. B. (1999). Molecular genetics of DNA repair in higher plants. *Trends in plant science*, *4*(1), 20–25. https://doi.org/10.1016/s1360-1385(98)01355-7
20. Bustin, S. A., Benes, V., Garson, J. A., Hellemans, J., Huggett, J., Kubista, M., Mueller, R., Nolan, T., Pfaffl, M. W., Shipley, G. L., Vandesompele, J., & Wittwer, C. T. (2009). The MIQE guidelines: minimum information for publication of quantitative real-time PCR experiments. *Clinical chemistry*, *55*(4), 611–622. https://doi.org/10.1373/clinchem.2008.112797
21. Campbell, R. (2005). Phylum Coniferophyta. *Biology. 7th*, 595.
22. Caplin, N., & Willey, N. (2018). Ionizing radiation, higher plants, and radioprotection: from acute high doses to chronic low doses. *Frontiers in plant science*, *9*, 847. https ://doi.org/10.3389/fpls.2018.00847
23. Carneros, E., Yakovlev, I., Viejo, M., Olsen, J. E., & Fossdal, C. G. (2017). The epigenetic memory of temperature during embryogenesis modifies the expression of bud burst-related genes in Norway spruce epitypes. *Planta*, *246*(3), 553–566. https://doi.org/10.1007/s00425-017-2713-9
24. Chatterjee, N., & Walker, G. C. (2017). Mechanisms of DNA damage, repair, and mutagenesis. *Environmental and molecular mutagenesis*, *58*(5), 235–263. https://doi.org/10.1002/em.22087
25. Chen, I. P., Haehnel, U., Altschmied, L., Schubert, I., & Puchta, H. (2003). The transcriptional response of *Arabidopsis* to genotoxic stress - a high-density colony array

study (HDCA). *The Plant journal: for cell and molecular biology*, *35*(6), 771–786. https://doi.org/10.1046/j.1365-313X.2003.01847.x

26. Choppin, G., Ekberg, C., Liljenzin, J. O., & Rydberg, J. (2013). *Radiochemistry and Nuclear Chemistry (4th ed.)*, Academic Press.
27. Culligan, K. M., Robertson, C. E., Foreman, J., Doerner, P., & Britt, A. B. (2006). ATR and ATM play both distinct and additive roles in response to ionizing radiation. *The Plant journal: for cell and molecular biology*, *48*(6), 947–961. https://doi.org/10.1111/j.1365-313X.2006.02931.x
28. Culligan, K., Tissier, A., & Britt, A. (2004). ATR regulates a G2-phase cell-cycle checkpoint in *Arabidopsis thaliana*. *The Plant cell*, *16*(5), 1091–1104. https://doi.org/10.1105/tpc.018903
29. De La Torre, A. R., Birol, I., Bousquet, J., Ingvarsson, P. K., Jansson, S., Jones, S. J. M., Keeling, C. I., MacKay, J., Nilsson, O., Ritland, K., Street, N., Yanchuk, A., Zerbe, P., & Bohlmann, J. (2014). Insights into conifer giga-genomes. *Plant physiology*, *166*(4), 1724–1732. https://doi.org/10.1104/pp.114.248708
30. De Schutter, K., Joubès, J., Cools, T., Verkest, A., Corellou, F., Babiychuk, E., Van Der Schueren, E., Beeckman, T., Kushnir, S., Inzé, D., & De Veylder, L. (2007). *Arabidopsis* WEE1 kinase controls cell cycle arrest in response to activation of the DNA integrity checkpoint. *The Plant cell*, *19*(1), 211–225. https://doi.org/10.1105/tpc.106.045047
31. Deckbar, D., Jeggo, P. A., & Löbrich, M. (2011). Understanding the limitations of radiation-induced cell cycle checkpoints. *Critical reviews in biochemistry and molecular biology*, *46*(4), 271–283. https://doi.org/10.3109/10409238.2011.575764
32. Desouky, O., Ding, N., & Zhou, G. (2015). Targeted and non-targeted effects of ionizing radiation. *Journal of radiation research and applied sciences*, *8*(2), 247-254. https://doi.org/10.1016/j.jrras.2015.03.003
33. Doutriaux, M. P., Couteau, F., Bergounioux, C., & White, C. (1998). Isolation and characterisation of the *RAD51* and *DMC1* homologs from *Arabidopsis thaliana*. *Molecular and general genetics: MGG*, *257*(3), 283–291. https://doi.org/10.1007/s004380050649
34. Dowlath, M. J. H., Karuppannan, S. K., Sinha, P., Dowlath, N. S., Arunachalam, K. D., Ravindran, B., Chang, S. W., Nguyen-Tri, P., & Nguyen, D. D. (2021). Effects of radiation and role of plants in radioprotection: A critical review. *The Science of the total environment*, *779*, 146431. https://doi.org/10.1016/j.scitotenv.2021.146431
35. Esnault, M. A., Legue, F., & Chenal, C. (2010). Ionizing radiation: advances in plant response. *Environmental and experimental botany*, *68*(3), 231-237. https://doi.org/10.1016/j.envexpbot.2010.01.007
36. Fesenko, S. V., Alexakhin, R. M., Geras'kin, S. A., Sanzharova, N. I., Spirin, Y. V., Spiridonov, S. I., Gontarenko, I. A., & Strand, P. (2005). Comparative radiation impact on biota and man in the area affected by the accident at the Chernobyl nuclear power plant. *Journal of environmental radioactivity*, *80*(1), 1–25. https://doi.org/10.1016/j.jenvrad.2004.08.011
37. Freitas, A. C., & Alencar, A. S. (2004). Gamma dose rates and distribution of natural radionuclides in sand beaches--Ilha Grande, Southeastern Brazil. *Journal of*

*environmental radioactivity*, *75*(2), 211–223. https://doi.org/10.1016/j.jenvrad.2004.01.002

38. Friesner, J. D., Liu, B., Culligan, K., & Britt, A. B. (2005). Ionizing radiation-dependent gamma-H2AX focus formation requires ataxia telangiectasia mutated and ataxia telangiectasia mutated and Rad3-related. *Molecular biology of the cell*, *16*(5), 2566–2576. https://doi.org/10.1091/mbc.e04-10-0890
39. Ganguly, T., & Duker, N. J. (1991). Stability of DNA thymine hydrates. *Nucleic acids research*, *19*(12), 3319–3323. https://doi.org/10.1093/nar/19.12.3319
40. Garcia, V., Bruchet, H., Camescasse, D., Granier, F., Bouchez, D., & Tissier, A. (2003). *AtATM* is essential for meiosis and the somatic response to DNA damage in plants. *The Plant cell*, *15*(1), 119–132. https://doi.org/10.1105/tpc.006577
41. García-Rodríguez, L. J., De Piccoli, G., Marchesi, V., Jones, R. C., Edmondson, R. D., & Labib, K. (2015). A conserved Polϵ binding module in Ctf18-RFC is required for S-phase checkpoint activation downstream of Mec1. *Nucleic acids research*, *43*(18), 8830–8838. https://doi.org/10.1093/nar/gkv799
42. Geras'kin, S. A., & Volkova, P. Y. (2014). Genetic diversity in Scots pine populations along a radiation exposure gradient. *The Science of the total environment*, *496*, 317–327. https://doi.org/10.1016/j.scitotenv.2014.07.020
43. Geras'kin, S. A., Fesenko, S. V., & Alexakhin, R. M. (2008). Effects of non-human species irradiation after the Chernobyl NPP accident. *Environment international*, *34*(6), 880–897. https://doi.org/10.1016/j.envint.2007.12.012
44. Geras'kin, S. A., Zimina, L. M., Dikarev, V. G., Dikareva, N. S., Zimin, V. L., Vasiliyev, D. V., Oudalova, A. A., Blinova, L. D., & Alexakhin, R. M. (2003). Bioindication of the anthropogenic effects on micropopulations of *Pinus sylvestris*, L. in the vicinity of a plant for the storage and processing of radioactive waste and in the Chernobyl NPP zone. *Journal of environmental radioactivity*, *66*(1-2), 171–180. https://doi.org/10.1016/S0265-931X(02)00122-4
45. Geras'kin, S., Oudalova, A., Dikareva, N., Spiridonov, S., Hinton, T., Chernonog, E., & Garnier-Laplace, J. (2011). Effects of radioactive contamination on Scots pines in the remote period after the Chernobyl accident. *Ecotoxicology*, *20*(6), 1195–1208. https://doi.org/10.1007/s10646-011-0664-7
46. Gichner, T., Patková, Z., & Kim, J. K. (2003). DNA damage measured by the Comet assay in eight agronomic plants. *Biologia plantarum*, *47*(2), 185-188. https://doi.org/10.1023/B:BIOP.0000022249.86426.2a
47. Gill, S. S., & Tuteja, N. (2010). Reactive oxygen species and antioxidant machinery in abiotic stress tolerance in crop plants. *Plant physiology and biochemistry: PPB*, *48*(12), 909–930. https://doi.org/10.1016/j.plaphy.2010.08.016
48. Gill, S. S., Anjum, N. A., Gill, R., Jha, M., & Tuteja, N. (2015). DNA damage and repair in plants under ultraviolet and ionizing radiations. *The scientific world journal*, *2015*, 250158. https://doi.org/10.1155/2015/250158
49. Goltsova, N., Abaturov, Y., Abaturov, A., Melankholin, P., Girbasova, A., & Rostova, N. (1991). Chernobyl radionuclide accident: effects on the shoot structure of *Pinus sylvestris*. *Annales Botanici Fennici*, *28*(1), 1–13

50. Hahlbrock, K., & Scheel, D. (1989). Physiology and molecular biology of phenylpropanoid metabolism. *Annual review of plant physiology and plant molecular biology*, *40*(1), 347-369. https://doi.org/10.1146/annurev.pp.40.060189.002023
51. Hansen, E. L., Lind, O. C., Oughton, D. H., & Salbu, B. (2019). A framework for exposure characterization and gamma dosimetry at the NMBU FIGARO irradiation facility. *International journal of radiation biology*, *95*(1), 82–89. https://doi.org/10.1080/09553002.2018.1539878
52. Holiaka, D., Fesenko, S., Kashparov, V., Protsak, V., Levchuk, S., & Holiaka, M. (2020). Effects of radiation on radial growth of Scots pine in areas highly affected by the Chernobyl accident. *Journal of environmental radioactivity*, *222*, 106320. https://doi.org/10.1016/j.jenvrad.2020.106320
53. Hong, M. J., Kim, D. Y., Ahn, J. W., Kang, S. Y., Seo, Y. W., & Kim, J. B. (2018). Comparison of radiosensitivity response to acute and chronic gamma irradiation in colored wheat. *Genetics and molecular biology*, *41*(3), 611–623. https://doi.org/10.1590/1678-4685-GMB-2017-0189
54. Hosoya, N., & Miyagawa, K. (2014). Targeting DNA damage response in cancer therapy. *Cancer science*, *105*(4), 370–388. https://doi.org/10.1111/cas.12366
55. Hu, Z., Cools, T., & De Veylder, L. (2016). Mechanisms Used by Plants to Cope with DNA Damage. *Annual review of plant biology*, *67*, 439–462.https://doi.org/10.1146/annurevarplant-043015-111902
56. Hurem, S., Gomes, T., Brede, D. A., Lindbo Hansen, E., Mutoloki, S., Fernandez, C., Mothersill, C., Salbu, B., Kassaye, Y. A., Olsen, A. K., Oughton, D., Aleström, P., & Lyche, J. L. (2017). Parental gamma irradiation induces reprotoxic effects accompanied by genomic instability in zebrafish (*Danio rerio*) embryos. *Environmental research*, *159*, 564–578. https://doi.org/10.1016/j.envres.2017.07.053
57. IAEA, (2006). Environmental consequences of the Chernobyl accident and their remediation: Twenty years of experience. IAEA-STI/PUB/1239, Vienna.
58. Jackson, S. P., & Bartek, J. (2009). The DNA-damage response in human biology and disease. *Nature*, *461*(7267), 1071–1078. https://doi.org/10.1038/nature08467
59. Jan, S., Parween, T., Siddiqi, T. O., & Mahmooduzzafar. (2012). Enhancement in furanocoumarin content and phenylalanine ammonia lyase activity in developing seedlings of *Psoralea corylifolia* L. in response to gamma irradiation of seeds. *Radiation and environmental biophysics*, *51*(3), 341–347. https://doi.org/10.1007/s00411-012-0421-1
60. Jansen, M. A. K. (2017). Ultraviolet-B radiation: stressor and regulatory signal. In: Shabala S (ed). Plant stress physiology, 2nd edn. CAB International, Oxfordshire, 253–278.
61. Jansen, M. A. K., & Bornman, J. F. (2012). UV-B radiation: from generic stressor to specific regulator. *Physiologia plantarum*, *145*(4), 501–504. https://doi.org/10.1111/j.1399-3054.2012.01656.x
62. Kal'chenko, V. A. & Fedotov, I. S. (2001). Genetic effects of acute and chronic ionizing irradiation on *Pinus sylvestris* L. inhabiting the Chernobyl meltdown area. *Russian journal of genetics*, *37*(4): 341-350. https://doi.org/10.1023/A:1016646806556

63. Kal'chenko, V. A., Rubanovich, A. V., Fedotov, I. S., & Arkhipov, N. P. (1993). Genetic effects in gametes of *Pinus sylvestris* L. induced in the Chernobyl accident. *Genetika*, *29*(7), 1205-1212.
64. Kashparov, V. A., Lundin, S. M., Khomutinin, Y. V., Kaminsky, S. P., Levchuk, S. E., Protsak, V. P., Kadygrib, A. M., Zvarich, S. I., Yoschenko, V. I., & Tschiersch, J. (2001). Soil contamination with 90Sr in the near zone of the Chernobyl accident. *Journal of environmental radioactivity*, *56*(3), 285–298. https://doi.org/10.1016/s0265-931x(00)00207-1
65. Kashparov, V. A., Lundin, S. M., Zvarych, S. I., Yoshchenko, V. I., Levchuk, S. E., Khomutinin, Y. V., Maloshtan, I. M., & Protsak, V. P. (2003). Territory contamination with the radionuclides representing the fuel component of Chernobyl fallout. *The Science of the total environment*, *317*(1-3), 105–119. https://doi.org/10.1016/S0048-9697(03)00336-X
66. Kashparov, V., Yoschenko, V., Levchuk, S., Bugai, D., Van Meir, N., Simonucci, C., & Martin-Garin, A. (2012). Radionuclide migration in the experimental polygon of the Red Forest waste site in the Chernobyl zone - Part 1: Characterization of the waste trench, fuel particle transformation processes in soils, biogenic fluxes and effects on biota. *Applied geochemistry*, *27*(7), 1348-1358. https://doi.org/10.1016/j.apgeochem.2011.11.004
67. Kashparova, E., Levchuk, S., Morozova, V., & Kashparov, V. (2020). A dose rate causes no fluctuating asymmetry indexes changes in silver birch (*Betula pendula* (L.) Roth.) leaves and Scots pine (*Pinus sylvestris* L.) needles in the Chernobyl Exclusion Zone. *Journal of environmental radioactivity*, *211*, 105731. https://doi.org/10.1016/j.jenvrad.2018.05.015
68. Kim, D. S., Kim, J. B., Goh, E. J., Kim, W. J., Kim, S. H., Seo, Y. W., Jang, C. S., & Kang, S. Y. (2011). Antioxidant response of *Arabidopsis* plants to gamma irradiation: Genome-wide expression profiling of the ROS scavenging and signal transduction pathways. *Journal of plant physiology*, *168*(16), 1960–1971. https://doi.org/10.1016/j.jplph.2011.05.008
69. Koppen, G., Azqueta, A., Pourrut, B., Brunborg, G., Collins, A. R., & Langie, S. A. S. (2017). The next three decades of the comet assay: a report of the 11th International Comet Assay Workshop. *Mutagenesis*, *32*(3), 397–408. https://doi.org/10.1093/mutage/gex002
70. Kovács, E., & Keresztes, A. (2002). Effect of gamma and UV-B/C radiation on plant cells. *Micron*, *33*(2), 199–210. https://doi.org/10.1016/s0968-4328(01)00012-9
71. Kovalchuk, I., Molinier, J., Yao, Y., Arkhipov, A., & Kovalchuk, O. (2007). Transcriptome analysis reveals fundamental differences in plant response to acute and chronic exposure to ionizing radiation. *Mutation research/fundamental and molecular mechanisms of mutagenesis*, *624*(1-2), 101-113. https://doi.org/10.1016/j.mrfmmm.2007.04.009
72. Kovalchuk, O., Kovalchuk, I., Titov, V., Arkhipov, A., & Hohn, B. (1999). Radiation hazard caused by the Chernobyl accident in inhabited areas of Ukraine can be monitored by transgenic plants. *Mutation research/genetic toxicology and environmental mutagenesis*, *446*(1), 49–55. https://doi.org/10.1016/s1383-5718(99)00147-3

73. Kozubov, G. M., & Taskaev, A. I. (1994). [Radiobiological and radioecological studies of woody plants]. *St. Petersburg: Nauka*, 167-190.
74. Kozubov, G. M., & Taskaev, A. I. (2002). Radiobiology Investigations of Conifers in Region of the Chernobyl Disaster (1986-2001). Moscow: PPC. "Design. Information. Cartography".
75. Kozubov, G. M., & Taskaev, A. I. (2007). [Characteristics of morphogenesis and growth processes of conifers in the Chernobyl nuclear accident zone]. *Radiatsionnaia biologiia, radioecologiia*, *47*(2), 204–223.
76. Kozubov, G., Taskaev, A., Ignatenko, E., Artemov, V., Ostapenko, E., Ladanova, N., Kuzivanova, S., Kozlov, V., & Larin, V. (1990). Radiation influence to the pine forests in the zone of the accident at the Chernobyl NPP. *Syktyvkar: Komi Branch of AS USSR*.
77. Lachumy, S. J., Oon, C. E., Deivanai, S., Saravanan, D., Vijayarathna, S., Choong, Y. S., Yeng, C., Latha, L. Y., & Sasidharan, S. (2013). Herbal remedies for combating irradiation: a green anti-irradiation approach. *Asian Pacific journal of cancer prevention: APJCP*, *14*(10), 5553–5565. https://doi.org/10.7314/apjcp.2013.14.10.5553
78. Lafarge, S., & Montané, M. H. (2003). Characterization of *Arabidopsis thaliana* ortholog of the human breast cancer susceptibility gene 1: *AtBRCA1*, strongly induced by gamma rays. *Nucleic acids research*, *31*(4), 1148–1155. https://doi.org/10.1093/nar/gkg202
79. Lind, O. C., Helen Oughton, D., & Salbu, B. (2019). The NMBU FIGARO low dose irradiation facility. *International journal of radiation biology*, *95*(1), 76–81. https://doi.org/10.1080/09553002.2018.1516906
80. Luckey, T. D. (2006). Radiation hormesis: the good, the bad, and the ugly. *Dose-response: a publication of International Hormesis Society*, *4*(3), 169–190. https://doi.org/10.2203/dose-response.06-102.Luckey
81. Mackay, I. M. (2004). Real-time PCR in the microbiology laboratory. *Clinical microbiology and infection*, *10*(3), 190–212. https://doi.org/10.1111/j.1198- 743x.2004.00722.x
82. Mackay, J., Dean, J. F. D., Plomion, C., Peterson, D. G., Cánovas, F. M., Pavy, N., Ingvarsson, P. K., Savolainen, O., Guevara, M. Á., Fluch, S., Vinceti, B., Abarca, D., Díaz-Sala, C., & Cervera, M. T. (2012). Towards decoding the conifer giga-genome. *Plant molecular biology*, *80*(6), 555–569. https://doi.org/10.1007/s11103-012-9961-7
83. Macovei, A., & Tuteja, N. (2013). Different expression of miRNAs targeting helicases in rice in response to low and high dose rate γ-ray treatments. *Plant signaling & behavior*, *8*(8), e25128. https://doi.org/10.4161/psb.25128
84. Makarenko, E. S., Oudalova, A. A., & Geras'kin, S. A. (2016). Study of needle morphometric indices in Scots pine in the remote period after the Chernobyl accident. *Radioprotection*, *51*(1), 19-23. https://doi.org/10.1051/radiopro/2015026
85. Makarenko, E. S., Oudalova, A. A., & Geras'kin, S. A. (2016). Study of needle morphometric indices in Scots pine in the remote period after the Chernobyl accident. *Radioprotection*, *51*(1), 19-23. https://doi.org/10.1051/radiopro/2015026
86. Manova, V., & Gruszka, D. (2015). DNA damage and repair in plants - from models to crops. *Frontiers in plant science*, *6*, 885. https://doi.org/10.3389/fpls.2015.00885

87. Maréchal, A., & Zou, L. (2013). DNA damage sensing by the ATM and ATR kinases. *Cold Spring Harbor perspectives in biology*, *5*(9), a012716. https://doi.org/10.1101/cshperspect.a012716
88. Marinich, A., & Powell, K. (2017). Scots Pine (*Pinus sylvestris*): best management practices in Ontario. Ontario invasive plants. https://www.ontarioinvasiveplants.ca/wp-content/uploads/2020/10/ScotsPine_BMP.pdf (accessed on June 26, 2021)
89. McIlwraith, M. J., Van Dyck, E., Masson, J. Y., Stasiak, A. Z., Stasiak, A., & West, S. C. (2000). Reconstitution of the strand invasion step of double-strand break repair using human Rad51 Rad52 and RPA proteins. *Journal of molecular biology*, *304*(2), 151–164. https://doi.org/10.1006/jmbi.2000.4180
90. Mergen, F., & Strøm Johansen, T. (1964). Effect of ionizing radiation on seed germination and seedling growth of *Pinus rigida* (mill). *Radiation Botany*, *4*(4), 417-427. https://doi.org/10.1016/S0033-7560(64)80009-0
91. Miller, M. W., & Miller, W. M. (1987). Radiation hormesis in plants. *Health physics*, *52*(5), 607–616. https://doi.org/10.1097/00004032-198705000-00012
92. Mittler, R., Vanderauwera, S., Gollery, M., & Van Breusegem, F. (2004). Reactive oxygen gene network of plants. *Trends in plant science*, *9*(10), 490–498. https://doi.org/10.1016/j.tplants.2004.08.009
93. Morgan, W. F. (2003). Non-targeted and delayed effects of exposure to ionizing radiation: I. Radiation-induced genomic instability and bystander effects in vitro. *Radiation research*, *159*(5), 567–580. https://doi.org/10.1667/0033-7587(2003)159[0567:nadeoe]2.0.co;2
94. Morgan, W. F., Day, J. P., Kaplan, M. I., McGhee, E. M., & Limoli, C. L. (1996). Genomic instability induced by ionizing radiation. *Radiation research*, *146*(3), 247–258. https://doi.org/10.2307/3579454
95. Mothersill, C., & Seymour, C. B. (1998). Mechanisms and implications of genomic instability and other delayed effects of ionizing radiation exposure. *Mutagenesis*, *13*(5), 421–426. https://doi.org/10.1093/mutage/13.5.421
96. Mousseau, T. A., & Møller, A. P. (2020). Plants in the light of ionizing radiation: what have we learned from Chernobyl, Fukushima, and other "hot" places?. *Frontiers in plant science*, *11*, 552. https://doi.org/10.3389/fpls.2020.00552
97. Mousseau, T. A., Welch, S. M., Chizhevsky, I., Bondarenko, O., Milinevsky, G., Tedeschi, D. J., Bonisoli-Alquati A., & Møller A. P. (2013). Tree rings reveal extent of exposure to ionizing radiation in Scots pine *Pinus sylvestris*. *Trees 27*(5), 1443–1453. https://doi.org/10.1007/s00468-013-0891-z
98. Mrdakovic Popic, J., Bhatt, C. R., Salbu, B., & Skipperud, L. (2012). Outdoor 220Rn, 222Rn and terrestrial gamma radiation levels: investigation study in the thorium rich Fen Complex, Norway. *Journal of environmental monitoring: JEM*, *14*(1), 193–201. https://doi.org/10.1039/c1em10726g
99. Murashige, T., & Skoog, F. (1962). A revised medium for rapid growth and bio assays with tobacco tissue cultures. *Physiologia plantarum*, *15*(3), 473-497. https://doi.org/10.1111/j.1399-3054.1962.tb08052.x
100. Nisa, M. U., Huang, Y., Benhamed, M., & Raynaud, C. (2019). The plant DNA damage response: signaling pathways leading to growth inhibition and putative role in response to

stress conditions. *Frontiers in plant science*, *10*, 653. https://doi.org/10.3389/fpls.2019.00653

101. Nystedt, B., Street, N. R., Wetterbom, A., Zuccolo, A., Lin, Y. C., Scofield, D. G., Vezzi, F., Delhomme, N., Giacomello, S., Alexeyenko, A., Vicedomini, R., Sahlin, K., Sherwood, E., Elfstrand, M., Gramzow, L., Holmberg, K., Hällman, J., Keech, O., Klasson, L., Koriabine, M., Kucukoglu, M., Käller, M., Luthman, J., Lysholm, F., Niittylä, T., Olson, A., Rilakovic, N., Ritland, C., Rosselló, J. A., Sena, J., Svensson, T., Talavera-López, C., Theißen, G., Tuominen, H., Vanneste, K., Wu, Z. Q., Zhang, B., Zerbe, P., Arvestad, L., Bhalerao, R., Bohlmann, J., Bousquet, J., Garcia Gil, R., Hvidsten, T. R., de Jong, P., MacKay, J., Morgante, M., Ritland, K., Sundberg, B., Thompson, S. L., Van de Peer, Y., Andersson, B., Nilsson, O., Ingvarsson, P. K., Lundeberg, J., & Jansson, S. (2013). The Norway spruce genome sequence and conifer genome evolution. *Nature*, *497*(7451), 579–584. https://doi.org/10.1038/nature12211
102. Ossowski, S., Schneeberger, K., Lucas-Lledó, J. I., Warthmann, N., Clark, R. M., Shaw, R. G., Weigel, D., & Lynch, M. (2010). The rate and molecular spectrum of spontaneous mutations in *Arabidopsis thaliana*. *Science*, *327*(5961), 92–94. https://doi.org/10.1126/science.1180677
103. Paschoa, A. S. (1998). Potential environmental and regulatory implications of naturally occurring radioactive materials (NORM). *Applied radiation and isotopes*, *49*(3), 189–196. https://doi.org/10.1016/s0969-8043(97)00239-x
104. Puizina, J., Siroky, J., Mokros, P., Schweizer, D., & Riha, K. (2004). Mre11 deficiency in Arabidopsis is associated with chromosomal instability in somatic cells and Spo11-dependent genome fragmentation during meiosis. *The Plant cell*, *16*(8), 1968–1978. https://doi.org/10.1105/tpc.104.022749
105. Pyhäjärvi, T., Kujala, S. T., & Savolainen, O. (2020). 275 years of forestry meets genomics in *Pinus sylvestris*. *Evolutionary applications*, *13*(1), 11–30. https://doi.org/10.1111/eva.12809
106. Quintiliani, M. (1986). The oxygen effect in radiation inactivation of DNA and enzymes. *International journal of radiation biology and related studies in physics, chemistry, and medicine*, *50*(4), 573–594. https://doi.org/10.1080/09553008614550981
107. Rastogi, R. P., Richa, Kumar, A., Tyagi, M. B., & Sinha, R. P. (2010). Molecular mechanisms of ultraviolet radiation-induced DNA damage and repair. *Journal of nucleic acids*, *2010*, 592980. https://doi.org/10.4061/2010/592980
108. Ravnikar, M., Mehle, N., Gruden, K., & Dreo, T. (2016). Real-time PCR. Molecular Methods in Plant Disease Diagnostics: Principles and Protocols, In: Boonham, N., Tomlinson, J., Mumford, R. (eds), 28-58. https://doi.org/10.1079/9781780641478.0028
109. Real, A., Sundell-Bergman, S., Knowles, J. F., Woodhead, D. S., & Zinger, I. (2004). Effects of ionising radiation exposure on plants, fish and mammals: relevant data for environmental radiation protection. *Journal of radiological protection: official journal of the Society for Radiological Protection*, *24*(4A), A123–A137. https://doi.org/10.1088/0952-4746/24/4a/008
110. Ricaud, L., Proux, C., Renou, J. P., Pichon, O., Fochesato, S., Ortet, P., & Montané, M. H. (2007). ATM-mediated transcriptional and developmental responses to γ-rays in *Arabidopsis*. *PloS one*, *2*(5), e430. https://doi.org/10.1371/journal.pone.0000430

111. Roldán-Arjona, T., & Ariza, R. R. (2009). Repair and tolerance of oxidative DNA damage in plants. *Mutation research*, *681*(2-3), 169–179. https://doi.org/10.1016/j.mrrev.2008.07.003
112. Rozen, S., & Skaletsky, H. (2000). Primer3 on the WWW for general users and for biologist programmers. *Methods in molecular biology*, *132*, 365–386. https://doi.org/10.1385/1-59259-192-2:365
113. Rudolph, T. D. (1971). Gymnosperm seedling sensitivity to gamma radiation: its relation to seed radiosensitivity and nuclear variables. *Radiation botany*, *11*(1), 45-51. https://doi.org/10.1016/S0033-7560(71)91371-8
114. Rushforth, K. (1986) [1980]. Bäume [Pocket Guide to Trees] (in German) (2nd ed.). Bern: Hallwag AG. p. 91. ISBN 978-3-444-70130-6.
115. Saldivar, J. C., Cortez, D., & Cimprich, K. A. (2017). The essential kinase ATR: ensuring faithful duplication of a challenging genome. *Nature reviews. Molecular cell biology*, *18*(10), 622–636. https://doi.org/10.1038/nrm.2017.67
116. Shevchenko, V. A., Abramov, V. I., Kal'chenko, V. A., Fedotov, I. S., & Rubanovich, A. V. (1996). [The genetic sequelae for plant populations of radioactive environmental pollution in connection with the Chernobyl accident]. *Radiatsionnaia biologiia, radioecologiia*, *36*(4), 531-545.
117. Shevchenko, V. V., & Grinikh, L. I. (1995). The cytogenetic effects in *Crepis tectorum* populations growing in Bryansk Province observed in the 7th year after the accident at the Chernobyl Atomic Electric Power Station. *Radiatsionnaia biologiia, radioecologiia*, *35*(5), 720–725.
118. Sidorov, V. P. (1994). [The cytogenetic effect in the cells of the needles of the common pine from irradiation resulting from the accident at the Chernobyl Atomic Power Station]. *Radiatsionnaia biologiia, radioecologiia*, *34*(6), 847–851.
119. Sidrak, G. H., & Suess, A. (1973). Effects of low doses of gamma radiation on the growth and yield of two varieties of tomato. *Radiation botany*, *13*(6), 309-314. https://doi.org/10.1016/S0033-7560(73)90040-9
120. Singh, J., Birbian, N., Sinha, S., & Goswami, A. (2014). A critical review on PCR, its types and applications. *International journal of advanced research in biological science, 1*(7), 65-80.
121. Sorochinsky, B., & Zelena, L. (2003). Is the cytoskeleton involved in the irradiation-induced abnormal morphogenesis of coniferous plants?. *Cell biology international*, *27*(3), 275–277. https://doi.org/10.1016/s1065-6995(02)00323-2
122. Spampinato, C. P. (2017). Protecting DNA from errors and damage: an overview of DNA repair mechanisms in plants compared to mammals. *Cellular and molecular life sciences: CMLS*, *74*(9), 1693–1709. https://doi.org/10.1007/s00018-016-2436-2
123. Sreedhar, M., Anurag, C., Aparna, M., Kumar, D. P., Singhal, R. K., & Venu-Babu, P. (2013). Influence of γ-radiation stress on scavenging enzyme activity and cell ultra-structure in groundnut (*Arachis hypogaea* L.). *Advances in applied science research*, *4*(2), 35-44.
124. Steinhauser, G., Brandl, A., & Johnson, T. E. (2014). Comparison of the Chernobyl and Fukushima nuclear accidents: a review of the environmental impacts. *The Science of the total environment*, *470-471*, 800–817. https://doi.org/10.1016/j.scitotenv.2013.10.029

125. Tamura, K., Adachi, Y., Chiba, K., Oguchi, K., & Takahashi, H. (2002). Identification of Ku70 and Ku80 homologues in *Arabidopsis thaliana*: evidence for a role in the repair of DNA double-strand breaks. *The Plant journal: for cell and molecular biology*, *29*(6), 771–781. https://doi.org/10.1046/j.1365-313x.2002.01258.x
126. Tikhomirov, F. A., & Shcheglov, A. I. (1994). Main investigation results on the forest radioecology in the Kyshtym and Chernobyl accident zones. *The Science of the total environment*, *157*(1-3), 45–57. https://doi.org/10.1016/0048-9697(94)04266-P
127. Tulik, M. (2001). Cambial history of Scots pine trees (*Pinus sylvestris*) prior and after the Chernobyl accident as encoded in the xylem. *Environmental and experimental botany*, *46*(1), 1–10. https://doi.org/10.1016/s0098-8472(01)00075-2
128. Tulik, M., & Rusin, A. (2005). Microfibril angle in wood of Scots pine trees (*Pinus sylvestris*) after irradiation from the Chernobyl nuclear reactor accident. *Environmental pollution*, *134*(2), 195–199. https://doi.org/10.1016/j.envpol.2004.08.009
129. United Nations Scientific Committee on the Effects of Atomic Radiation [UNSCEAR]. (2010). Summary of low-dose radiation effects on health. *New York*, 1-14.
130. United Nations Scientific Committee on the Effects of Atomic Radiation [UNSCEAR]. (2017). Sources, effects and risks of ionizing radiation. *New York*, 184.
131. Van Hoeck, A., Horemans, N., Van Hees, M., Nauts, R., Knapen, D., Vandenhove, H., & Blust, R. (2015). Characterizing dose response relationships: Chronic gamma radiation in *Lemna minor* induces oxidative stress and altered polyploidy level. *Journal of environmental radioactivity*, *150*, 195–202. https://doi.org/10.1016/j.jenvrad.2015.08.017
132. Van Hoeck, A., Horemans, N., Nauts, R., Van Hees, M., Vandenhove, H., & Blust, R. (2017). *Lemna minor* plants chronically exposed to ionising radiation: RNA-seq analysis indicates a dose rate dependent shift from acclimation to survival strategies. *Plant science*, *257*, 84-95. https://doi.org/10.1016/j.plantsci.2017.01.010
133. Vandenhove, H., Vanhoudt, N., Cuypers, A., van Hees, M., Wannijn, J., & Horemans, N. (2010). Life-cycle chronic gamma exposure of *Arabidopsis thaliana* induces growth effects but no discernable effects on oxidative stress pathways. *Plant physiology and biochemistry: PPB*, *48*(9), 778–786. https://doi.org/10.1016/j.plaphy.2010.06.006
134. Vanhoudt, N., Cuypers, A., Vangronsveld, J., Horemans, N., Wannijn, J., Van Hees, M., & Vandenhove, H. (2011). Study of biological effects and oxidative stress related responses in gamma irradiated *Arabidopsis thaliana* plants. *Radioprotection*, *46*(6), S401–S407. https://doi.org/10.1051/radiopro/20116510s
135. Vanhoudt, N., Horemans, N., Wannijn, J., Nauts, R., Van Hees, M., & Vandenhove, H. (2014). Primary stress responses in *Arabidopsis thaliana* exposed to gamma radiation. *Journal of environmental radioactivity*, *129*, 1–6. https://doi.org/10.1016/j.jenvrad.2013.11.011
136. Vanhoudt, N., Vandenhove, H., Horemans, N., Wannijn, J., Van Hees, M., Vangronsveld, J., & Cuypers, A. (2010). The combined effect of uranium and gamma radiation on biological responses and oxidative stress induced in *Arabidopsis thaliana*. *Journal of environmental radioactivity*, *101*(11), 923–930. https://doi.org/10.1016/j.jenvrad.2010.06.008

137. Volkova, P. Y., Geras'kin, S. A., & Kazakova, E. A. (2017). Radiation exposure in the remote period after the Chernobyl accident caused oxidative stress and genetic effects in Scots pine populations. *Scientific reports*, *7*, 43009. https://doi.org/10.1038/srep43009
138. Wang, X. Q., & Ran, J. H. (2014). Evolution and biogeography of gymnosperms. *Molecular phylogenetics and evolution*, *75*, 24–40. https://doi.org/10.1016/j.ympev.2014.02.005
139. Watanabe, Y., Ichikawa, S., Kubota, M., Hoshino, J., Kubota, Y., Maruyama, K., Fuma, S., Kawaguchi, I., Yoschenko, V. I., & Yoshida, S. (2015). Morphological defects in native Japanese fir trees around the Fukushima Daiichi Nuclear Power Plant. *Scientific reports*, *5*, 13232. https://doi.org/10.1038/srep13232
140. Waterworth, W. M., Altun, C., Armstrong, S. J., Roberts, N., Dean, P. J., Young, K., Weil, C. F., Bray, C. M., & West, C. E. (2007). NBS1 is involved in DNA repair and plays a synergistic role with ATM in mediating meiotic homologous recombination in plants. *The Plant journal: for cell and molecular biology*, *52*(1), 41–52. https://doi.org/10.1111/j.1365-313X.2007.03220.x
141. Wegrzyn, J. L., Liechty, J. D., Stevens, K. A., Wu, L. S., Loopstra, C. A., Vasquez-Gross, H. A., Dougherty, W. M., Lin, B. Y., Zieve, J. J., Martínez-García, P. J., Holt, C., Yandell, M., Zimin, A. V., Yorke, J. A., Crepeau, M. W., Puiu, D., Salzberg, S. L., de jong, P. J., Mockaitis, K., Main D., Langley, C. H., & Neale, D. B. (2014). Unique features of the Loblolly pine (*Pinus taeda* L.) megagenome revealed through sequence annotation. *Genetics*, 196(3), 891–909. https://doi.org/10.1534/genetics.113.159996
142. Weimer, A. K., Biedermann, S., Harashima, H., Roodbarkelari, F., Takahashi, N., Foreman, J., Guan, Y., Pochon, G., Heese, M., Van Damme, D., Sugimoto, K., Koncz, C., Doerner, P., Umeda, M., & Schnittger, A. (2016). The plant-specific CDKB1-CYCB1 complex mediates homologous recombination repair in *Arabidopsis*. *The EMBO journal*, *35*(19), 2068–2086. https://doi.org/10.15252/embj.201593083
143. Weng, M. L., Becker, C., Hildebrandt, J., Neumann, M., Rutter, M. T., Shaw, R. G., Weigel, D., & Fenster, C. B. (2019). Fine-grained analysis of spontaneous mutation spectrum and frequency in *Arabidopsis thaliana*. *Genetics*, *211*(2), 703–714. https://doi.org/10.1534/genetics.118.301721
144. West, C. E., Waterworth, W. M., Jiang, Q., & Bray, C. M. (2000). *Arabidopsis* DNA ligase IV is induced by γ-irradiation and interacts with an *Arabidopsis* homologue of the double strand break repair protein XRCC4. *The Plant journal: for cell and molecular biology*, *24*(1), 67–78. https://doi.org/10.1046/j.1365-313x.2000.00856.x
145. Wi, S. G., Chung, B. Y., Kim, J. S., Kim, J. H., Baek, M. H., Lee, J. W., & Kim, Y. S. (2007). Effects of gamma irradiation on morphological changes and biological responses in plants. *Micron*, *38*(6), 553–564. https://doi.org/10.1016/j.micron.2006.11.002
146. Wong, M. L., & Medrano, J. F. (2005). Real-time PCR for mRNA quantitation. *Biotechniques*, *39*(1), 75–85. https://doi.org/10.2144/05391RV01
147. Woodwell, G. M. & Rebuck, A. L. (1967). Effects of chronic gamma radiation on the structure and diversity of an oak-pine forest. *Ecological monographs*, *37*(1), 53-69. https://doi.org/10.2307/1948482

148. Woodwell, G. M. (1962). Effects of ionizing radiation on terrestrial ecosystems: experiments show how ionizing radiation may alter normally stable patterns of ecosystem behavior. *Science*, *138*(3540), 572–577. https://doi.org/10.1126/science.138.3540.572
149. Xie, L., Solhaug, K. A., Song, Y., Brede, D. A., Lind, O. C., Salbu, B., & Tollefsen, K. E. (2019). Modes of action and adverse effects of gamma radiation in an aquatic macrophyte *Lemna minor*. *The Science of the total environment*, *680*, 23–34. https://doi.org/10.1016/j.scitotenv.2019.05.016
150. Yokota, Y., Funayama, T., Hase, Y., Hamada, N., Kobayashi, Y., Tanaka, A., & Narumi, I. (2010). Enhanced micronucleus formation in the descendants of γ-ray-irradiated tobacco cells: evidence for radiation-induced genomic instability in plant cells. *Mutation research/fundamental and molecular mechanisms of mutagenesis*, *691*(1-2), 41–46. https://doi.org/10.1016/j.mrfmmm.2010.07.001
151. Yokota, Y., Shikazono, N., Tanaka, A., Hase, Y., Funayama, T., Wada, S., & Inoue, M. (2005). Comparative radiation tolerance based on the induction of DNA double-strand breaks in tobacco BY-2 cells and CHO-K1 cells irradiated with gamma rays. *Radiation research*, *163*(5), 520–525. https://doi.org/10.1667/rr3355
152. Yoschenko, V. I., Kashparov, V. A., Melnychuk, M. D., Levchuk, S. E., Bondar, Y. O., Lazarev, M., Yoschenko, M. I., Farfán, E. B., & Jannik, G. T. (2011). Chronic irradiation of Scots pine trees (*Pinus sylvestris*) in the Chernobyl exclusion zone: dosimetry and radiobiological effects. *Health physics*, *101*(4), 393–408. https://doi.org/10.1097/HP.0b013e3182118094
153. Yoschenko, V., Nanba, K., Yoshida, S., Watanabe, Y., Takase, T., Sato, N., & Keitoku, K. (2016). Morphological abnormalities in Japanese red pine (*Pinus densiflora*) at the territories contaminated as a result of the accident at Fukushima Dai-Ichi Nuclear Power Plant. *Journal of environmental radioactivity*, *165*, 60–67. https://doi.org/10.1016/j.jenvrad.2016.09.006
154. Yoschenko, V., Ohkubo, T., & Kashparov, V. (2018). Radioactive contaminated forests in Fukushima and Chernobyl. *Journal of forest research*, *23*(1), 3-14. https://doi.org/10.1080/13416979.2017.1356681
155. Yoshiyama, K. O., Sakaguchi, K., & Kimura, S. (2013). DNA damage response in plants: conserved and variable response compared to animals. *Biology*, *2*(4), 1338–1356. https://doi.org/10.3390/biology2041338
156. Yoshiyama, K., Conklin, P. A., Huefner, N. D., & Britt, A. B. (2009). Suppressor of gamma response 1 (*SOG1*) encodes a putative transcription factor governing multiple responses to DNA damage. *Proceedings of the National Academy of Sciences of the United States of America*, *106*(31), 12843–12848. https://doi.org/10.1073/pnas.0810304106
157. Zelena, L., Sorochinsky, B., von Arnold, S., van Zyl, L., & Clapham, D. H. (2005). Indications of limited altered gene expression in *Pinus sylvestris* trees from the Chernobyl region. *Journal of environmental radioactivity*, *84*(3), 363–373. https://doi.org/10.1016/j.jenvrad.2005.03

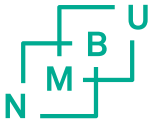


**Norges miljø- og biovitenskapelige universitet**
Noregs miljø- og biovitskapelege universitet
Norwegian University of Life Sciences

Postboks 5003
NO-1432 Ås
Norway